LIMITATIONS TO THE RATES OF RECOMBINANT PROTEIN PRODUCTION BY MAMMALIAN CELLS

by

Chorng-Hwa Fann

B.Sc., Chung-Yuan University, Taiwan, 1984
M.Sc., National Taiwan University, Taiwan, 1986

A THESIS SUBMITTED IN PARTIAL FULFILLMENT OF THE REQUIREMENTS FOR THE DEGREE OF DOCTOR OF PHILOSOPHY

in

THE FACULTY OF GRADUATE STUDIES

BIOTECHNOLOGY LABORATORY
&
DEPARTMENT OF CHEMICAL AND BIO-RESOURCE ENGINEERING

We accept this thesis as confirming to the required standard

THE UNIVERSITY OF BRITISH COLUMBIA

1999

In presenting this thesis in partial fulfilment of the requirements for an advanced degree at the University of British Columbia, I agree that the Library shall make it freely available for reference and study. I further agree that permission for extensive copying of this thesis for scholarly purposes may be granted by the head of my department or by his or her representatives. It is understood that copying or publication of this thesis for financial gain shall not be allowed without my written permission.

Department of Chemical & Bio-Resource Engineering

The University of British Columbia
Vancouver, Canada

Date April 29 '99

DE-6 (2/88)

ABSTRACT

Mammalian cells have been genetically engineered to produce a large number of recombinant proteins for research, diagnostic and therapeutic applications. However, low cellular production rate generally limits production yields and increases production costs. To select strategies to maximize production, it is important to identify the intracellular limitations of the mammalian cell production rates. Recombinant human activated protein C (APC) and tissue plasminogen activator (t-PA) have served as low and high producing systems for this investigation, respectively. The transcription, translation, and secretory efficiencies were analyzed in clones with wide ranges of APC and t-PA productivities. A structured kinetic model was used to quantify the changes in intracellular parameters when recombinant protein expression became limiting.

The production rate of APC by baby hamster kidney (BHK) cells was increased 35-fold by increasing the cDNA copy number per cell from 50 to 240. In this range, the transcription efficiency (APC mRNA per cDNA) was not constant, as had been expected, but instead increased 7 fold. This apparent cooperative effect of multiple cDNA copies could be explained by their integration in tandem. For cDNA copy numbers higher than 240, the transcription efficiency decreased dramatically, possibly due to cosuppression.

Two strategies were employed to maximize APC mRNA levels and APC production rate. Sodium butyrate treatment or re-transfection of an APC producing cell line with a vector containing additional APC cDNA resulted in over 2-fold higher mRNA levels and cell specific APC production rates. At high mRNA levels, the APC secretion rate but not translation efficiency was decreased, revealing a saturation of the secretory pathway. In

batch cultures of a mRNA limited clone, the levels of total cellular RNA, APC mRNA and β-actin mRNA were relatively stable while cells were in the exponential growth phase, but rapidly decreased during the stationary phase. Decreasing APC mRNA level was correlated with a decline in APC secretion rate, indicating that the mRNA levels limited the rates of APC production beyond the exponential phase, into the declining growth and stationary phases. The γ-carboxylation of glutamic acid residues, a post-translational modification required for APC biological activity, was also analyzed. The proportion of APC that was fully γ-carboxylated decreased as batch cultures progressed and in clones with increased APC production rates.

The production of recombinant t-PA in Chinese hamster ovary (CHO) cells was increased by cDNA amplification using stepwise adaptation to increasing methotrexate (MTX) concentrations. Subcloning of the amplified cells showed no apparent correlation between t-PA production rate and cell specific growth rate. The highest producing clones were isolated at 5 μM MTX and yielded 26,000 U/10^6cells·day (~43 μg/10^6cells·day) of t-PA. In the absence of MTX, an up to 90% decline in t-PA production rate was observed within 40 days, which could be explained by an up to 60% loss of cDNA copies. In long-term serum-free culture without MTX (108 days), the maximum t-PA production rate obtained (for 320 days) was 7,000 ± 750 U/10^6cells·day (~12 ± 1 μg/10^6cells·day*). This stable level of production was significantly lower than the unstable levels of production that CHO cells attained under selective pressure.

The intracellular factors which influence the rates of recombinant t-PA production by CHO cells were investigated in 24 clones with a wide range of t-PA production rates from 300 to 25,000 U/10^6cells·day (0.5 to 42 μg/10^6cells·day). The cDNA copy number data revealed a cooperative increase of t-PA production rates up to 350 copies, with apparent cosuppression at higher copy numbers. A linear relation between the t-PA mRNA levels and t-PA production rates suggested that the t-PA mRNA levels limited production for all clones. The intracellular t-PA content and pulse-chase analysis of intracellular t-PA confirmed that the recombinant protein did not accumulate in the CHO cells. The mRNA half-lives of t-PA producing clones were analyzed to determine if decreased mRNA stability limited the high t-PA mRNA levels, but the mRNA half-lives (7±2 h) were not decreased at higher expression levels. Instead, the transcription rates of t-PA appeared to limit production rate, even in the unstable range of t-PA production rates (12-42 μg/10^6cells·day).

In batch culture, the levels of t-PA mRNA were relatively stable and correlated well with cell specific t-PA production rates, while cells were in the exponential growth phase. When cells reached the stationary phase, a more rapid decline in cell specific t-PA production rates than mRNA levels was observed, which implied that in the declining growth phase, factors other than mRNA levels may limit t-PA production rates.

TABLE OF CONTENTS

LIST OF TABLES

LIST OF FIGURES

TABLE OF ABBREVIATIONS

Ad	Adenovirus
ADA	Adenosine deaminase
APC	Activated protein C
BHK cells	Baby Hamster Kidney cells
BPV	Bovine papillomavirus
CD4IgG	Anti-CD4 protein - immunoglobulin G
cDNA	Complementary DNA
CHO cells	Chinese Hamster Ovary cells
CMV	Cytomegalovirus
CMV-MIE	CMV major immediate-early gene
dCF	2'-Deocycoformycin
DHFR	Dihydrofolate reductase
DIG	Digoxigenin
DM	Double minute (DNA)
DNA	Deoxyribonucleic Acid
eIF-2	Eucaryotic initiation factor - 2
EF-1	Elongation factor-1
ELISA	Enzyme-linked Immunosorbent Assay
EPO	Erythropoietin
ER	Endoplasmic reticulum
FBS	Fetal bovine serum
FISH	Fluorescence *in-situ* hybridization
FVIII	Factor VIII
GC-rich	DNA sequences contain abundant guanine and cytosine bases
G-CSF	Granulocyte-colony-stimulating factor
Gla	γ-carboxyglutamic acid
GS	Glutamine synthetase

GTP	Guanosine tri-phosphate
hATIII	Human antithrombin III
HbsAg	Hepatitis B surface antigen
HPV-IE	Human papillomavirus-immediate-early gene
HSRs	Homogeneous staining regions
HSV-TK	Herpes simplex virus thymidine kinase
ICAM-1	Intercellular adhesion molecule-1
M-CSF	Macrophage-colony stimulating factor
Met-tRNA	Methionine-transfer RNA
MMTV-LTR	Mouse mammary tumor virus long terminal repeat
mRNA	Messenger ribonucleic acid
MSX	Methionine sulphoximine
mt t-PA	Mutant t-PA
MTX	Methotrexate
NEO	Neomycin phosphotransferase gene
NCS	Newborn calf serum
PAGE	Polyacrylamide Gel Electrophoresis
PBS	Phosphate-buffered saline
RNase	Ribonuclease
rRNA	Ribosome ribonucleic acid
RSV	Rous sarcoma virus
SDS	Sodium Dodecyl Sulfate
SRP	Signal recognition particles
SV40	Simian Virus 40
SV-TK	Simplex virus thymidine kinase
TCA	Trichloroacetic acid
TdT	Terminal deoxynucleotidyl transferase
TIMP	Tissue inhibitor of metalloproteinases
TNFrFc	Tumor necrosis factor receptor
t-PA	Tissue-type Plasminogen Activator

TUNEL	TdT mediated dUTP-biotin nick end labeling
VP16	A herpesvirus transactivator
vWF	von Willebrand factor

LIST OF SYMBOLS AND UNITS

m_{cDNA}	Amount of plasmid DNA
m_g	Amount of genomic DNA
S_g	Molecular size of the mammalian genome (5.6×10^6 kb/ cell)
S_p	Molecular size of the plasmid (7 kb/plasmid for APC and 6.6 kb/plasmid for t-PA)
$[mRNA]$	Intracellular recombinant protein mRNA concentration (mRNA transcripts/cell)
k_D	cDNA transcription rate (mRNA/cDNA·h)
$[cDNA]$	Cellular cDNA copy number (cDNA copies/cell)
k_m	mRNA turnover rate (h^{-1})
$[P_i]$	Intracellular concentration of recombinant protein (pg/cell)
k_R	Translation rate (pg protein/mRNA·h)
k_S	Secretion rate (h^{-1})
k_P	Intracellular protein degradation rate (h^{-1})
q_p	Cell specific recombinant protein production rate (pg protein/cell/h)
q_p	Cell specific production rate (pg/cell·day)
X	Cell concentration (cells/L) in the culture
$[P_e]$	Secreted recombinant protein concentration (pg/L)
$\mathcal{E}_R$	Transcription efficiency (mRNA/cDNA)
$\mathcal{E}_P$	Translation efficiency (protein/mRNA)

k_a	Cell Specific t-PA production decay rate (day^{-1})
q_p^{max}	Predicted maximum cell specific protein production rate
$[P_i^{max}]$	Intracellular recombinant protein saturation concentration (approximately 1 pg/cell) in secretory pathway
μ	Cell specific growth rate (h^{-1})
t	Time (h)
U	International unit, the amount of enzyme required to turn over 1 μmole substrate/ min.

ACKNOWLEDGMENTS

I am very grateful to my supervisor, Dr. James Piret, for his excellent guidance on my research work during all these years. He has provided me an outstanding research environment and fully supported my doctoral studies in the Biotech Lab. I would also like to thank Dr. Marta Guarna for her great contributions on the activated protein C studies and her excellent advice for my thesis work.

Dr. Hélène Côté, Dr. Sharon Busby (Zymogenetics, Seattle, WA), and my committee advisors, Dr. Douglas Kilburn and Dr. Ross MacGillivray, are gratefully acknowledged for their excellent instructions. I would also like to thank Dr. Faiz Guirgis for providing great technical support and Jason Dowd for helpful discussions. Dr. Loida Escote-Carlson, Mr. John Huang and Mr. Darius Panaligan in the Teaching Lab, and Dr. Robert McMaster in Medical Genetics are also greatly appreciated for generously providing me the access to their facilities.

I am also grateful to Cangene Corp. (Winnipeg, MB) and the Natural Sciences and Engineering Research Council of Canada for financial support.

Finally, I want to express my special thanks and greatest love to my wife, Grace Chen. She has not only taken care of the whole family, but also provided excellent contributions to my research projects. My project would not have been accomplished without her support.

CHAPTER 1 INTRODUCTION AND LITERATURE REVIEW

1.1 RECOMBINANT PROTEIN PRODUCTION BY MAMMALIAN CELLS

Mammalian cell based expression systems have been widely employed to produce recombinant proteins, especially those requiring complex post-translational modifications for diagnostic and therapeutic applications (Bially, 1987). However, major drawbacks of using mammalian cells for production are the limited protein production rates and low product concentrations in expensive medium. Other expression systems, such as *Escherichia coli* or yeast, usually produce recombinant proteins at higher rates in relatively inexpensive growth media. However, many complex post-translational modifications of proteins are not properly performed in these microbial systems. Thus, to efficiently produce complex recombinant proteins, it is often necessary to maximize foreign protein production rates in mammalian cells.

1.1.1 Introduction of Foreign cDNA Carrying Vectors Into Mammalian Cells

Introduction of foreign genes (cDNAs) into mammalian cells can be efficiently achieved by various methods (Keown et al., 1990). The most common procedure to obtain stable transfected cells is to add DNA directly in the form of a calcium phosphate precipitate, taken up by the host cells via endocytosis (Graham and van der Eb, 1973; Chen and Okayama, 1987). Other methods such as polyethylene glycol (PEG)-induced fusion (Schaffner, 1980), DNA microinjection (Capecchi, 1980), electroporation (Potter et al.,

1984), and DNA encapsulated liposomes (Felgner et al., 1987) have also been used. These techniques can increase transfection efficiencies (Chu et al., 1987; Barsoum, 1990) compared to calcium phosphate mediated DNA transfer, but the results are variable and depend on many parameters in each protocol (Chen and Okayama, 1987).

1.1.2 Expression of Heterologous cDNAs

To maximize expression, transfected cDNA are commonly placed in high expression cassettes with heterologous promoter sequences. Signals for termination and processing of the RNA transcripts are also included at the end of the coding sequence. With some exceptions, the rates of transcription in mammalian cells are generally controlled by three elements (Wasylyk, 1986): (1) The TATA box in the promoter, which contains a consensus sequence 5'-TATAAAT-3' upstream of the RNA transcription initiation (Gorden et al., 1980). (2) Further upstream of the coding region, several sequence elements have been identified, such as the CAAT box and a GC-rich region. These elements bind to transcriptional factors involved in the regulation of transcription (Benoist and Chambon, 1981; Dierks et al., 1983). (3) Finally, enhancer sequences, which may be distant upstream or downstream of the coding sequence, stimulate promoter expression (Khoury and Gruss, 1983; Boshart et al., 1985).

Constitutive viral promoters are the most widely used to express transfected genes. These promoters include Simian Virus 40 (SV40) early and late promoters, herpes simplex virus thymidine kinase promoter (SV-TK), Rous sarcoma promoter, and human cytomegalovirus (CMV) promoter (Boshart et al., 1985). To enhance expression rates, dual

or hybrid promoters have also been used, for example, the SV40 early promoter/ adenovirus major late promoter system was used for the production of Factor VIII (Wood et al., 1984).

In contrast to constitutive promoters, inducible promoters are mainly derived from cellular genes. Metallothionein promoters, which contain a consensus sequence for heavy metal induction, have been used in bovine papillomavirus (BPV)-based vectors for the transfection of mouse, rat and kidney cells (Mayo et al., 1982). Although these promoters can be induced by adding toxic heavy metals such as zinc or cadmium, the genes regulated by metallothionein promoters also have relatively high basal level of expression (0.2 $\mu g/10^6$ cells·day) (Gebert and Gray, 1994). Heat shock promoters derived from *Drosophila* cells are active in a wide variety of cells (Nover , 1987). These promoters have been used to express several genes including histone H3 (Morris et al., 1986) and *c-myc* (Wurm et al., 1986); however, the activation of heat shock promoters can disrupt normal cellular physiology and affect protein processing and secretion. Hormone inducible promoters, containing sequences responsive to glucocorticoid and other steroid hormones, have been used to express high levels of hormone receptors (Lee et al., 1981; Giguere et al., 1986). In the presence of virus infection and double-stranded RNA, a 200-fold induction of β-interferon promoter has been reported (Lengyel, 1982).

It is important not only to select a powerful promoter but also to match the promoter with the host cell line. For instance, the SV40 promoter is very active in the CHO cells and less active in mouse cells, whereas the metallothionein promoter is active in mouse but not in CHO cells (McIvor et al., 1985). These variations are likely due to variable affinities of transcriptional factors to different promoters.

1.1.3 mRNA Processing and Translation

The final steps of mRNA synthesis involve termination, cleavage of the 3' end and polyadenylation. Transcription from an upstream promoter sometimes can skip its termination site and occlude transcription from a downstream promoter (Cullen et al., 1984). In the case of histone H2-A or mouse β-globin genes, strong termination regions inserted into expression cassettes to prevent this read-through have resulted in a 7-fold increase in expression of a downstream gene (Proudfoot, 1986). Although most transfected cDNAs do not require the presence of introns and mRNA splicing, in a few exceptions, such as factor VIII cDNA, expression is maximized if introns are included (Kaufman et al., 1987). A sequence AAUAAA, 11-30 nucleotides upstream of the poly-A addition site, is essential for polyadenylation of mRNA, which increases mRNA stability (McLauchlan et al., 1985). Another repeated sequence AUUUA in the 3' regions of some cytokines and growth factor mRNAs de-stabilizes mRNA and its removal can increase levels of expression (Cosmon, 1987; Wilson and Treisman, 1988).

The formation of a ternary complex which contains eIF-2, GTP and Met-tRNA initiates mRNA translation (Pain, 1986). This complex binds the 40S rRNA subunit and starts the translation with the addition of a 60 S rRNA subunit (Hershey, 1991). The overall rate of translation is largely controlled by phosphorylation/ dephosphorylation of the initiation factors, mainly eIF-2 and eIF-4F (Hershey, 1989; Kaufman et al., 1989), regulated by proteins, such as protein kinase C.

1.1.4 Post-translational Modification and Secretion

Translocation of nascent secreted or membrane proteins into the lumen of the endoplasmic reticulum (ER) occurs simultaneously with translation of mRNA containing a hydrophobic signal sequence at or near the amino terminus. These sequences are recognized by the signal recognition particles (SRP), then the resulting complex interacts with a receptor (docking protein) on the rough ER and the nascent protein is translocated through the ER membrane (Garoff, 1985). The signal peptide is cleaved by the signal peptidase during translocation.

Most human proteins expressed in mammalian cells are also post-translationally processed (Darnell et al., 1990). Formation of disulfide bonds first occurs soon after protein translocation. This time-consuming process requires minutes to hours and is catalyzed by protein disulfide isomerase (PDI) (Bergman and Kuehl, 1979).

Glycosylation is the main modification of the foreign protein done in the mammalian cell secretory pathway. Asparagine-linked (N-linked) glycosylation occurs at Asn-X-Ser/Thr recognition sites as the protein enters the ER (Kornfield and Kornfield, 1985). After this high-mannose core oligosaccharide addition, some trimming of terminal glucose and mannose residues and fatty acid addition can occur in the ER. The proteins are then transported to the Golgi apparatus through transport vesicles. The N-linked carbohydrates are further modified by the additions of galactose and sialic acid. More post-translational modifications occur in the Golgi, such as sulfation of tyrosine and carbohydrate residues, protein phosphorylation, serine and threonine O-linked glycosylation, processing of propeptides, γ-carboxylation of glutamate residues and β-hydroxylation of aspartate

residues (Farquhar, 1986). Membrane-bound proteins and secreted proteins (Figure 1.1) are transported to the cell surface (Griffith and Simons, 1986), lysosomal enzymes to the lysosomes (Sly and Fisher, 1982), while regulated secretory proteins are stored in secretory granules to be released upon appropriate stimulus (Griffith and Simons, 1986), such as the secretion of insulin stimulated by D-glucose (Cerasi, 1975). The final destination as well as the post-translational modifications of proteins are mainly dependent on their primary structure (Griffith and Simons, 1986).

1.2 MODEL PRODUCTION SYSTEMS

Activated protein C (APC) and tissue-type plasminogen activator (t-PA) production by BHK cells and CHO cells, respectively, were analyzed in this work to investigate the limits to cell specific recombinant protein production rates. Despite their sharing of some sequence homology, the maximum production rate of recombinant APC was approximately 20-fold lower than that of recombinant t-PA, as shown in this work. Thus, these proteins provide model systems for investigating production limitations to two proteins with relatively limited (APC) or high (t-PA) production rates in the range generally observed for mammalian cells (0.003~22 $\mu g/10^6$cells·day, Sanders, 1990).

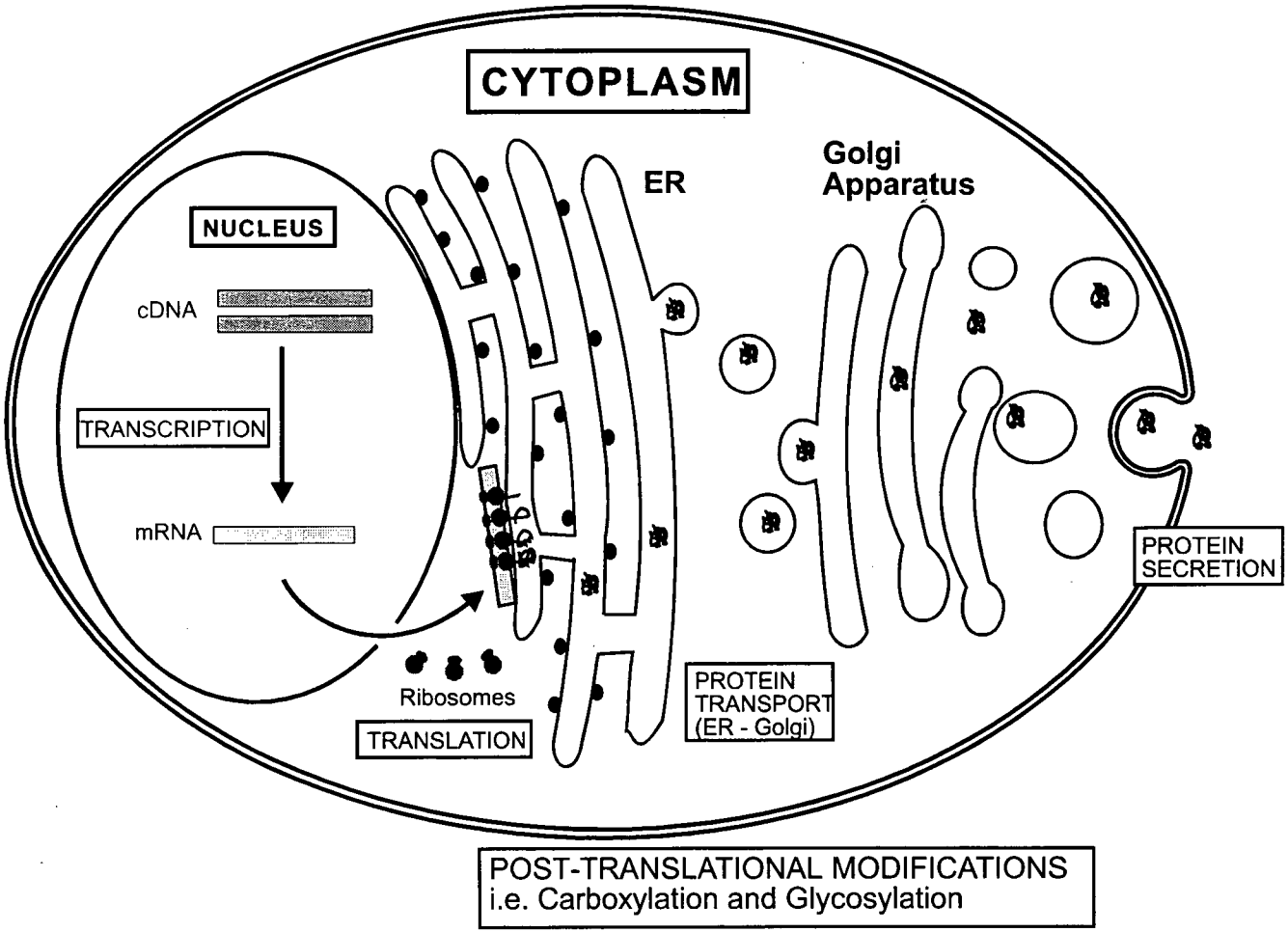

Figure 1.1 A schematic diagram of recombinant protein production pathway in mammalian cells.

1.2.1 Human Activated Protein C (APC)

Human protein C (Figure 1.2) is one of the vitamin K dependent proteins in the blood that plays a critical role in the regulation of blood coagulation (Figure 1.3). *In vivo,* the thrombin thrombomodulin complex activates the inactive protein C zymogen on the endothelial cell surface by cleavage of a 12-residue peptide (158-169), resulting in a two-chain activated protein C (APC) (Esmon, 1989). While binding with protein S, which may prompt the binding of APC to phospholipid membranes and abrogate the protection of factor Va by factor Xa (Walker, 1981; Solymoss et al., 1988), APC inactivates factors Va and VIIIa by limited proteolysis. With this anti-coagulant activity, APC is a potential therapeutic for the treatment of septic shock, stroke, disseminated intravascular coagulation, deep vein thrombosis, and to prevent reocclusion in patients treated with fibrinolytic agents (Esmon, 1987).

Human protein C has five types of post-translational modifications: (1) Disulfide formation at 28 cysteine residues. (2) γ-Carboxylation of the first nine glutamic acid residues by a vitamin K-dependent microsomal carboxylase to become γ-carboxyglutamic acids (Gla) (Suttie, 1985). γ-Carboxylation is essential to the anticoagulant function of APC (Zhang et al., 1992). (3) β-Hydroxylation of an aspartic acid residue (Asp 71) is believed to be involved in a Gla-region independent calcium-binding site, and is required for functional activity (Stenflo et al., 1989). (4) N-glycosylation at three of four available sites. Plasma human protein C has a molar mass of approximately 66 kDa and has been reported to be 23 % carbohydrate mass (Kisiel and Davie, 1981). (5) Proteolytic cleavage of an 18 amino acid signal peptide targeting the nascent polypeptide to the lumen of ER,

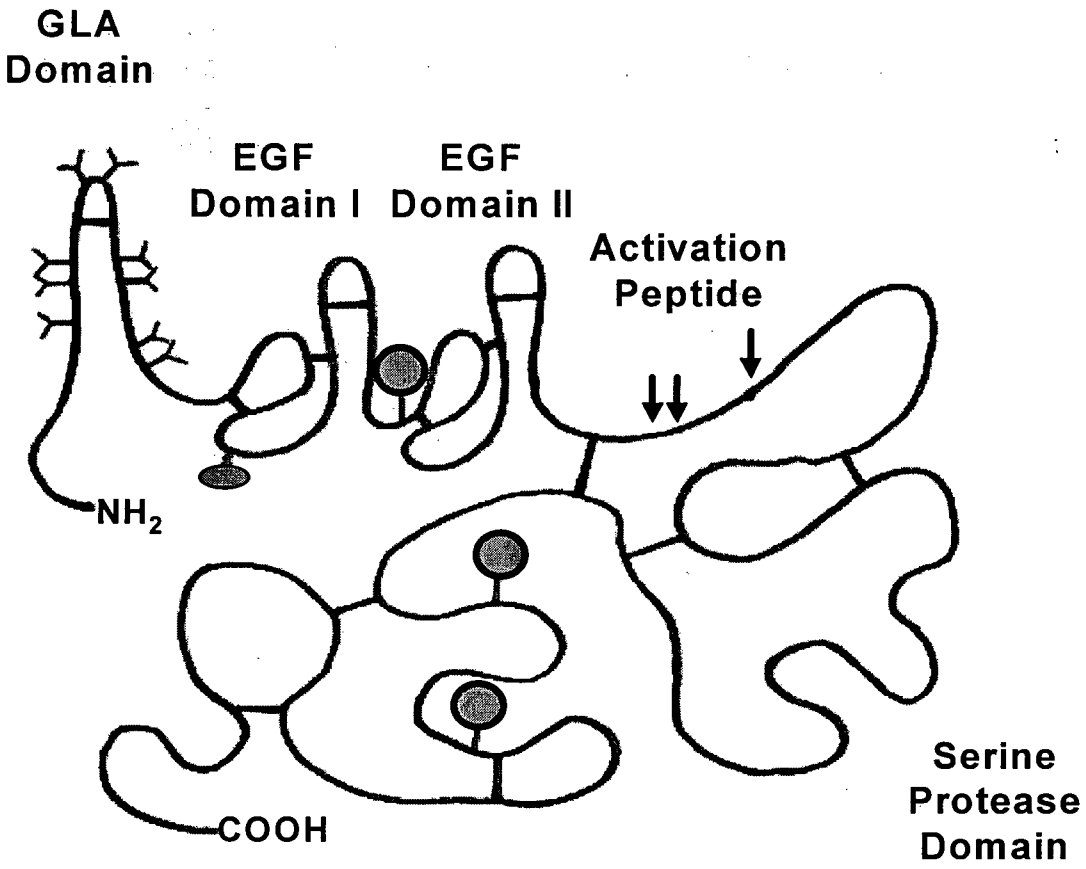

Figure 1.2 Schematic representation of protein C single chain precursor. The bars represent the proposed disulfide bonds. The gray circles represent N-glycosylated sites. The oval represents the β-hydroxy aspartic acid. The Y-shaped bars represent γ-carboxyglutamic acids in the GLA domain. The EGF domains are epidermal growth factor-like domains. The three known proteolytic cleavage sites resulting in two-chain, activated protein C are shown with arrows. (adapted from Grinnell et al., 1990)

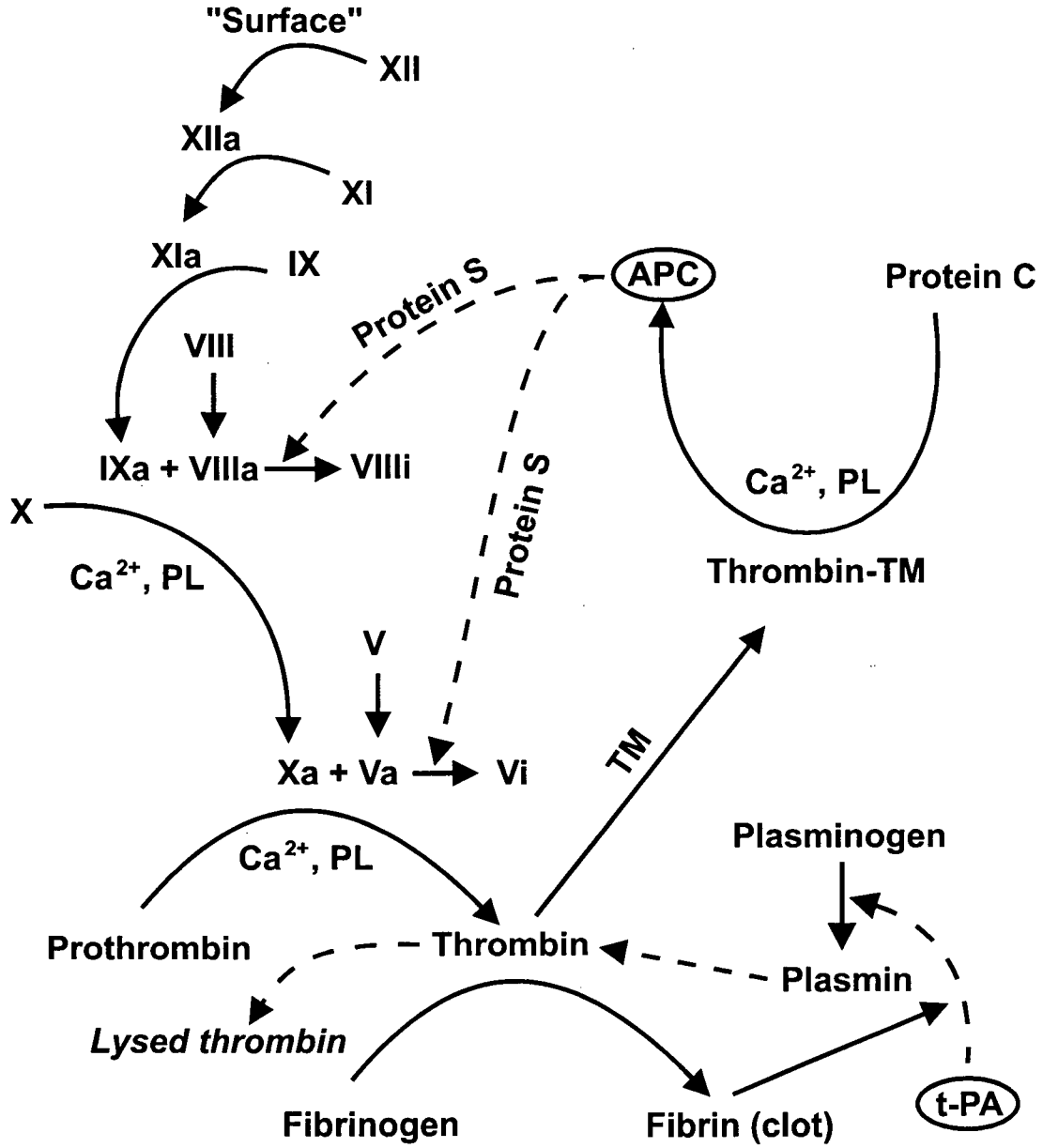

Figure 1.3 Intrinsic pathway for blood coagulation and the anti-coagulant roles of APC and t-PA. The extrinsic pathway (not shown) enters the above path at the point of factor X activation in the presence of tissue factor, Ca^{2+}, and phospholipid (PL), i.e., altered cell surface. Va, VIIIa, IXa, Xa, XIa, and XIIa are activated blood coagulation factors; Vi and VIIIi are inactivated factors; TM is thrombomodulin. The anti-coagulant and thrombolytic effects of APC and t-PA, respectively, are indicated by dashed lines.
(modified from Long, 1986)

and proteolytic cleavage of a 24 amino acid propeptide which is required for carboxylation (Foster et al., 1987; Suttie et al., 1987).

Protein C is synthesized in the liver, but in a hepatoma cell line, recombinant protein C was produced at very low levels and was not fully active (Suttie, 1986). However, attempts to express high levels of protein C in CHO cells or mouse fibroblast C127 cells resulted in partial carboxylation and low functional activity (Suttie, 1986). With a cell specific protein C production rates up to 15 $\mu g/10^6$cells·day in various CHO cell clones, a maximum of 56% γ-carboxylation ratio was observed (Sugiura, 1992). In addition, in CHO cells, only 10% of protein C was processed into the two-chain form, and 40% of the protein secreted by the CHO cells still had the propeptide attached. Two cell lines, human kidney 293 and baby hamster kidney (BHK) cells can produce protein C at high rates and with 80-100% specific activity (Table 1.1). Of 55 clones obtained from 293 cells after gene amplification, the cell specific protein C production rates varied from 0.02 up to 25 $\mu g/10^6$cells·day with an average of 3 $\mu g/10^6$cells·day cells (Walls et al., 1989).

In this work, a modified protein C cDNA was used to produce APC in BHK cells. The activation peptide sequence in the APC cDNA was deleted and the sequences for two arginine residues were inserted to improve intracellular proteolytic cleavage to the two-chain form of APC (Foster et al., 1990). To date, only the production rates of protein C but not APC have been reported in mammalian cells (Table 1.1).

Table 1.1 Summary of reported maximum cell specific protein C production rates by mammalian cells (modified from Grinnell et al., 1990)

Cell Type	Promoter	Cell Specific protein Production Rate ($\mu g/10^6 cells \cdot day$)	References
Human kidney 293	Ad2-ML	25	(Walls et al., 1989)
CHO	SV40	15.5	(Takeshita et al., 1988)
BHK-Ad	Ad2-ML	15	(Yan et al., 1990)
AV12-664	Ad2-ML	38*	(Grinnell et al., 1990)
SA7	Ad2-ML	0.19	(Grinnell et al., 1990)
SV20	Ad2-ML	0.15	(Grinnell et al., 1990)

* This highest protein C production rate was listed in a review article only; no research articles have been found confirming this high production rate.

1.2.2 Human Tissue-type Plasminogen Activator (t-PA)

Human tissue-type plasminogen activator (t-PA) (Figure 1.4) is a serine protease secreted by endothelial cells which converts plasminogen into plasmin by proteolytic cleavage (Collen and Lijnen, 1986). This results in the degradation of fibrin networks and the dissolution of blood clots (Rijken et al., 1982). Unlike enzymes with similar biological functions, such as streptokinase and urokinase, t-PA binds to fibrin-bound plasminogen and not circulating plasminogen (Thorsen et al., 1972; Rijken and Collen, 1981), which allows t-PA preferentially to activate the plasminogen entrapped in the clots. This specificity reduces the risk of hemorrhaging caused by circulating plasmin and makes t-PA a more effective thrombolytic therapeutic to treat heart attacks and strokes (Rouf et al., 1996).

Nascent t-PA contains a leader sequence consisting of a signal peptide and a pre-pro-leader sequence with unclear function (Pennica et al., 1983). Mature t-PA contains a fibronectin finger domain, an epidermal growth factor (EGF) domain, two kringle domains, and the catalytic serine domain (Figure 1.4). The finger domain and the kringle domains are associated with fibrin binding, and thus are important to clot-specific therapeutic function. Mature t-PA also contains 35 cysteine residues and 17 disulfide bonds. Either two or three glycosylation sites are occupied (type II or type I t-PA, respectively) at Asn-184 (not glycosylated in type II t-PA), 117 and 448 (Vehar et al., 1984; Parekh et al., 1989). The occupancy of N-glycosylation sites influences t-PA clearance rates *in vivo* (Spellman, 1990; Keyt et al., 1994). Recombinant t-PA expressed in CHO or human embryonic kidney cells, as well as melanoma-derived t-PA, contain an O-linked fucose residue in the EGF domain (Harris et al., 1991). The molecular weight of t-PA is approximately 66~68 kDa,

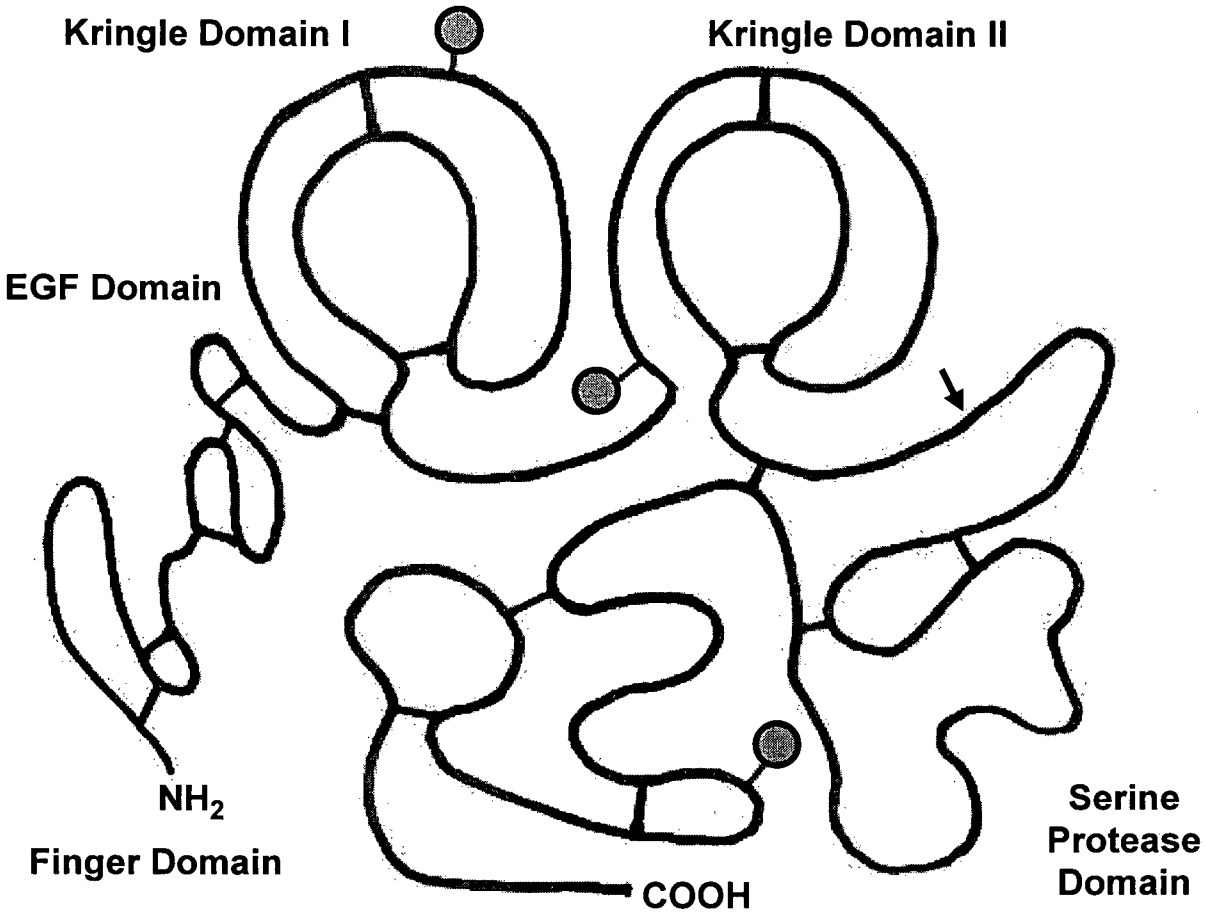

Figure 1.4 Schematic of single chain t-PA molecule. Amino acid are represented by one-letter codes. The bars represent the proposed disulfide bonds. EGF: epidermal growth factor like domain. The solid circles indicate potential glycosylation sites. The arrow indicates the potential cleavage site that generates the two-chain form from the one-chain form. (adapted from Pohl et al., 1984; Rouf et al., 1996)

with 7% (mass %) carbohydrate. Like many other serine proteases, t-PA is synthesized as a single polypeptide-chain form, but can be proteolytically cleaved by plasmin at a specific sensitive site (Arg275-Ile276) to become a two-chain protein (Rijken et al., 1982; Pohl et al., 1984). The two-chain form of t-PA remains catalytically active and exhibits biological properties that are very similar to those of the single-chain form (Cartwright, 1992).

Currently therapeutic t-PA is being produced by mammalian cells at the 10,000 L scale (Lubiniecki et al., 1989). A wide range of production rates have been reported for recombinant t-PA production in mammalian cells (Table 1.2), up to 50 $\mu g/10^6$cells·day under MTX selection (Goeddel et al., 1989). There have only been a few reports of higher rates than those for t-PA (Table 1.3).

Table 1.2 Summary of reported maximum t-PA production rates by various mammalian cell types

Cell Type	Promoter	Amplification Method	Cell Specific Protein Production Rates ($\mu g/10^6 cells \cdot day$)	References
Bowes melanoma	t-PA	None	0.3	(Brown et al., 1985)
Human Melanoma TRBM6	NA	NEO/G418	3.1	(Brown et al., 1985)
Rat myeloma	RSV	DHFR/MTX	4	(Kenten and Boss, 1985)
Chinese Hamster Ovary	Ad2	DHFR/MTX	10	(Kaufman et al., 1985)
Mouse C127	BPV	Spontaneous	20	(Reddy et al., 1987)
Chinese Hamster Ovary	SV40	DHFR/MTX	50	(Goeddel et al., 1989)
Baby Hamster Kidney/ Herpes virus VP16	HPV-IE	ADA/hygromycin B	20	(Hippenmeyer and Highkin, 1993)

NA - not available

Table 1.3 Examples of Recombinant Proteins Produced by Mammalian Cells at High rates

Recombinant Protein	Host Cell	Promoter	Amplification Method	Production Rates ($\mu g/10^6 cells \cdot day$)	References
Hepatitis B surface antigen	CHO	SV40	DHFR/MTX	15	(Michel et al., 1985)
Antithrombin III	CHO	MMTV-LTR	DHFR/MTX	22	(Zettlmeissl et al., 1987)
Protein C	293	Ad	DHFR/MTX	25	(Walls et al., 1989)
Tissue plasminogen activator	CHO	SV40	DHFR/MTX	50	(Goeddel et al., 1989)
Tissue inhibitor of metalloproteinases	CHO	CMV	GS/MSX	110	(Cockett et al., 1990)
Human monoclonal antibody	CHO	β-actin	DHFR/MTX	100	(Page and Sydenham, 1991)
Human monoclonal antibody	CHO	Ad-ML/ SV40 enhancer	ADA/dCF	110	(Fouser et al., 1992)
Intercellular adhesion molecule-1	BHK/VP16	BPV	ADA/hygromycin B	100	(Warren et al., 1994)
Granulocyte-colony stimulating factor (G-CSF)	CHO	CMV-MIE	DHFR/MTX	90	(Rotondaro et al., 1997)

VP16: herpesvirus VP16 transactivator; SV40: Simian Virus 40; MMTV-LTR: Mouse mammary tumor virus long terminal repeat; Ad: Adenovirus; CMV: Cytomegalovirus; Ad-ML: Adenovirus major late; BPV: Bovine papillomavirus; CMV-MIE: CMV- major immediate-early; DHFR: dihydrofolate reductase; MTX: methotrexate; GS: Glutamine synthetase; MSX: Methionine sulphoximine; ADA: Adenosine deaminase; dCF: 2'-Deocycoformycin.

1.3 GENE AMPLIFICATION

The most common strategy to increase recombinant protein production rate is by performing amplification of the integrated cDNA copies in the host cell genome. This is achieved by constructing a vector which carries both the cDNA for the desired recombinant protein and a gene for a selectable marker. Under selection pressure, both cDNA copy numbers can be increased by co-amplification, increasing mRNA levels and the corresponding protein synthesis. Gene amplification has been used successfully to express a large number of recombinant proteins with high production rate, particularly in CHO cells (Table 1.3). The cell specific production rate of co-transfected recombinant proteins can also decrease at high selective pressure (Kaufman et al., 1985; Pendse et al., 1992). Moreover, the protein production rate obtained in the presence of selective pressure is generally not stable, and the amplification protocols for maximizing stable production rate have been very cell culture labor-intensive.

1.3.1 Amplifiable Markers and Amplification

More than 17 pairs of amplifiable markers/selectable agents are now available to genetic engineers for mammalian cell expression (Kellems, 1991), including dihydrofolate reductase (DHFR)/MTX, thymidylate synthetase/5-fluorodeoxyuridine, and adenosine deaminase (ADA)/2'-deocycoformycin. Most of the amplifiable markers are key enzymes in DNA precursor biosynthesis (Figure 1.5). DHFR is the original and most widely employed marker and has the advantage that its drug for selection (MTX) is relatively

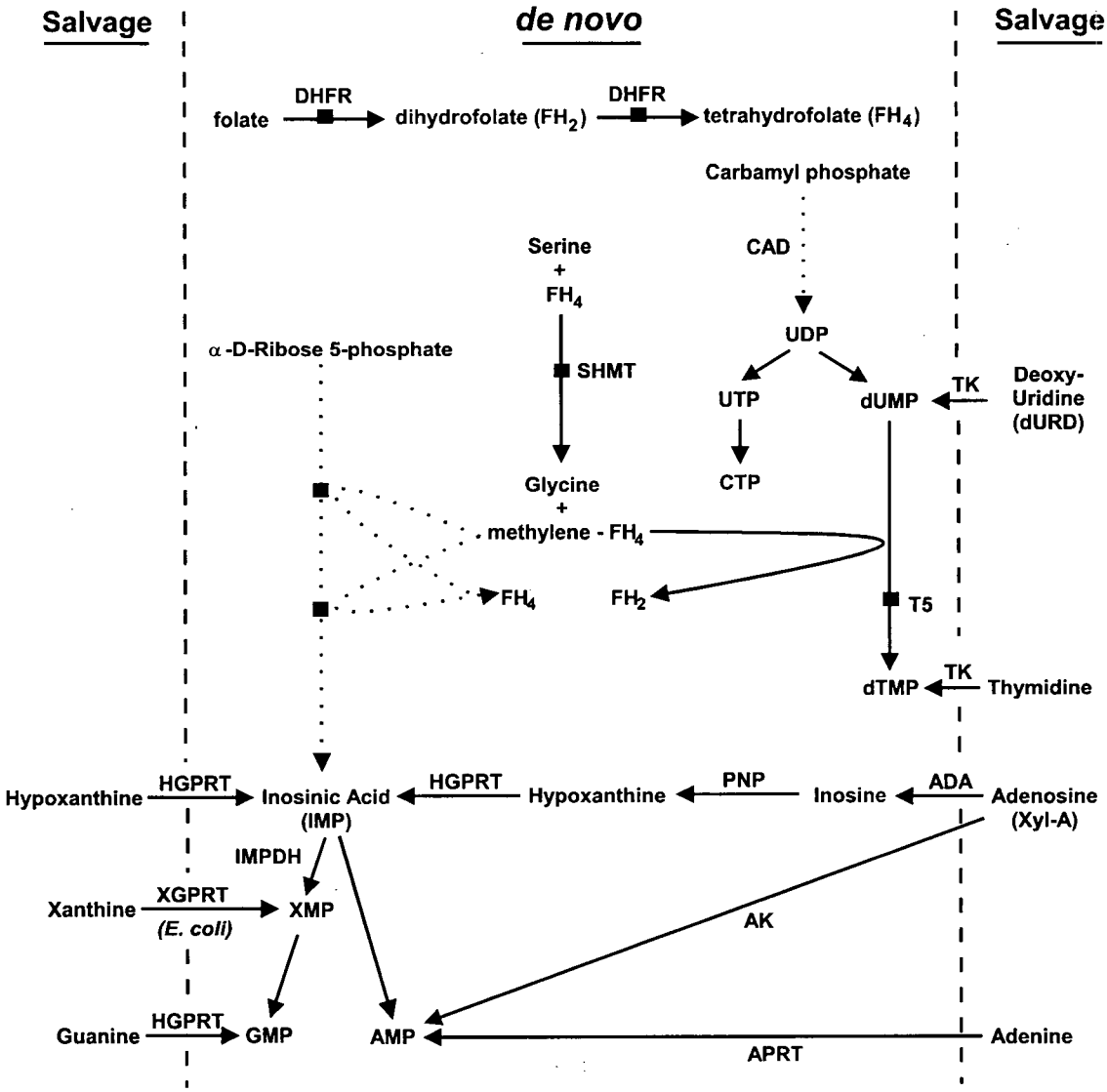

Figure 1.5 De *novo* and salvage biosynthesis pathways for purines and pyrimidines involving available selectable markers. Abbreviations for *de novo* enzymes: DHFR, dihydrofolate reductase; CAD, carbamyl-P synthesis, asparate transcarbamylase, and dihydroorotase; SHMT, serine hydroxymethyltransferase; TS, thymidylate synthetase; and IMPDH, inosine monophosphate dehydrogenase. Abbreviations for salvage enzymes: TK, thymidine kinase; ADA, adenosine kinase; PNP, purine nucleotide phosphorylase; AK, adenosine kinase; APRT, adenine phosphoribosyltransferase; and XGPRT, *E. coli* xanthine-guanine phosphoribosyltransferase. Solid arrows indicate single reactions. Dashed arrows indicate multiple reactions. The solid squares indicate reactions that are inhibited by the folate analog methotrexate and aminopterin. (Modified from Kaufman, 1990)

inexpensive and stable. DHFR catalyzes the conversion of folate to tetrahydrofolate and is required for the biosynthesis of (1) glycine from serine, (2) thymidine monophosphate from deoxyuridine monophosphate and (3) providing the precursors for purine nucleotides (Figure 1.5). DHFR containing vectors have mostly been used in DHFR minus cell lines, such as CHO K1, and selected in glycine/hypoxanthine/thymidine (GHT)-minus medium (Urlaub and Chasin, 1980) (Figure 1.6A). They can also be used in cell lines containing a functional endogenous DHFR gene if a mutant DHFR gene is used (Palmiter et al., 1987), that provides the ability to grow in previously lethal concentrations of MTX. Using stepwise increasing selection with MTX (Figure 1.6B), cell lines have been developed with high copy number of the transfected plasmid and high recombinant protein production rate (e.g. Kaufman et al., 1985; Wurm et al., 1986; Pallavicini et al., 1990; Page and Sydenham, 1991; Fouser et al., 1992).

In most reports, cloning at each selection level was employed to obtain high producing clones for subsequent amplification at higher MTX levels (Kaufman et al., 1985; Zettlmeissl et al., 1987). Although this multiple cloning and amplification strategy can provide high producing clones, the practice is very tedious and labor-intensive, often requiring culture and analysis of over one hundred subclones. For instance, Michel et al. (1985) amplified five HbsAg producing clones after transfection at 0.05, 0.1 and 0.15 μM MTX. Following subcloning, three high producing amplified clones were selected for further amplification at 5, 10 and 25 μM MTX. A total of 150 clones were individually analyzed during this procedure, and a clone with the highest cell specific production rate approximately 15 $\mu g/10^6 cell \cdot day$ was obtained after subcloning from 10 μM MTX selected cells.

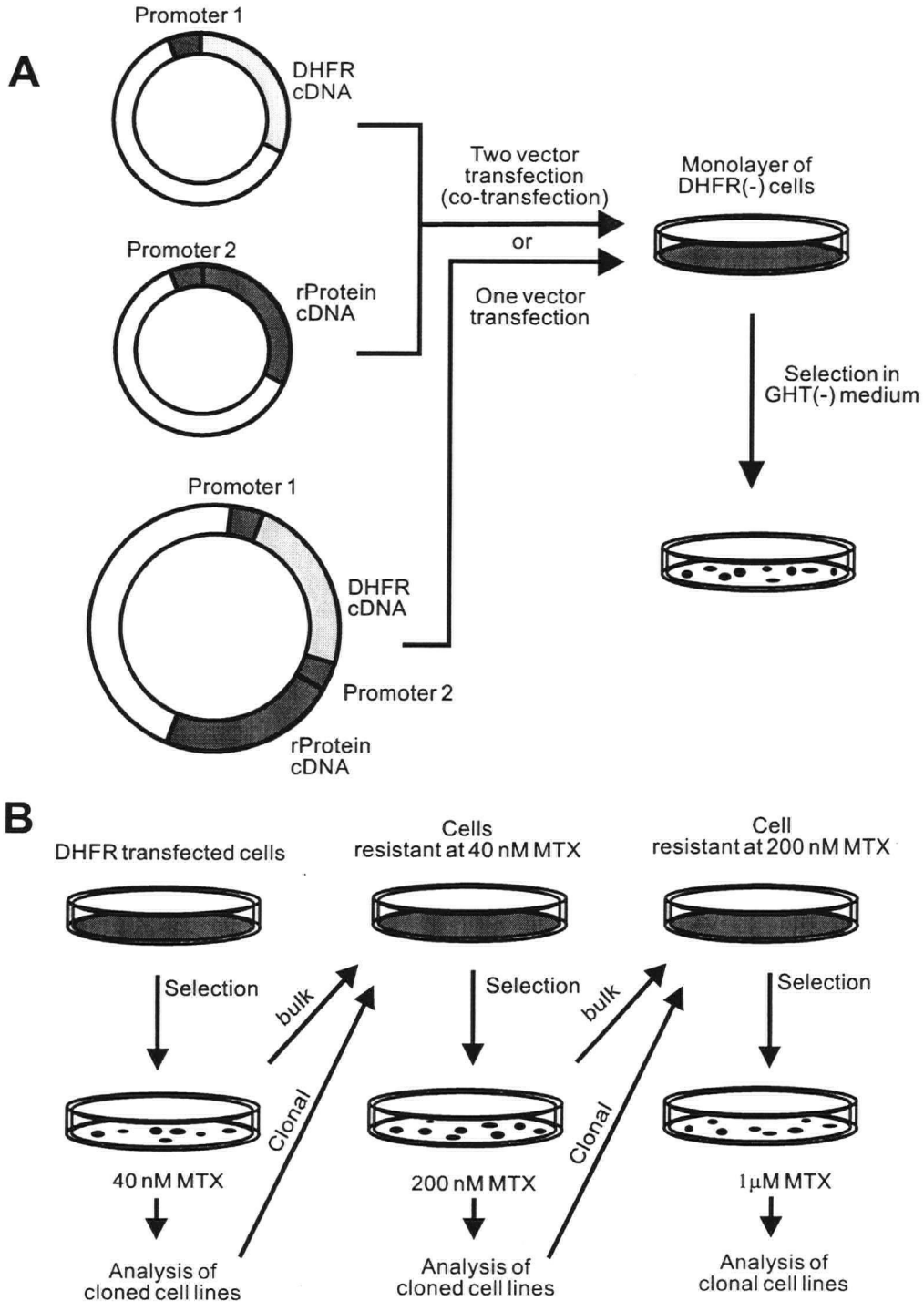

Figure 1.6 (A) Transfection and co-transfection of DHFR containing expression vectors into CHO cells deficient in endogenous DHFR activity. Selection of recombinant clones in GHT minus medium lacking glycine, hypoxanthine and thymidine. (B) Example of incremental increases in methotrexate (MTX) concentration and selection of subpopulations of cell clones resistant to high levels of methotrexate. Both bulk and clonal amplifications are shown.

Interestingly, most of the results showed that highest selective pressure did not necessarily maximize the protein production rate, implying that a maximum production rate limitation exists that blocks higher recombinant protein production rates despite cDNA amplification. To date, the achievable maximum recombinant protein production rate by mammalian cells has been limited to approximately 100 $\mu g/10^6$cells·day (Table 1.3).

1.3.2 Mechanisms of Gene Amplification

Linearization of plasmid DNA has been found to be a prerequisite for integration of the plasmid DNA into host cell chromosomes (Finn et al., 1989). Specific restriction enzyme digestion has been performed prior to transfection to open the circular plasmid molecule and increase the rate of homologous integration (Jasin and Berg, 1988; Zheng and Wilson, 1990). Amplified DHFR genes have often been reported to localize in expanded chromosomal regions termed homogeneously staining regions (HSRs) (Nunberg et al., 1978). The HSRs which contain amplified DHFR genes are elongated. Judging from the size of DHFR gene and the size of HSRs, it is suggested that individual repeating units (amplicons) were several hundred kb long (Dolnick et al., 1979; Milbrant et al., 1981), including chromosomal sequences in addition to the plasmid. Looney et al. (1988) analyzed five independently isolated MTX-resistant CHO cell clones, and concluded that the DHFR amplicons in most of the CHO cells shared a 273 kb core sequence; moreover, these amplicons were in end-to-end arrays. The mechanism of forming these amplicon arrays was proposed by Kaufman and Sharp (1982) and confirmed by Ma et al. (1993). When CHO cells were exposed to MTX, the initial event of amplification was found to be

a duplication of the endogenous DHFR gene locus by two versions of sister chromatid fusions, and resulting in dicentric chromosomes which contained two centromeres and a duplication of the DHFR locus. After mitotic separation of the two centromeres, another round of chromatid fusion and, possibly, further duplication events could occur. This bridge-breakage-fusion mechanism was accompanied by the loss of telomeres, which in turn decreased the stability of chromosomes (Cowell and Miller, 1983). Repeated cycles would generate chromosomal translocation, inverted duplication and eventually, gene amplification (Robins et al., 1981a; Ruiz and Wahl, 1988).

Other than the intrachromosomal amplification mechanism, the submicroscopic extrachromosomal elements named "amplisomes" or "episomes" were also reported to be part of the amplification mechanism (Maurer et al., 1987). These amplisomes are mostly homogenous in size, and contain multiple copies of DHFR replication units. Amplisomes appeared during the stepwise selection in MTX, and had gene loss kinetics similar to chromosomal DHFR genes for gene loss upon removal of the selective pressure in HeLa cells (Pauletti et al., 1990). Based on the observation of a mammalian replication origin in the amplisomes, Carroll et al. (1987) and Windle et al. (1991) suggested that host sequences might be involved in the facilitation and/or generation of excisional amplisome formation following plasmid integration.

1.3.3 Production Stability of Amplified Clones

It is important to obtain relatively stable cell lines for recombinant protein production to maintain high product concentrations, to ensure product consistency, and to

satisfy regulatory requirements. This stability has to be maintained in the long-term as well as in each production batch (Wiebe and Builder, 1994). Although high protein cell specific production rates up to 110 $\mu g/10^6$cells·day has been achieved using gene amplification (Table 1.1), these high production rates are generally temporary and only existed with the selective pressure. The maximum reported stable recombinant protein production rate without selective pressure was only 20 $\mu g/10^6$cells·day for antithrombin III (up to 30 days, Zettlmeissl et al., 1987).

In the absence of selective pressure, instability of recombinant expression has been reported for DHFR (Kaufman et al., 1981; Sinacore et al., 1995), t-PA (Kaufman et al., 1985; Weidle et al., 1988), *c-myc* (Pallavicini et al., 1990), γ-interferon (Cossons et al., 1991) and chimeric antibody (Kim et al., 1998a). There have been relatively fewer published reports of stable expression. Dyring and Mellstrom (1997) reported 130 days of stable human insulin-like growth factor binding protein-1 production. Extended culture for at least 50 cell doublings in the presence of MTX has been reported to improve the stability of amplified CHO cells after the MTX was removed (Kaufman et al., 1981). However, it is controversial whether the continued presence of a selective agent (i.e. MTX) in long-term cultures of recombinant CHO cells ensures production stability. Whereas MTX has been reported to maintain stable t-PA production by CHO cells (Weidle et al., 1988), others have reported that protein production instability could still occur in the presence of MTX (Cossons et al., 1991; Morrison et al., 1997; Kim et al., 1998b). Furthermore, using fluorescence *in situ* hybridization (FISH), Pallavicini et al. (1990) demonstrated that the presence of MTX in the culture medium resulted in the

generation of mostly unstable chromosomal rearrangements that were lost in the absence of MTX.

The loss of DHFR expression in the absence of MTX can be due to unstable localization in double minute chromosomes (DMs) (Kaufman et al., 1979; Brown et al., 1981). DMs are small-paired chromosomal elements that lack centromeric function and thus segregate randomly at mitosis; hence, they can be rapidly lost upon propagation in the absence of selective pressure. However, these extrachromosomal DMs could also integrate into the chromosome to become stably amplified genes (Murray et al., 1983). In the absence of MTX selection, Weidle et al. (1988) observed both a reduction in copy number and a gradual decline of t-PA production rate for 40 to 60 days after adapting the cells in MTX-free medium. In this case, loss of DMs was not responsible for t-PA production rate loss, since all t-PA cDNAs were localized in HSRs (Weidle et al., 1988; Koehler et al., 1995). Interestingly, the t-PA production rate stabilized at lower production levels after 40 days without MTX selective pressure. This instability in HSRs may be explained by the mechanism proposed by Wurm et al. (1997). Based on their cytogenetic analyses of stable or unstable recombinant protein producing cells (Wurm et al., 1986; Pallavicini et al., 1990; Wurm et al., 1992), they proposed that there were three "master integration" patterns that were associated with high degree of genetic stability in the absence of methotrexate. These three master integration sites for stable FISH signals of heterologous genes were: (1) the short arm of one midsize submetacentric chromosome (probably chromosomes 3, 4, or X), (2) the telomeric end of a small acrocentric chromosome (either chromosomes 5, 6, or 7), or (3) the center of the long arm in chromosome 2. When MTX-resistant cells were adapted in MTX-free medium, the

frequency of the variant or multiple integrations declined, whereas the frequency of master integration increased from 50% to 96% of the cells analyzed after 40 days. This master integration mechanism seems to provide a reasonable explanation for the t-PA instability in the amplified HSRs, followed by stabilization after 40 days without MTX as reported by Weidle et al. (1988).

1.4 INTRACELLULAR LIMITATIONS TO MAMMALIAN PROTEIN PRODUCTION

The level of protein expression from heterologous genes introduced into mammalian cells can depend on multiple factors including copy number, promoter strength, mRNA stability and protein secretory pathway capacity. The limitations to hybridoma monoclonal antibody production have been more thoroughly investigated than mammalian cell recombinant protein production. The literature has been quite confusing, in part due to the fact that proteins were expressed in different host systems.

1.4.1 Limitations to Hybridoma Monoclonal Antibody Production

The intracellular parameters that limit monoclonal antibody production rate have been studied over a range of batch culture conditions (Dalili and Ollis, 1990; Bibila and Flickinger, 1991; Leno et al., 1991; 1992). Total RNA content (Dalili and Ollis, 1990) and specific monoclonal antibody mRNA levels (Bibila and Flickinger, 1991) were

roughly constant in the exponential phase and then decreased when the hybridoma cells passed from exponential growth into the stationary phase. A correlation was also observed between the total cellular RNA content and the antibody secretion rate (Dalili and Ollis, 1990). Leno et al. (1992) reported a correlation between the relative levels of heavy and light chain mRNA and the total intracellular monoclonal antibody. However, they reported a lack of correlation between intracellular antibody levels and the cell specific monoclonal antibody production rates, suggesting that the secretion process might be rate-limiting for antibody production. A similar post-transcriptional limiting step was proposed by Flickinger et al. (1992). Compared to most recombinant proteins, analysis of the hybridoma system is complicated by the potentially confounding influences of both heavy and light chain mRNA on monoclonal antibody production rates. In addition, multiple hybridomas expressing the same monoclonal antibody at different rates have not been investigated.

1.4.2 Recombinant Protein: cDNA Copy Number and mRNA Level

Gene amplification is commonly used to increase recombinant protein expression. However, correlation between gene dosage and recombinant protein production has not been consistently reported in the literature (Table 1.4). For instance, Kaufman et al. (1985) increased the number of t-PA cDNA copies by MTX selection, which in turn was paralleled by increased mRNA levels and corresponding higher t-PA production. A similar correlation was observed by Hendricks et al. (1989) for t-PA expression by recombinant myeloma cells. On the contrary, Jalanko et al. (1990) using an Epstein-Barr

Table 1.4 Reported Limiting Factors to the Rates of Recombinant Protein Production by Mammalian Cells

Recombinant Protein	Host Cell	Number of samples	cDNA vs. q_p	mRNA vs. q_p	cDNA vs. mRNA	mRNA vs. P_i	P_i vs. q_p	(q_p) Specific production rate range (μg/10^6cell·day)	Reference
HbsAg	CHO	5	–	+	–	NA	NA	0.1~1	Michel et al., 1985
t-PA	CHO	3	+	+	+	+	+	0.6~10	Kaufman et al., 1985
EPO	CHO	1	NA	+	NA	+	+	NA	Dorner et al., 1989
FVIII	CHO	3	NA	–	NA	+	–	<1.4	Kaufman et al., 1989
vWF	CHO	3	NA	+	NA	+	+	0.1~24	Kaufman et al., 1989
t-PA	Myeloma	14	+	+	+	NA	NA	0.8~8	Hendricks et al., 1989
Protein C	293	15	NA	NA	+	NA	NA	0.02~25	Walls et al., 1989
t-PA	Various	13	–	NA	NA	NA	NA	0.1~11	Jalanko et al., 1990
HbsAg	CHO	3	+	+	+	+	+, –	0.2~11	Pendse et al., 1992
t-PA	BHK	7	–	+	–	NA	NA	1~20	Hippenmyer and Highkin, 1993
hIGFBP-1	CHO	3	+	NA	NA	NA	NA	0.1~6	Dyring and Mellstrom, 1997
hATIII	CHO	4	NA	NA	NA	NA	+, –	0.4~7	Schroder and Friedl, 1997
TNFrFc	CHO	6	NA	+, –	NA	NA	NA	NA	Morris et al., 1997

NA: not available. P_i: intracellular protein concentration. +: positive correlation, with correlation coefficient larger than 0.85 (where available). –: poor correlation, with correlation coefficient lower than 0.6 (where available). +, –: positive correlation below saturation level, then poor correlation at saturation levels.

virus-based vector for t-PA production in CHO, HeLa, leukemia and 293 cells, observed no correlation between copy numbers up to 100 and up to 0.1~11 $\mu g/10^6$cells·day t-PA expression. Hippenmeyer and Highkin (1993) also reported no correlation between t-PA cDNA copy numbers and the level of t-PA expression in BHK cells, whereas mRNA levels were positively correlated with t-PA expression.

For human insulin-like growth factor binding protein-1 (hIGFBP-1) in CHO cells (Dyring and Mellstrom, 1997), a positive correlation between cDNA copy number up to 100 and protein production rate has been reported. A linear correlation between cDNA copy number up to 40 and mRNA levels was also reported for human protein C production by 16 clones of 293 cells (Walls et al., 1989); however, they did not report if protein C production rate correlated with mRNA level. Morris et al. (1997) observed increased mRNA levels of recombinant tumor necrosis factor receptor (TNFrFc) with increasing MTX concentration and protein expression levels up to 150 nM MTX, but from 150 to 500 nM MTX, there was no increase in protein expression but only an increase in mRNA levels. Overall, there are more reports of recombinant protein production rate correlation with mRNA than with cDNA levels (Table 1.4). This is likely due to different transcription rates at different sites in chromosomes.

1.4.3 Recombinant Protein: Secretory Pathway Limitations

The rate-limiting step between translation and protein secretion is generally in transit from the endoplasmic reticulum (ER) to the Golgi apparatus (Lodish et al., 1983; Shuster, 1991). Unfolded, misfolded or partly folded and assembled proteins are selectively

retained in the ER, or retrieved to the ER from the cis-Golgi (Hurtley and Helenius, 1989; Doms et al., 1993). At high recombinant expression rates, protein processing in the ER can become saturated and limit further increases to the specific protein production rate. However, exit from the ER does not necessary limit the cell specific rates (i.e. $\mu g/10^6 cells \cdot day$) of recombinant protein production (e.g. mRNA can be the limiting factors, section 1.4.1). In most reported cases (Table 1.4), mRNA, intracellular protein levels and secretion rates are positively correlated (see next section for discussion of exceptions).

Accumulation in the secretory pathway is protein dependent. For instance, wild-type t-PA is efficiently secreted, whereas aglycosylated (not glycosylated) t-PA is blocked in the ER (Dorner et al., 1988), due to stable association with GRP78, a 78kDa glucose responsive chaperone protein that binds to misfolded or incorrectly post-translational modifed nascent proteins to prevent their secretion. Reduction of GRP78 levels by introducing an antisense expression vector resulted in a 10-fold decrease in GRP78 expression and a parallel increase in aglycosylated t-PA secretion (Dorner et al., 1988). Overexpression of GRP78 reduced the rates of some recombinant protein secretion (e.g. factor VIII and von Willebrand factor, vWF), which were shown to be at least transiently associated with GRP78. However, overexpression of GRP78 did not decrease production rates of macrophage-colony stimulating factor, which does not associate with GRP78 (Dorner et al., 1992). Increased expression of factor VIII using sodium butyrate led to increased accumulation in the ER and caused the enlargement of rough ER cisternae (Dorner et al.,1989).

Another important ER resident protein that can limit recombinant protein secretion rates is protein disulfide isomerase (PDI), which catalyzes disulfide bond formation and exchanges (Lyles and Gilbert, 1991). Overexpression of recombinant proteins such as erythropoietin (EPO) or human granulocyte colony stimulating factor (G-CSF) have been shown to decrease PDI levels in yeast, and overexpression of PDI increased the secretion rates of platelet derived growth factor 10-fold (Robinson et al., 1994; Robinson and Wittrup, 1995). These results indicate that the limitation in these secretory pathways were due to inefficient protein folding that was overcome by increasing PDI levels. However, no apparent antibody secretion increase was observed in NSO-based recombinant transfectomas with increased PDI levels (Greenall et al., 1995).

1.4.4 Quantitative Investigations of Recombinant Protein Production Limitations

Most of the articles introduced in the previous two sections only provided qualitative observations instead of systematic quantification of the production rate limitations. Some only provide partial quantitative results (Walls et al., 1989; Jalanko et al., 1990), or investigate only in a low production rate range (Michel et al., 1985). To date, only a few reports have focused on quantitatively determining the intracellular factors that limit maximum recombinant protein production in mammalian cells (Table 1.4). Pendse et al. (1992) observed that HbsAg mRNA levels and production rates increased when cDNA copy numbers were increased in late-log phase cells. At the maximum production rate, there were increases in intracellular protein degradation rates and it was concluded that the cellular secretory pathway capacity was limiting at higher HbsAg production rates.

However, this conclusion failed to explain the linear relationship between mRNA and HbsAg production rate in the same report. Schroder and Friedl (1997) reported a decrease in the secretion efficiency (defined as the protein production rate per intracellular concentration) of human antithrombin III (hATIII) with increasing intracellular hATIII levels (in confluent CHO cells). This result also suggested a saturation in the secretory pathway at the highest levels of hATIII.

For both HbsAg and ATIII, only three or four CHO cell populations were studied. Pendse et al. (1992) investigated three MTX-amplified cell populations with HbsAg productivities from 0.2 to 11$\mu g/10^6$cells·day. Schroder and Friedl (1997) reported results from four CHO cell populations with ATIII production rates from 0 to 7 $\mu g/10^6$cells·day. Due to the limited sample numbers and production rate ranges, the data in both reports did not strongly support their conclusions. For example, the secretory pathway saturation at 7 $\mu g/10^6$cells·day described by Schroder and Friedl (1997) conflicted with the previous report by Zettlmeissl et al. (1987) of a 22 $\mu g/10^6$cells·day maximum ATIII production rate in CHO cells. Furthermore, these experiments were conducted with confluent growth phase cells, and it was not reported whether the limitations varied in different phases of batch culture. Another concern is that most of the studies listed in Table 1.4 were performed in the presence of MTX. The HbsAg degradation and ATIII secretory pathway saturation at high expression rates reported by Pendse et al. (1992) and Schroder and Friedl (1997), respectively, were correlated with higher MTX concentrations. As a strong inhibitor of purine biosynthesis (McBurney and Whitemore, 1975), MTX toxicity might have had direct effects on cell physiology and secretion efficiency. Therefore, to study

production limitations, it is preferable to avoid any possible negative influence of MTX and use MTX-free medium adapted cells.

1.5 THESIS OBJECTIVES

To optimize recombinant protein production by mammalian cells, it is critical to develop efficient strategies to maximize stable expression rates, because gene amplification, transcription promoter optimization, and manipulation of processing enzymes in the secretory pathway are labor-intensive and result in significant delays. An incorrect choice could easily lead to futile results and unnecessary costs. Identification of the intracellular limiting factors which determine recombinant production rates can provide guidance to efficient mammalian cell process optimization. For in stance, if mRNA levels are limiting then further amplification or promoter improvement would be advised. On the other hand, if the secretory pathway is saturated, increased levels of processing proteins may yield increased expression.

In this work, we investigated the production of APC and t-PA by mammalian cells as the model systems. Relative to other proteins (Table 1.4), t-PA can be produced at high rates, while APC is limited to much lower levels of production (i.e. ~1 $\mu g/10^6$cells·day) clones. The intracellular kinetic parameters of both these recombinant proteins were also systematically calculated based on a structured model. Upon understanding the roles of essential intracellular factors in recombinant protein expression, it is conceivable that these parameters may help to simplify the searching procedure for the limiting factors.

Furthermore, the amplification and stability of t-PA production by CHO cells were also analyzed, with the aim of developing a strategy to shorten the time and efforts required to achieve high and stable producing clones, and understand the possible limitations in cDNA amplification procedure for obtaining maximum t-PA production rates.

In Chapter 2, the materials and methods are described. In Chapter 3, a kinetic model is developed to help identify the limiting factors as well as quantitate intracellular kinetic parameters. Chapter 4 describes the limitations to APC production in BHK cells, and the relationship between intracellular factors, such as gene dosage, intracellular rates, and protein production rate. Amplification and stability of t-PA production rate is considered in Chapter 5. Chapter 6 focuses on the limitations in t-PA production by CHO cells. The intracellular parameters were analyzed as well. Chapters 7 and 8 provide conclusions and suggestions for future work, respectively.

CHAPTER 2

MATERIALS AND METHODS

2.1 CELL CULTURE AND GENETIC ENGINEERING

2.1.1 APC Transfection Vectors

Two vectors were employed for mammalian cell APC expression. The vector pNUT-1058 contains a 1722 bp insert for APC and a mutant dihydrofolate reductase (DHFR) cDNA (Figure 2.1A). The vector was constructed by ligation of APC cDNA into *Sma*I-cut pNUT. The pNUT vector contains a mouse metallothionein-1 promoter to induce cDNA transfection, pUC 18 sequences to allow replication and selection in *E. coli*, and a mutant DHFR cDNA driven by the SV40 early promoter to allow selection in culture. The DHFR cDNA sequence encodes a mutant form of the enzyme which has a 270-fold lower affinity for the competitive inhibitor MTX. Thus, high concentrations of MTX are required for the selection of transfected cells (approximately 0.5 mM MTX). The activation peptide sequence in the APC cDNA was deleted to produce the activated form of protein C (APC) and the sequences for two arginine residues were inserted to improve intracellular proteolytic cleavage to the two-chain form of protein C (Foster et al., 1987). The insertion and orientation of the APC cDNA into pNUT were verified by restriction enzyme digestion and by DNA sequence analysis using the Sequenase Kit (United States Biochemical Corporation, Cleveland, OH).

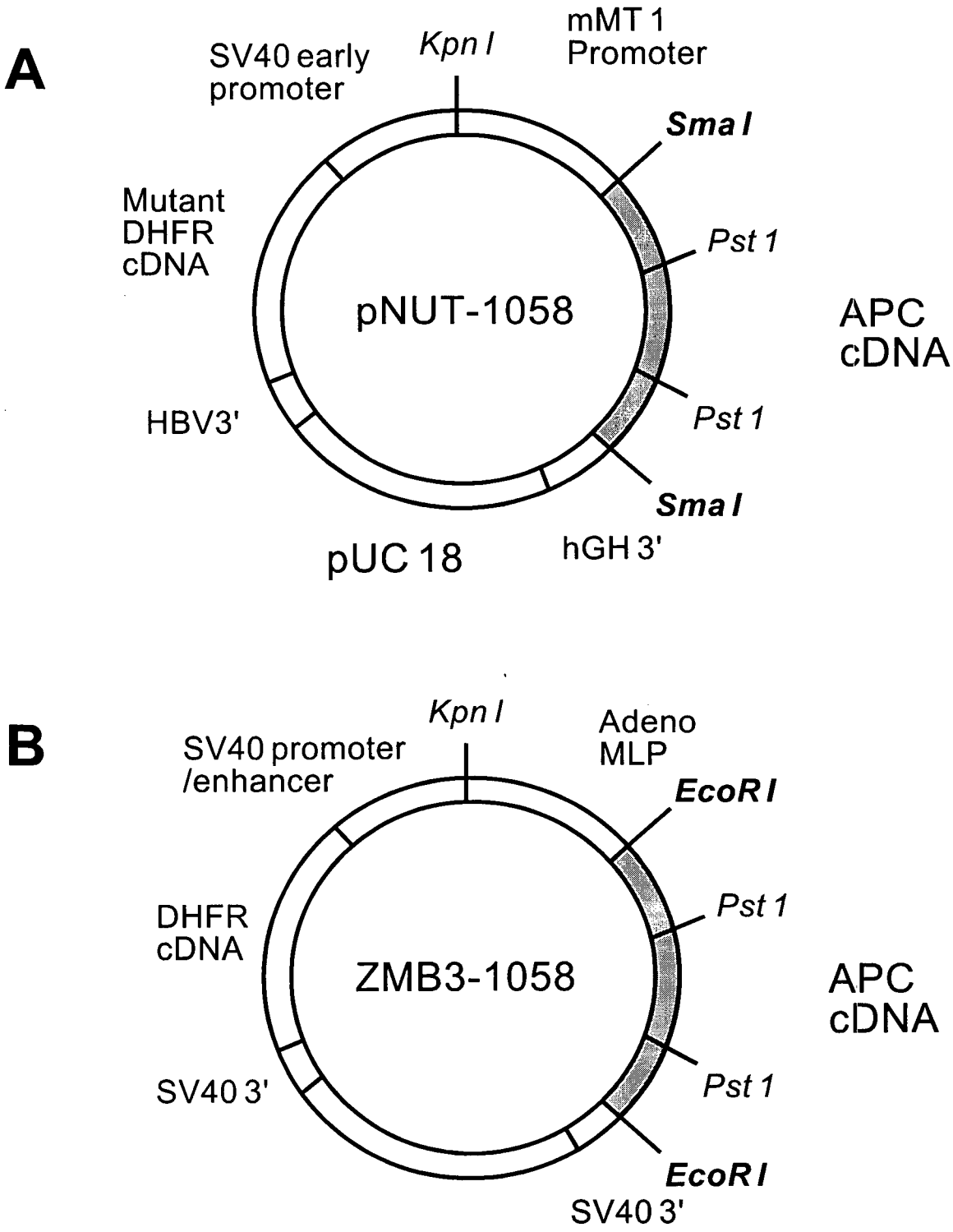

Figure 2.1 Mammalian expression vectors pNUT-1058 (A) and ZMB3-1058 (B).

The vector ZMB3-1058 (obtained from Zymogenetics, Inc, Seattle, WA., Figure 2.1B) encodes the same APC cDNA insert as pNUT-1058. ZMB3 contains the adenovirus major late promoter, tripartite leader and an immunoglobulin splice set (Berkner et al., 1986) substituted for the metallothionein promoter in the vector Zem229 (Foster et al., 1991). The wild-type normal DHFR cDNA in this vector allows selection of transfected cells at low MTX concentrations (approximately 40 nM MTX).

2.1.2 Cell Culture of APC Producing BHK Cells

BHK cells were grown in Dubelcco's modified Eagle's medium: Ham's F- 1 2 (1: 1) (DMEM/F-12) (Life Technologies, Burlington, ON) containing 5% newborn calf serum (NCS) (Life Technologies, Burlington, ON) to approximately 10^6 cells per 10 cm Petri dish and transfected with pNUT-1058 by calcium phosphate coprecipitation method as described (Guarna et al., 1995) and selected in 0.05 or 0.5 mM sodium methotrexate (MTX, David Bull Laboratories, Mulgrave, Australia). Twelve days after transfection, visible MTX resistant colonies were isolated as clones and then expanded for 3-4 weeks in DMEM/F-12 with 5 % NCS and 5 μg/mL of vitamin K, (Abbott Laboratories, Montreal, PQ). The cells were cultured in the absence of MTX to minimize the genetic instability induced by MTX selections (Pallavicini et al., 1990). However, instability is a potential problem when analyzing the specific production rate of cells both in the presence and in the absence of MTX. Thus, we measured the cDNA copy number, APC production rate and proportion of γ-carboxylated APC in the same experiments. Medium samples were cleared by centrifugation at 1000 ×g, room temperature, and stored in aliquots at -70°C for

APC and glucose analysis. For the determination of APC secretion rates and for DNA extraction, 12 clones were first analyzed. Eight clones were from the first transfection series and 2 clones were selected by maintaining the highest expressing clone (clone A-27) in 0.5 mM MTX for 3 and 8 weeks. The 2 additional clones (B-1 and B-2) were the highest expressing clones from another transfection in which 0.5 mM MTX was maintained throughout the expansion of the isolated clones.

To avoid possible toxic effects of MTX on secretion during the experiment, the amplified clones were maintained without MTX for 5 days before the determination of secretion rates and cDNA copy number. Cells growing in DMEM/F-12 containing 5% (v/v) NCS and 5 μg/mL of vitamin K, were harvested from subconfluent 175 cm^2 T-flasks and counted. Approximately 10^7 cells were washed with PBS and stored at -70°C for DNA extraction. For mRNA analysis, the cells were washed twice with ice cold PBS, resuspended in guanidium thiocyanate solution (Solution D) and then stored in liquid nitrogen for mRNA extraction. The cell specific APC secretion rates were determined in parallel cultures, where 10^4 cell/cm^2 were seeded in 6-well plates (Life Technologies, Burlington, ON) and the medium (2.5 mL/well) changed after 24 h; after an additional 72 h the medium was sampled and the cells were harvested by trypsin digestion.

Harvested cells were counted by hemocytometer and with a particle data analyzer (Elzone 280 PC, Particle Data, Inc.). Glucose analysis was performed using a Beckman glucose analyzer and APC was analyzed by ELISA. Intracellular APC content was analyzed by a similar method but using 75 cm^2 T-flasks for culture. The harvested cells were washed once with PBS then lysed with the lysis buffer (5 mM Tris, 15 mM NaCl and

10% w/v NP-40, pH 8.0). The cell lysate was centrifuged at 10,000 ×g, 4°C, and analyzed by ELISA.

2.1.3 Sodium Butyrate Treatment of APC Producing BHK Cells

Each clone subjected to sodium butyrate treatment was seeded at 10^4 cell/cm^2 in two 175 cm^2 T-flasks with 58 mL of medium per flask. After culturing for 72 h, the medium in the two T-flasks was replaced by fresh medium with or without 5 mM sodium butyrate (J. T. Baker, Toronto, ON), respectively. Cells were then cultivated for an additional 24 h, and then the conditioned medium was collected for protein C analysis and the cells were counted or prepared for mRNA analysis as described in section 2.1.2.

2.1.4 Re-transfection of APC Producing BHK Cells

The highest expressing clone from ZMB3-1058 transfection series, clone 27-4 (obtained from Zymogenetics Inc., Seattle, WA), was inoculated at 10^4 cells/cm^2 and cultured to 10^6 cells per 10-cm Petri dish containing DMEM/F-12 medium with 5% NCS and 5 μg/mL of vitamin K_1 before re-transfection. The pNUT-1058 vector was introduced into the cells by the calcium phosphate co-precipitation method (Keown et al., 1990). Briefly, 20 μg of vector DNA was added to each dish and incubated until the medium was changed after 4 h. The selection was started at 24 h in medium containing 0.50 mM MTX. After 2 weeks, MTX resistant colonies were isolated. The isolated clones were expanded in medium without MTX for 3-4 weeks before analysis. Control cells were treated with the same protocol except no pNUT-1058 vector DNA was introduced. No viable cells

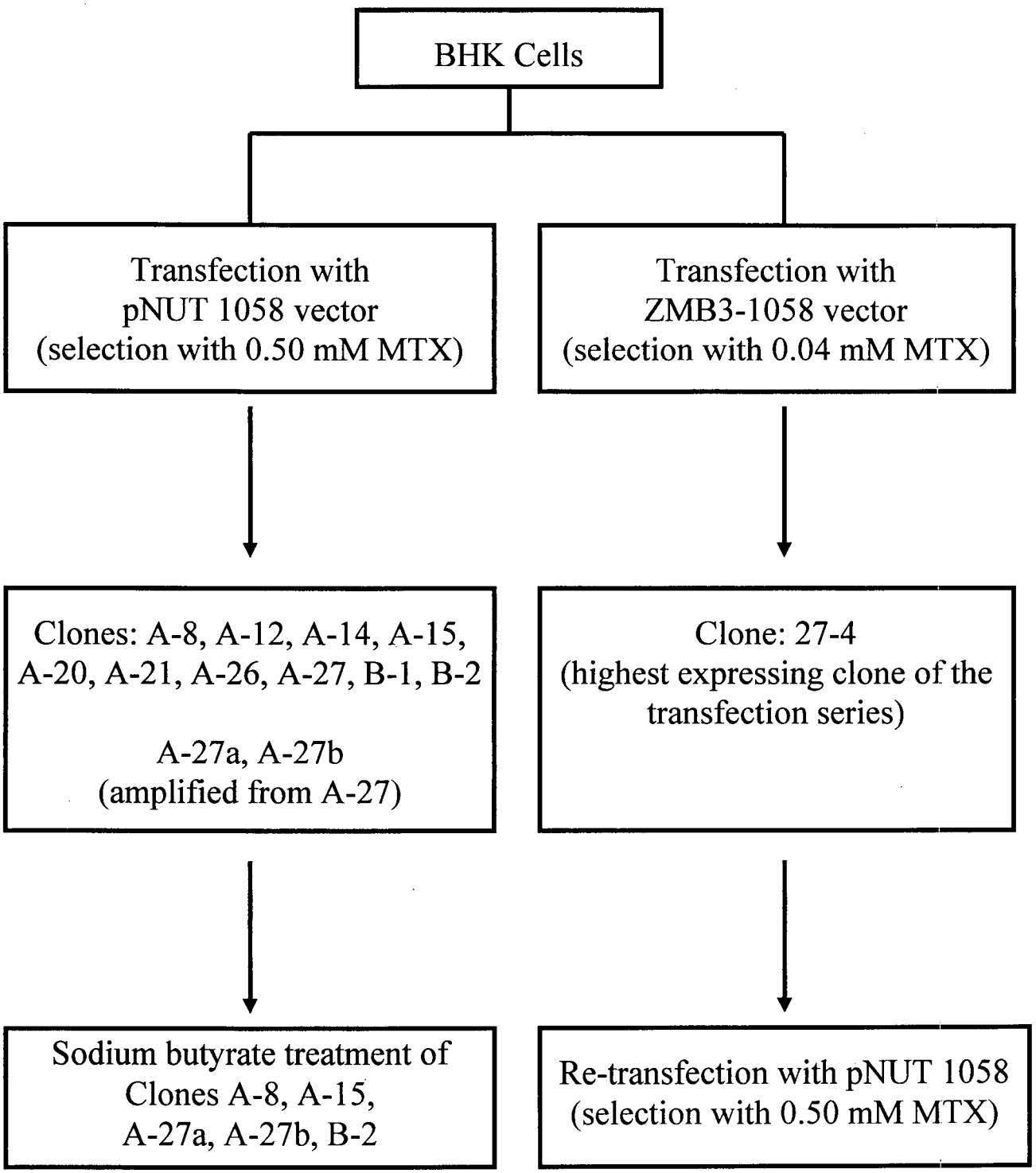

FIGURE 2.2 Strategies to increase APC mRNA levels and APC secretion rates in transfected BHK cells. The vectors used for transfection were: a) pNUT 1058 which contains the APC cDNA sequence and a mutant DHFR cDNA sequence; this mutant DHFR allows for clone selection at high MTX concentrations (0.50 mM MTX) and b) ZMB3-1058 which contains the APC cDNA sequence and wild type DHFR cDNA sequence.

were observed in the control dish after 2 weeks of selection in 0.5 mM MTX. The relationships among the transfected, re-transfected and sodium butyrate treated cells are summarized in Figure 2.2.

2.1.5 BHK Cell Batch Cultures

For the batch cultures, cell line 27-4 was inoculated at 1×10^4 cells/cm^2 into 175 m^2 T flasks containing 58 mL of DMEM/F-12 with 5% NCS and 5 μg/mL vitamin K_1. The cultures were operated in a 37°C incubator with 5% CO_2 and monitored on a daily basis. On successive days of the batch culture, the supernatant was withdrawn directly from the T flasks using a glass pipette, to minimize oxygen contamination to the sample. The dissolved oxygen concentration and pH were determined by a blood-gas analyzer (Corning, Acton, MD), while glucose and lactate concentrations were determined by an automated STAT 10 Nova analyzer (Waltham, MA). Individual T flasks were sacrificed and the cells were counted, harvested and stored in liquid nitrogen for mRNA analysis. Total secreted APC and γ-carboxylated APC were determined by ELISA. Total RNA was extracted and quantified from cell samples collected during the batch culture. APC mRNA and β-actin mRNA levels were estimated by Northern blot analysis.

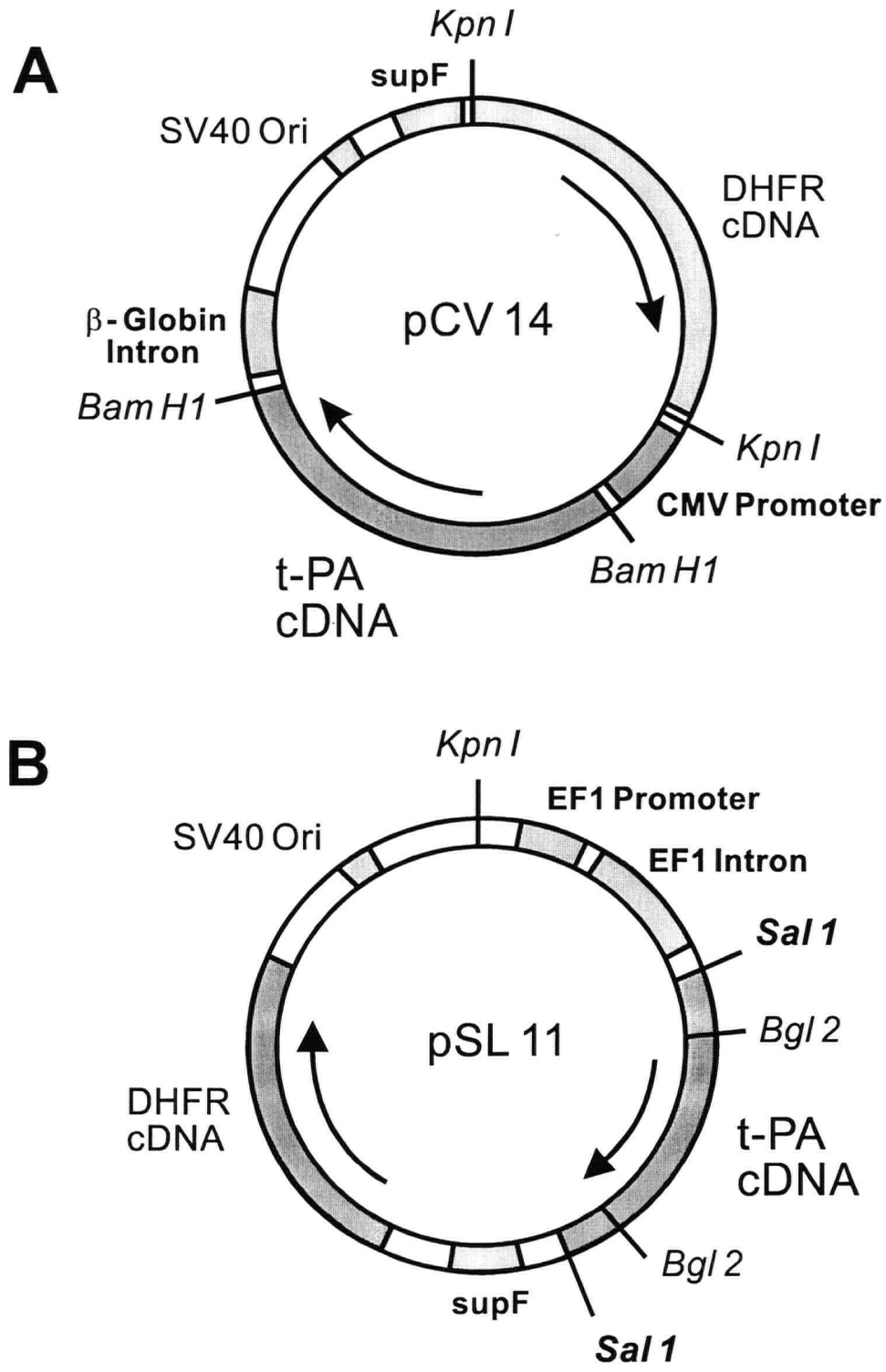

Figure 2.3 Mammalian expression vectors pCV14 (A) and pSL11 (B) for t-PA expression.

2.1.6 t-PA Producing CHO Cell Lines and Transfection Vectors

Four parental recombinant t-PA producing CHO cell lines were provided by Cangene (Winnipeg, MB). Cell lines SI9-12 and SI9-24 were transfected with vector pCV14 which contains one t-PA cDNA cassette with a human cytomegalovirus (CMV) promoter for t-PA expression and a DHFR cDNA for MTX selection (Figure 2.3A). Cell lines SI12-5 and SI12-7 were transfected with vector pSL11 which contains similar t-PA and DHFR cDNAs while t-PA production is controlled by the elongation factor-1 (EF-1) promoter (Figure 2.3B).

2.1.7 Cell Culture of t-PA Producing CHO Cells

The CHO cells were cultured in T75 flasks with Iscove's modified Dulbecco's medium (IMDM) / 10% v/v fetal bovine serum (FBS) (Life Technologies, Burlington, ON) at 37°C in a humidified incubator with 5% CO_2. Adaptation of the CHO cells to serum-free medium (APOSFM1.1, Cangene) was performed by stepwise decreasing the serum concentrations over 2~3 weeks from 10% to 5%, 1%, 0.2% and finally to 0%. The cell numbers and viability were determined using a hemocytometer and trypan blue dye exclusion.

To analyze cell specific t-PA production rate in serum-containing cultures, the cells were inoculated at 3×10^4 cells/mL in 6-well plates or 25-mL T flasks and cultured for 72 h. At the end of the culture, the cells were trypsinized and counted. The supernatants were aliquoted and stored at -20°C for t-PA assay (Section 2.2.2). For serum-free cultures,

cells were inoculated at 10^5 cells/mL in T flasks and then collected by centrifugation at the end of the culture. The cell specific t-PA production rates was calculated based on the final t-PA concentration and the log-mean average cell number during a 72 h culture period.

The cells were washed three times with ice cold PBS, then either frozen at -70°C for DNA analysis or resuspended in guanidinium thiocyanate solution then frozen in liquid nitrogen for mRNA analysis. To extract intracellular t-PA, cells were incubated on ice for 30 min in cell lysis buffer then centrifuge at 10,000 ×g for 10 min to remove cell debris. The collected cell extract was stored at -20°C for t-PA ELISA analysis.

2.1.8 CHO Cell Batch Cultures

Batch cultures were performed in two culture vessels, reactor and spinner, with the same culture volume (500 mL). The pH value in the reactor was controlled by head-space CO_2 input, but not controlled in the spinner culture. SI12-5.23 cells were inoculated at approximately 1×10^5 cells/mL in both serum-free cultures, with APOSFM1.1 medium. The cells and spent medium were sampled every day in an 8 day batch culture. Glucose concentration, pH value, and cell concentration were measured as described in Section 2.1.2. t-PA concentration was analyzed by the colorimetric assay (Section 2.2.2) and mRNA level was analyzed by Northern blot analysis (Section 2.3.4)..

2.1.9 Amplification, Subcloning and Stability Test of t-PA Producing CHO Cells

All four cell lines were subjected to bulk amplification, i.e. by stepwise increment of the MTX concentrations without subcloning at each level (Figure 1.6B). Since these cells had been originally selected after transfection at 0.04 μM MTX, the bulk amplification was initiated at that concentration. The MTX concentration was then increased by 5-fold steps, approximately every month, up to 0.2, 1 and 5 μM.

The bulk amplification of the SI12-5 cells was repeated and the MTX level increased further to 25, 125 and 625 μM. When the cell specific growth rate recovered to approximately 0.02 ~ 0.025 h^{-1}, the selection was increased to the next MTX level. The cell specific t-PA production rate and the growth rate of the amplified cells were analyzed every 4 days. The heterogeneity of the amplified cell population was analyzed by subcloning while maintaining the MTX level. Serum-cultured cells were diluted to a mean concentration of 1 or 10 cells per well in 96 well plates. After culturing for approximately 2 weeks, wells with single colonies were selected. The clones were cultured in 6 well culture plates and analyzed for their growth and cell specific t-PA production rates. A similar subcloning method was applied to cells in serum-free cultures. However, instead of using fresh medium, filtered conditioned serum-free medium from cultures with a maximum cell density of 1×10^6 cells/mL was used for the limiting dilution. Several strategies and consequences for developing subclones by limiting dilution in serum-free medium were summarized in Table 2.1.

TABLE 2.1 Summary of the efforts to clone SI12-5.23 cells in serum-free medium

Medium used for limiting dilution	**Result**
APOSFM-1	No growth below 5000 cells/mL
50% conditioned APOSFM-1	No growth below 5000 cells/mL
0.5% FBS/APOSFM-1	No growth below 5000 cells/mL
IMDM/10% FBS	A few cells grew below 5000 cells/mL but did not survive
100% well-conditioned APOSFM-1	Cells grew in 5 cells/mL and above, several single colonies obtained

2.1.10 Apoptosis Analysis of CHO Cells

Apoptosis of t-PA producing CHO cells was detected using a fluorescence *in situ* cell death detection kit (Boehringer Mannheim, Laval, PQ) to detect the breakage of genomic DNA. Briefly, cells were inoculated at 3×10^4 cells/mL in IMDM/10% FBS medium, then cultured for 5 days to the stationary phase (approximately 10^6 cells/mL). The cells were harvested by trypsinization and washed twice immediately with PBS/1% BSA at 4°C, then adjusted to $1\text{-}2 \times 10^7$ cells/mL in a final volume of 50 µL after cell counting. A cell fixation solution (4% v/v paraformaldehyde in PBS, pH 7.4) was added (100 µL) and incubated with cells for 30 min at room temperature. The cells were then washed and resuspended in 100 µL of permeabilisation solution (0.1% v/v Triton X-100 in 0.1% w/v sodium citrate) for 2 min on ice. Following a centrifugation at 3,000 ×g, the cells were resuspended in 50 µL of terminal deoxynucleotidyl transferase (TdT) mediated dUTP-biotin nick end labeling (TUNEL) solution which contained TdT and a fluorescein-labeled nucleotide mixture, and incubated for 60 min at 37°C. After washing with PBS, the cells were analyzed by flow cytometry using a Becton Dickinson FACScan (Franklin Lakes, NJ). Non-transfected CHO cells were treated with the same procedures as the negative control.

2.2 RECOMBINANT PROTEIN ANALYSIS

2.2.1 Enzyme Linked Immunosorbent Assay

ELISAs for analyzing APC were performed as described by Foster et al. (1987) with some modifications. Two anti-protein C monoclonal antibodies, PCH-1 and PCG-1 (obtained from Zymogenetics Inc.), were used for coating the plates (Immunosorb plates, Life Technologies, Burlington, ON). The antibody PCH-1 recognizes total Protein C while PCG-1 recognizes carboxylated protein C in a calcium-dependent fashion (Foster et al., 1987). The epitope of PCH-1 lies in the heavy chain and its binding is independent of the γ-carboxylation status of the protein. Thus, using both antibodies, it is possible not only to quantify protein C but also to estimate the proportion of protein C that is fully γ-carboxylated. Binding of protein C was detected using an affinity purified biotinylated sheep anti-human protein C antibody followed by streptavidin conjugated alkaline phosphatase (Life Technologies, Burlington, ON) and alkaline phosphatase substrate (Sigma 104, Sigma Chemical Co., St. Louis, MO). Plasma protein C (American Diagnostica, Greenwich, CT) was used as the standard for both ELISAs. All dilutions were in 50 mM TrisCl, 150 mM NaCl, 10 mM $CaCl_2$, 0.5% v/v Tween 20, pH 7.4. The ratio of spent medium to buffer was kept constant in the samples and standards by adding spent medium from a BHK cell line transfected with pNUT (no APC insert).

Concentrations of t-PA were also analyzed by ELISA with HI72C anti-t-PA monoclonal antibody (Life Technologies, Burlington, ON) for plate-coating and rabbit anti-t-PA antiserum (Cangene, Winnipeg, MB) as the secondary antibody as described in

Harlow and Lane's (1988) protocol. The immuno-complex formed by binding of t-PA with these antibodies was detected by alkaline phosphatase conjugated goat anti-rabbit antibody and alkaline phosphatase substrate (Sigma 104, Sigma Chemical Co., St. Louis, MO). Plasma t-PA (Calbiochem, La Jolla, CA) served as the standard in ELISA, diluted in the same medium/buffer (0.1 M TrisCl, 0.1% v/v Tween 80, 0.1% w/v IMDM/10% v/v FBS medium, pH 8.0) as were the analyzed samples. All ELISA plates were analyzed at 405 nm for optical density with a microtiter reader (Molecular Devices, Sunnyvale, CA).

2.2.2 t-PA Colorimetric Assay

The enzymatic activity of t-PA was analyzed by a colorimetric assay (Randy and Wallen, 1981; Verheijen et al., 1982) with some modifications. The standards for the assay were serial dilutions of plasma t-PA (Calbiochem, La Jolla, CA) from 0.25 to 10 U/mL in 0.1 M tris buffer, pH 8.0, containing 0.1% v/v Tween 80 and 0.1% w/v IMDM/10% v/v FBS medium. Supernatant samples were diluted with the 0.1 M tris buffer. The t-PA standards and samples were loaded onto 96-well flat-bottomed microtiter plates (Dynatech, Burlinton, MA) at 50 μL/well, followed by the addition of plasminogen (0.13 μM, Boehringer Mannheim, Laval, PQ), CNBr-fragmented fibrinogen (0.12 mg/mL, Calbiochem, La Jolla, CA) and the substrate, *D*-Val-Leu-Lys-*p*-Nitroanilide dihydrochloride (0.5 mM, Sigma Chemical Co., St. Louis, MO). The microtiter plates were incubated at 37°C for 2 h and the *p*-nitroanilide cleaved from the substrate was detected at 405 nm using a microtiter reader (Molecular Devices, Sunnyvale, CA).

2.2.3 Pulse-chase Analysis

To determine t-PA residence time in the secretory pathway , pulse-chase analysis (Harlow and Lane, 1988) was performed. Cells were inoculated at 10^4 cell/cm^2 (3×10^4 cells/mL) in 6-well plates and cultivated for 96 h in 3 mL/well of IMDM with 10% v/v FBS medium. The medium was withdrawn and the cells were washed once with sterile PBS, then cultivated for 1 h in methionine-free DMEM (Life Technologies, Burlington, ON) with dialyzed FBS. The medium was then replaced with methionine-free DMEM/dialyzed FBS containing 150 μCi of ^{35}S-methionine (ICN, Costa Mesa, CA) for each well. The cells were cultivated for another 30 min (pulse) followed by a washing step. A methionine-rich medium containing 500mg/L methionine was added to the culture (chase), then the cells were lysed by the cell lysis buffer at 0, 30, 60, 90 min followed by centrifugation at 10,000 g for 10 min. The cell extract was collected and stored at -20°C. To collect total ^{35}S-methionine-incorporated proteins, trichloroacetic acid (TCA, Sigma Chemical Co., St. Louis, MO) was added into the cell extract for 20% v/v final concentration. After incubation on ice for 30 min followed by centrifugation at 10,000 ×g for 10 min, the resulting pellet was washed with 20% w/v TCA and 95% v/v ethanol. Finally, the pellet was dissolved in 50 μl PBS for scintillation counting. Newly synthesized t-PA proteins were acquired by incubating monoclonal antibody HI72C with 1 mL of cell lysate at 4°C overnight (2 μg/mL final antibody concentration). The resulting immuno-complex was captured by 5 μL of protein A beads (0.5% v/v in lysis buffer, Repligen, Needham, MA). The acquired t-PA was released by heating in 40 μL of sample

loading buffer at 85°C for 10 min, then 20 μL of the resulting supernatant was loaded onto 10% polyacrylamide gel for SDS-PAGE. The dried gel was exposed to an X-ray film (Kodak, Rochester, NY) for three weeks, then the protein bands were quantified by laser densitometer (Molecular Dynamics, Sunnyvale, CA).

2.2.4 Sodium Dodecyl Sulfate - Polyacrylamide Gel Electrophoresis

The sodium dodecyl sulfate-polyacrylamide gel electrophoresis (SDS-PAGE) was performed using a Mini-Protein II Dual Slab Cell electrophoresis apparatus (Bio-Rad, Mississauga, ON). The 3% stacking and 10% resolving gels were prepared with acrylamid solution (30% w/v acrylamid:bis stock solution, Bio-Rad, Mississauga, ON), 0.05% potassium persulfate, 0.1% *N,N,N',N'*- tetramethylenediamine (TEMED; Bio-Rad, Mississauga, ON), 0.1% SDS, and Tris buffer (0.125 M TrisCl, pH6.8 for the stacking gel and 0.4 M TrisCl, pH 8.8 for the resolving gel) (Hames and Dickwood, 1982). Gel electrophoresis was carried out in the Tris running buffer (0.025 M TrisCl, 0.2 M Glycine, and 0.5% SDS, pH 8.3) at 90 V for 1 h, then the gel was dried on a gel drier (Bio-Rad, Mississauga, ON). The dried gel was exposed to an X-ray film (Kodak, Rochester, NY) for 3 weeks, then the protein bands were quantified by laser densitometer (Molecular Dynamics, Sunnyvale, CA).

2.3 GENETIC ANALYSIS OF RECOMBINANT MAMMALIAN CELLS

2.3.1 Preparation of DIG-labeled DNA Probes

The protocol described by Lanzillo (1990) was followed to prepare digoxigenin (DIG)-labeled DNA probes by the polymerase chain reaction (PCR) using DIG-11-dUTP (Boehringer Mannheim, Laval, PQ) in the reaction mixture on a DNA Thermocycler (Perkin-Elmer Cetus, Branchburg, NJ). The template for preparing APC probe was a 1.2 kb fragment purified from a *BamH*I restriction enzyme digest of the ZMB3-1058 plasmid. A 0.43 kb DIG-labeled human protein C probe was generated. In a similar procedure, a 0.52 kb t-PA DNA probe was prepared using a template of 1.9 kb fragment purified from a *Bgl*II restriction digested pSL-11 plasmid.

2.3.2 Estimation of cDNA Copy Number

Genomic DNA from cultured mammalian cells was isolated using a standard phenol/chloroform purification procedure (Strauss, 1987) followed by RNase treatment. For APC producing BHK cells, the plasmid pNUT-1058 standard and the genomic DNA samples were digested with restriction enzyme *Pst*I. For t-PA producing CHO cells, cells containing pCV14 plasmid (SI9-12 and SI9-24) were digested with *BamH*I, whereas cells containing pSL-11 plasmid were digested with *Bgl*II. Restrict digested genomic DNA as well as plasmid standards were subjected to Southern blot analysis (Southern, 1975) which DNA was resolved on a 0.8% w/v agarose gel then transferred to a positively charged

nylon membrane (Boehringer Mannheim, Laval, PQ). After hybridization and blocking, the hybridized DIG-labeled probe was detected using the DIG Luminescent Detection Kit (Boehringer Mannheim, Laval, PQ), which contained an alkaline phosphatase conjugated anti-DIG antibody and the chemiluminescent substrate LumiPPD (Boehringer Mannheim, Laval, PQ). Luminescent bands were documented by exposure to Hyperfilm-ECL and analyzed with a Fast Scan Computing densitometer (Molecular Dynamics, Sunnyvale, CA). A standard curve of peak area as a function of plasmid DNA loaded was generated (i.e. as in Figure 2.4). The cDNA copy number of the individual clones was calculated using:

$$[cDNA] = \frac{\mathrm{m}_{cDNA}}{\mathrm{m}_g} \times \frac{S_g}{S_p} \times \frac{1 \cdot copy}{plasmid} \qquad (2.1)$$

where m_{cDNA} is the amount of plasmid DNA estimated based on the values interpolated from the standard curve, m_g is the amount of genomic DNA loaded in the gel, S_g is the molecular size of the mammalian genome (5.6×10^6 kb/ cell) and S_p is the molecular size of the plasmid (7 kb/plasmid for APC and 6.6 kb/plasmid for t-PA).

2.3.3 Cytogenetic Analysis

The chromosomal integration of t-PA cDNA was analyzed by fluorescence *in-situ* hybridization (FISH). Cultured cells were arrested in the metaphase by incubation in 0.3 μg/mL of Colcemid (Boehringer Mannheim, Laval, PQ) for 2 h, then the cells were

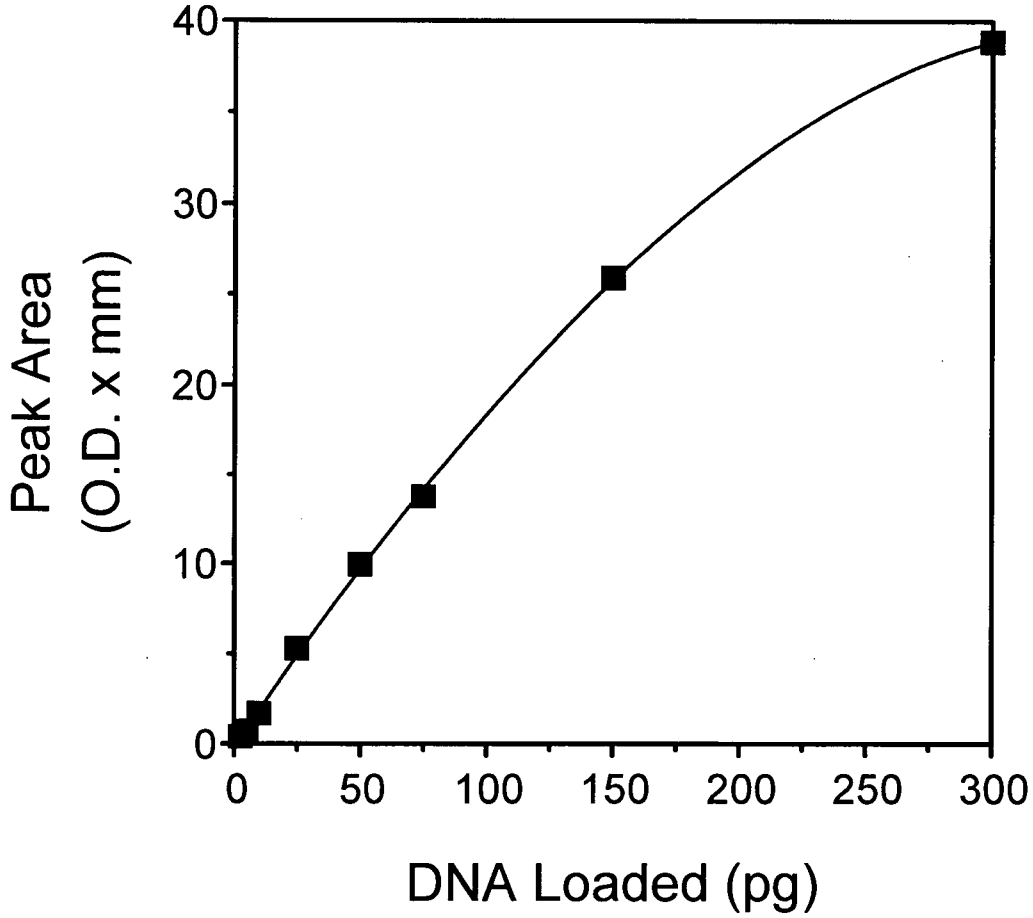

FIGURE 2.4 A representative DNA standard curve. Restriction enzyme *Pst*I digested pNUT-1058 vector was serial diluted from 5 to 300 pg and resolved by Southern blot analysis to serve as the standards for cDNA copy number estimation. The optical density (O.D.) of each DNA band was quantified by a laser densitometer, and the integral peak area was plotted to generate the standard curve.

swollen in 0.075 M KCl for 10 min and fixed in freshly prepared fixative solution (3:1 of methanol : acetic acid) as in the protocols described by Kaufman et al. (1985) and Pinkel et al. (1986). After centrifugation at 400 ×g for 10 min and re-suspending the cell pellet in 200 μL fixative solution, the slides carrying metaphase cells were prepared by dropping 50 μL of cell suspension onto the slides then air-drying them. The slides were first incubated in 60 mL of 2×SSC in a coplin jar at 37°C for 30 min, then dehydrated consecutively in 70%, 90% and 100% v/v ethanol at room temperature for 3 min each. After air-drying, 75 μL of RNAase (100 μg/mL in 2×SSC) was added onto each slide and covered with a plastic coverslip (Oncor, Gaithersburg, MD) then incubated at 37°C for 1 h. The chromosomal DNA was denatured by placing the slides in 70% v/v formamide at 73°C for 2 min, followed by immersing the slides in 70% v/v ethanol at -20°C for 10 min then dehydrated and air-dried. *In-situ* hybridization was carried out following a modified protocol of Pinkel et al. (1986). The DIG-labeled t-PA DNA probe used for FISH was purified (GeneClean, BIO 101, La Jolla, CA) after polymerase chain reaction. The *in-situ* hybridization was carried out by incubating the DIG-labeled t-PA probe with the slides carrying metaphase cells at 95°C for 10 min, then cooled to ice and finally incubated at 42°C for 16 h (Hybaid OmniGene thermocycler, Interscience, Markham, ON). The hybridized slides were then washed and detected by the FITC-labeled anti-digoxigenin detection kit (Oncor, Gaithersburg, MD). After counterstaining with propidium iodide, the slides were evaluated using an epi-fluorescence microscope (Photomicroscope II, Carl Zeiss, Don Mills, ON).

2.3.4 Estimation of mRNA Level and Half-lives

Total cellular RNA was isolated based on the protocol described by Chomczynski and Sacchi (1987). The purified RNA was quantified by optical absorbance then analyzed by Northern hybridization (Maniatis et al., 1982). In the case of APC study, 2.5 μg of RNA for each clone was loaded onto a 1.2% w/v agarose gel containing formaldehyde. After gel electrophoresis, resolved RNAs were transferred onto a positively-charged nylon membrane (Boehringer Mannheim, Laval, PQ) followed by hybridization with DNA probes in 50% v/v formamide at 50°C overnight. The luminescent bands were visualized by exposure to Hyperfilm-ECL (Amsham, Oakville, ON) and analyzed with a laser densitometer (Molecular Dynamics, Sunnyvale, CA). The mRNA levels of the housekeeping gene, β-actin, were used to normalize the APC mRNA data.

The t-PA mRNA level was analyzed in a similar way with a loading of 5 μg RNA per clone onto the 1.2% v/v formaldehyde contained agarose gel. The mRNA levels of the housekeeping gene, β-actin, were also used to normalize the t-PA mRNA data.

To determine t-PA mRNA half-life, clones were cultured in Petri dishes for 72 h. Actinomycin D (Boehringer Mannheim, Laval, PQ) was added to a final concentration of 5 μg/mL to inhibit RNA transcription. Cells were harvested every 2 h up to 10 h. Northern blot hybridization and densitometry were performed to quantify the mRNA levels.

CHAPTER 3

KINETIC MODEL OF MAMMALIAN RECOMBINANT PROTEIN PRODUCTION

A mechanistic model of protein synthesis and secretion will provide a mathematical framework for our analysis of possible intracellular limiting factors to protein expression (Figure 3.1). A model similar to the one described by Bibila and Flickinger (1992) for hybridoma antibody production can be readily adapted to mammalian cell recombinant protein production:

$$\frac{d[mRNA]}{dt} = k_D[cDNA] - k_m[mRNA] - \mu[mRNA] \qquad (3.1)$$

where $[mRNA]$ is the intracellular recombinant protein mRNA concentration (mRNA transcripts/cell), t is time (h), k_D is the cDNA transcription rate (mRNA/cDNA/h), [cDNA] is the cellular cDNA copy number (cDNA copies/cell), k_m is the mRNA turnover rate (h^{-1}) and μ is the cell specific growth rate (h^{-1}).

After translation, newly synthesized proteins are processed in the endoplasmic reticulum and Golgi before being secreted into the culture medium. A mass balance of the intracellular and secreted recombinant proteins obtains:

$$\frac{d[P_i]}{dt} = k_R[mRNA] - k_S[P_i] - k_P[P_i] - \mu[P_i] \qquad (3.2)$$

where $[P_i]$ is the intracellular concentration of recombinant protein (pg/cell), k_R is the translation rate (pg protein/mRNA/h), k_S is the secretion rate (h^{-1}), and k_P is the

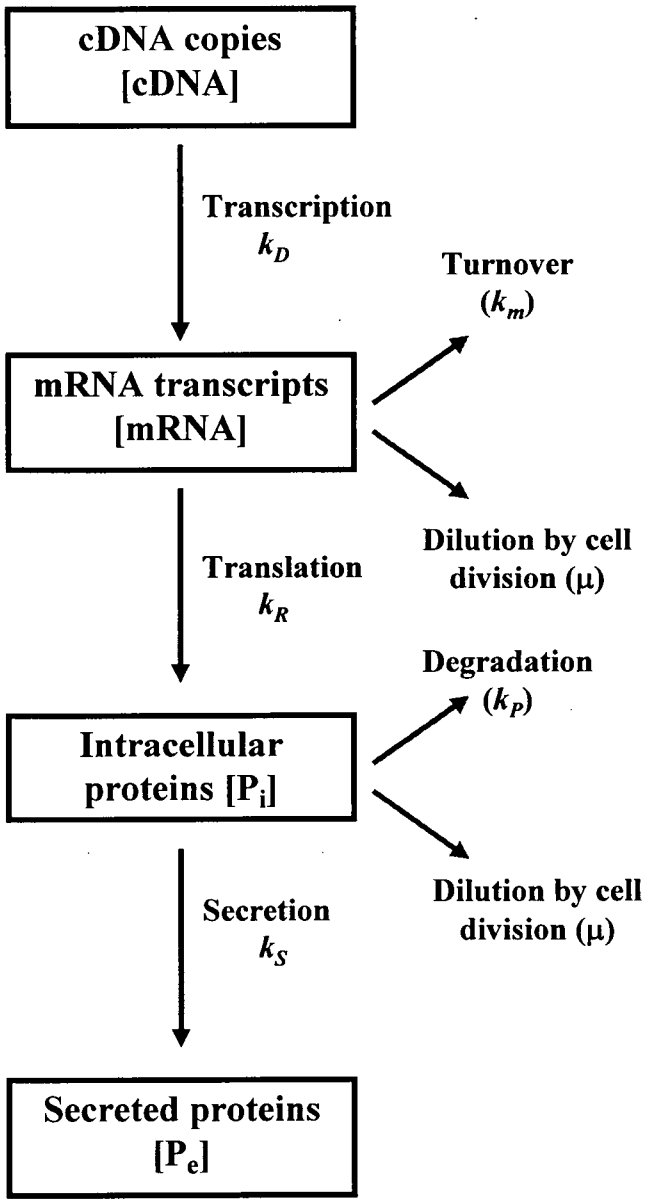

Figure 3.1 The intracellular factors and kinetic constants in mammalian recombinant protein production.

intracellular protein degradation rate (h^{-1}).

Finally, $$q_p = \frac{1}{X}\frac{d[P_e]}{dt} = k_S[P_i] \tag{3.3}$$

where q_p is the cell specific recombinant protein production rate (pg protein/cell/h), $[P_e]$ is the secreted recombinant protein concentration (pg/L), and X is the cell concentration (cells/L) in the culture. It is important to note that the secretion rate, k_S (h^{-1}), is different from the cell specific production rate, q_p, (pg/cell·day). The secretion rate k_S is identical to the secretion efficiency defined by Schroder and Friedl (1997).

In exponential growth phase, the cells are in quasi-steady-state balanced growth (as shown in Sections 4.2.8 and 6.2.7), the time derivatives in Equations 3.1 and 3.2 would be zero. Equation 3.1 provides an algebraic relation between kinetic constants and the ratio of mRNA and cDNA,

$$\frac{[mRNA]}{[cDNA]} = \frac{k_D}{k_m + \mu} \tag{3.4}$$

and the transcription efficiency ε_R can be defined as:

$$\varepsilon_R = \frac{[mRNA]}{[cDNA]} \tag{3.5}$$

Similarly, the relation between the intracellular recombinant protein and mRNA level can be derived from Equation 3.2,

$$\frac{[P_i]}{[mRNA]} = \frac{k_R}{k_S + k_P + \mu} \tag{3.6}$$

Equations (3.4) and (3.6) will allow us to estimate relative transcription (k_D) and translation rates (k_R) from other data. Similarly to Equation (3.5), the secretion efficiency ε_P can be defined as:

$$\varepsilon_P = \frac{[P_i]}{[mRNA]} \tag{3.7}$$

The relationship between cell specific recombinant protein production rate and intracellular factors can be simplified as:

$$q_p = k_S[P_i] = k_S\varepsilon_P[mRNA] = k_S\varepsilon_P\varepsilon_R[cDNA] \tag{3.8}$$

CHAPTER 4

TRANSCRIPTIONAL AND SECRETORY LIMITATIONS TO THE PRODUCTION OF RECOMBINANT ACTIVATED PROTEIN C BY BABY HAMSTER KIDNEY CELLS

4.1 INTRODUCTION

To investigate the limitation in APC production by BHK cells, the relationship between the gene dosage, i.e. cDNA copy number and mRNA level, and APC production rate by BHK cells was analyzed. cDNA copy number as well as mRNA level is usually the target for improving protein production rate in low producing recombinant mammalian cells, as reviewed in Chapter 1. To analyze the effects of cDNA copy number on the production rate and post-translational processing of APC, clones with multiple cDNA copies and various APC production rates were required. Transfection and MTX selection were performed to obtain BHK cells with a wide range of APC cDNA copy numbers. The rationale for using BHK cells is because they have been reported to synthesize a greater proportion of γ-carboxylated vitamin K-dependent proteins than CHO cells (Yan et al., 1990). The influence of various cell specific APC production rates on APC γ-carboxylation was also investigated. Quantitative analysis of intracellular APC and APC mRNA levels were performed to study the limitations to recombinant APC production. In addition, the impact of increased APC mRNA levels on protein secretion and production

rate was investigated using sodium butyrate treatment and re-transfection. Finally, APC mRNA levels and APC production were studied in batch cultures.

4.2 RESULTS

4.2.1 Molecular Cloning of APC Producing BHK Cells

A series of transfections were performed by varying the concentration of vector DNA and the selection conditions to generate clones producing different levels of APC (Guarna et al., 1995). APC production varied widely between the different clones with a range of production rate from 0.034 to 1.1 $\mu g/10^6$cells·day. For the collection of clones tested, a higher average of APC production was obtained from clones derived from transfection with the highest dose of vector DNA (20 $\mu g/10^6$cells) (Guarna et al., 1995).

4.2.2 Relationship between cDNA Copy Number and APC Production

Figure 4.1 shows a Southern blot of the plasmid used as standard and genomic DNA digested with the restriction enzymes *Pst*I and *Kpn*I. Scanning densitometer analysis of the 0.85 Kb band generated by *Pst*I digestion was used to estimate the number of cDNA copies in the BHK clones. Analysis of genomic DNA samples digested with *Kpn*I, which cleaves only once within the vector, was used to investigate whether the integration

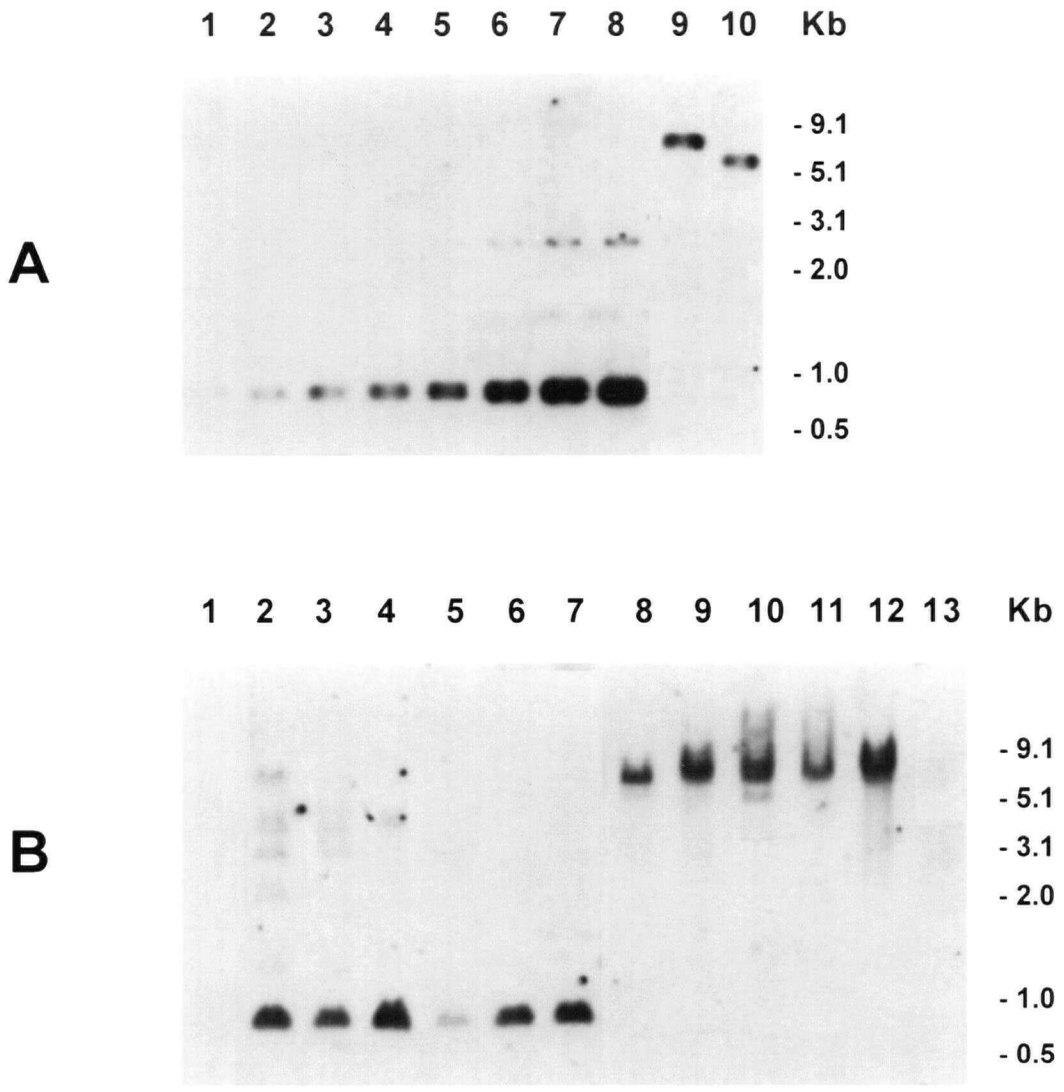

Figure 4.1 Representative Southern blot analysis. Two gels run in parallel were blotted to one membrane which was hybridized with a DIG-labeled PC probe and processed as described in Chapter 2. (A) Standard (vector) DNA digested with *Pst*I was loaded in lanes 1 to 8 in increasing amounts (1, 5, 10, 25, 50, 75, 150, and 300 pg). Vector digested with *Kpn*I (lane 9) and uncut vector (lane 9) were also analyzed. (B) Analysis of genomic DNA samples (1.5 μg) from a clone transfected with the pNUT vector (no insert) after digestion with *Pst*I (lane 1) and *Kpn*I (lane 13) and genomic DNA samples (1.5 μg) from clones A-26, A-15, A-27a, A-21, A-20, and A-8 (left to right) as described in Figure 2.2 after digestion with *Pst*I (lane 2 to 7) and clones A-20, A-26, A-8, A-15, and A-27a (left to right) after digestion with *Kpn*I (lanes 8 to 12).

occurred in tandem repeats. The appearance of a full length (7 kb) predominant fragment upon *Kpn*I digestion indicates that the majority of the integrations occurred in a tandem head-to-tail fashion (Figure 4.1B).

The APC production as a function of cDNA copy number is shown in Figure 4.2. The protein production rates were analyzed during exponential growth to minimize the effects of nutrient limitations or accumulation of toxic metabolites. For instance, on average the glucose concentration decreased only from 3.0 to 1.5 g/L. The APC production rate per cell increased with copy number up to 240 and then decreased (Figure 4.2). Similar bell-shaped patterns were obtained both when the APC production was expressed as APC secreted per glucose utilized and as the rate of APC production per cell. The results expressed in terms of mg APC secreted per g of glucose correlated with the rate of APC produced per 10^6 cells per day (r - 0.95). This correlation indicated that APC production rate could be estimated based on APC secreted per g glucose consumption, which could be useful for the analysis of APC production rate with large sample numbers.

The nonlinear relation between production and cDNA indicated that the rate of APC production per copy (The product of $k_S \mathcal{E}_P \mathcal{E}_R$ in Equation 3.8) was not constant. Instead, the protein production rate per cDNA copy increased for up to 240 copies per cell and then decreased at higher copy numbers (Figure 4.3). At high cDNA copy numbers, not only the APC production rate per cDNA copy but also the production rate per cell decreased (Figures 4.2 and 4.3).

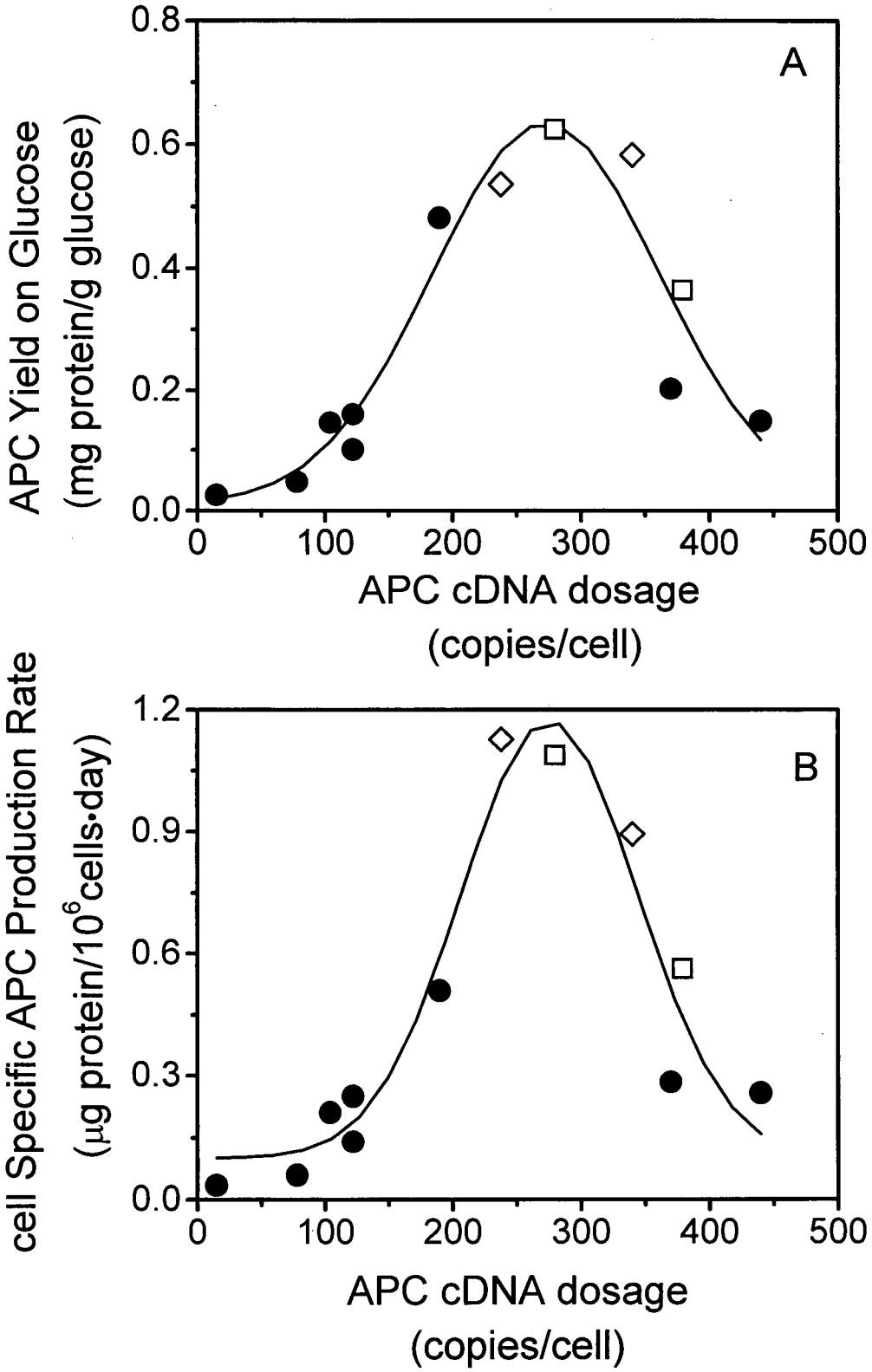

Figure 4.2 Production of total APC by BHK cells with a range of recombinant cDNA copy numbers. APC production was expressed as APC produced per glucose utilized by the culture (A) and as the rate of APC production per cell (B). Gaussian curves were fit to both sets of data. In order of increasing cDNA, closed circles represent clones A-21, A-12, A-14, A-15, A-20, A-27, A-8, and A-26 from the first transfection series. Open diamonds represent the two highest producing clones from a second transfection and open squares represent clone A-27 after additional MTX amplification.

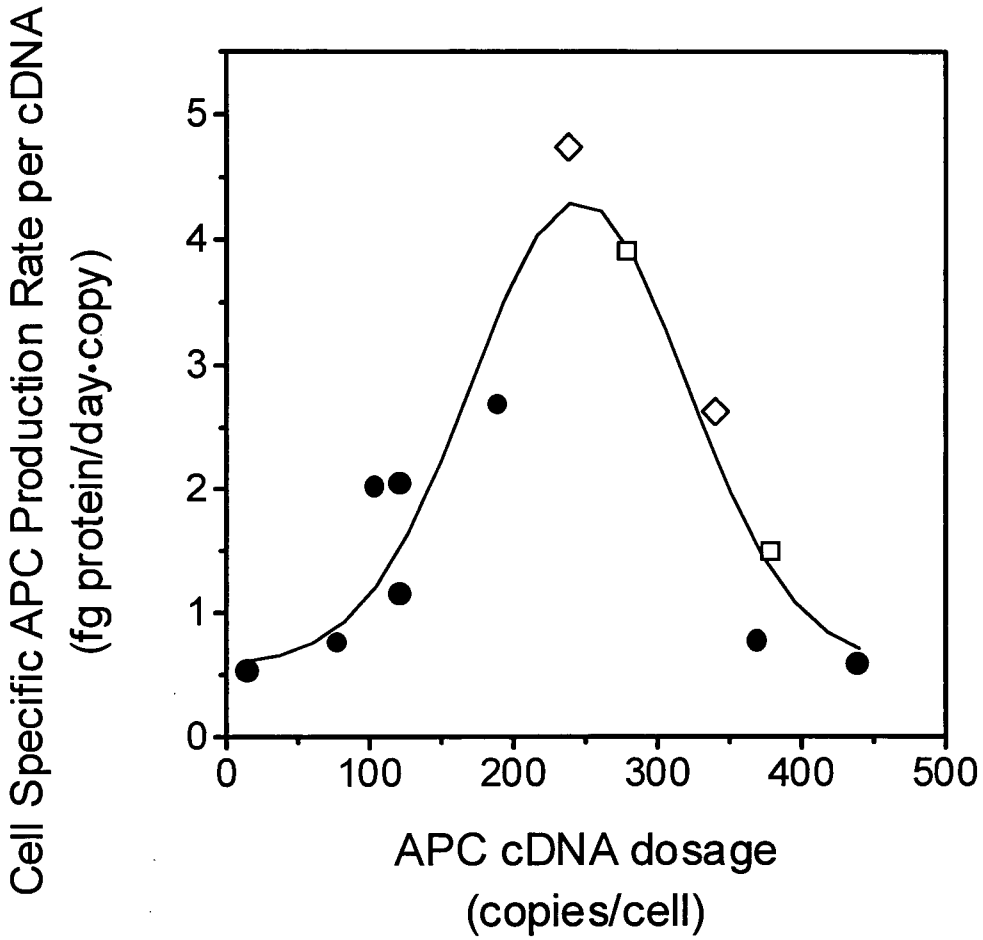

Figure 4.3 Total APC production rate per cDNA copy. Clones from the first transfection series (closed circles) and clones from a second transfection (open diamonds) and clone A-27 after additional MTX amplification (open squares) were analyzed.

4.2.3 Intracellular APC Retention Time in BHK Cells

To further investigate the variations in the rate of APC production per cDNA copy, pulse-chase experiments were performed to analyze the secretion status of two clones, A-26 and A-27, which had distinct production rates per copy (0.58 vs. 2.6 fg protein/day·copy, respectively, Figure 4.3). After a pulse with ^{35}S-methionine and followed by 3 h of chase, A-26 and A-27 secreted, respectively, approximately 22% and 27% of labeled APC into the medium (Figure 4.4). The secretion rates were estimated as approximately $k_S = 0.11$ and $k_S = 0.13$ h^{-1} for A-26 and A-27, respectively. The average retention half-life for these two clones was 5.8 ± 0.7 h. Only a small portion of the newly synthesized APC was degraded within 3 h (1~2%), at a protein degradation rate of k_P = 0.004 ± 0.004 h^{-1}.

4.2.4 Dependence of APC γ-carboxylation on Production Rate

To determine if the post-translational γ-carboxylation of APC was influenced by the production rate, we developed an ELISA based on a monoclonal antibody specific for γ-carboxylated protein C (PCG-1). Total APC was measured by an ELISA based on an antibody insensitive to the degree of carboxylation (PCH-1). Thus, by comparison of these results, we estimated the proportion of γ-carboxylated APC (Figure 4.5). Although APC produced by BHK cells was not fully γ-carboxylated at any of the expression levels,

A

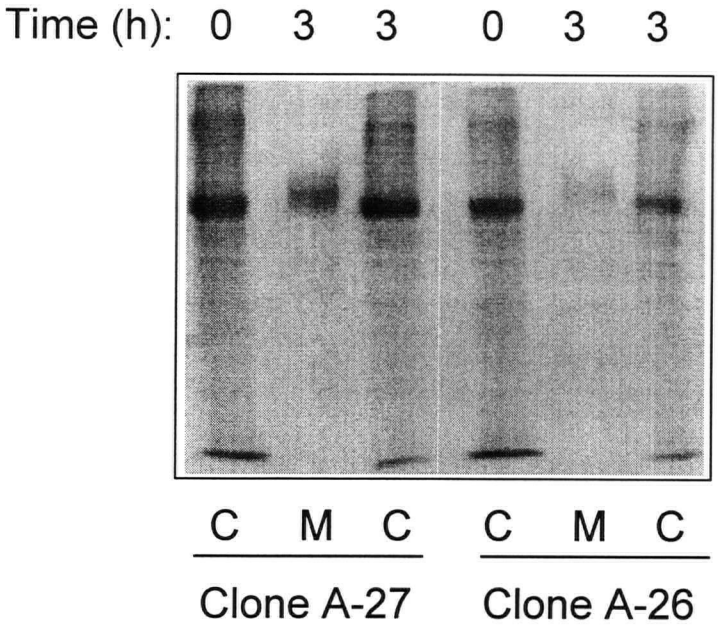

B

Chase Time (h)	Location	Clone A-27	Clone A-26
0	Cell extract	100%	100%
3	Cell extract	72%	68%
3	Medium	27%	22%

Figure 4.4 Pulse-chase analysis of APC secretion. Two APC producing clones were pulsed with ^{35}S-methionine then chased with unlabeled methionine for 0~3 h. Intracellular and secreted APC on a 10% SDS-acrylamide gel are shown in (A). (B) Summary of the quantitated results of intracellular and secreted APC from (A). The two clones analyzed by pulse-chase are clones A-26 and A-27, which had APC production rates of 0.26 and 0.45 μg/10^{6}cells·day, and cDNA copy numbers of 440 and 170, respectively.

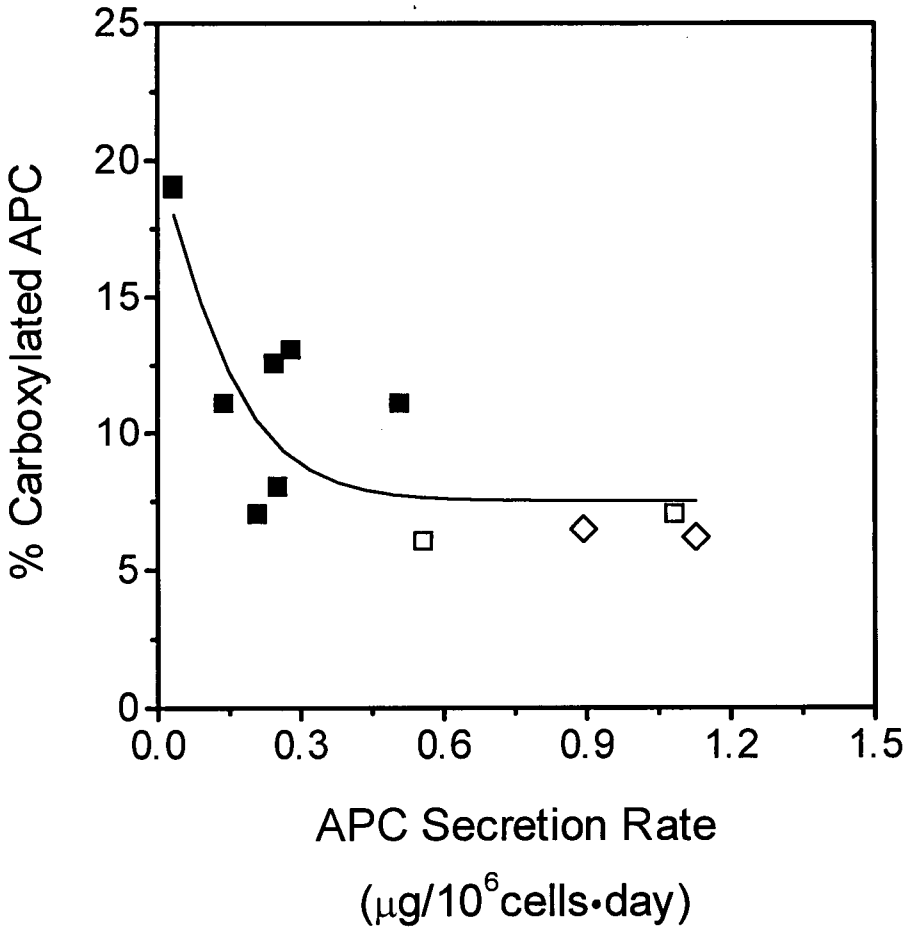

Figure 4.5 Percentage of fully γ-carboxylated activated protein C produced by individual clones with increasing APC production rates. The percentage of fully γ-carboxylated APC was estimated by ELISA using antibodies specific to total protein C and to γ-carboxylated protein C. Clones from the first transfection series (closed circles) and clones from a second transfection (open diamonds) and clone A-27 after additional MTX amplification (open squares) were analyzed.

the proportion of APC that was γ-carboxylated decreased from 19% to 6% as the specific APC production increased from 0.06 to 1. 1 μg APC/10^6 cells·day.

4.2.5 Relation between mRNA Levels and APC Production Rates

The mRNA levels of the transfected clones were analyzed in exponential growth by Northern blot analysis (Figure 4.6). The β-actin mRNA levels were used to normalize the APC mRNA data to minimize the deviations due to variable mRNA recovery. A proportional increase of cell specific APC production rate with increasing clonal APC mRNA level was observed (Figure 4.7A). This linear relationship (r - 0.94) indicated that the mRNA levels limited the APC production rates. A non-linear bell-shape relationship between APC mRNA level and cDNA copy number was also observed which indicated the clonal transcription efficiencies per APC cDNA copy varied in these clones (Figure 4.7B).

4.2.6 Induction of APC mRNA Levels and APC Production Rates by Sodium Butyrate

If APC mRNA level limits APC production rates then increasing APC mRNA levels should increase APC production rates. Two strategies were employed to increase APC mRNA transcripts (Figure 2.2 in Chapter 2). Sodium butyrate treatment was the first strategy to increase the transcriptional activity of APC cDNA transiently and consequently increase the APC mRNA levels (Figure 4.8). The cell growth was reduced 30 to 40% by

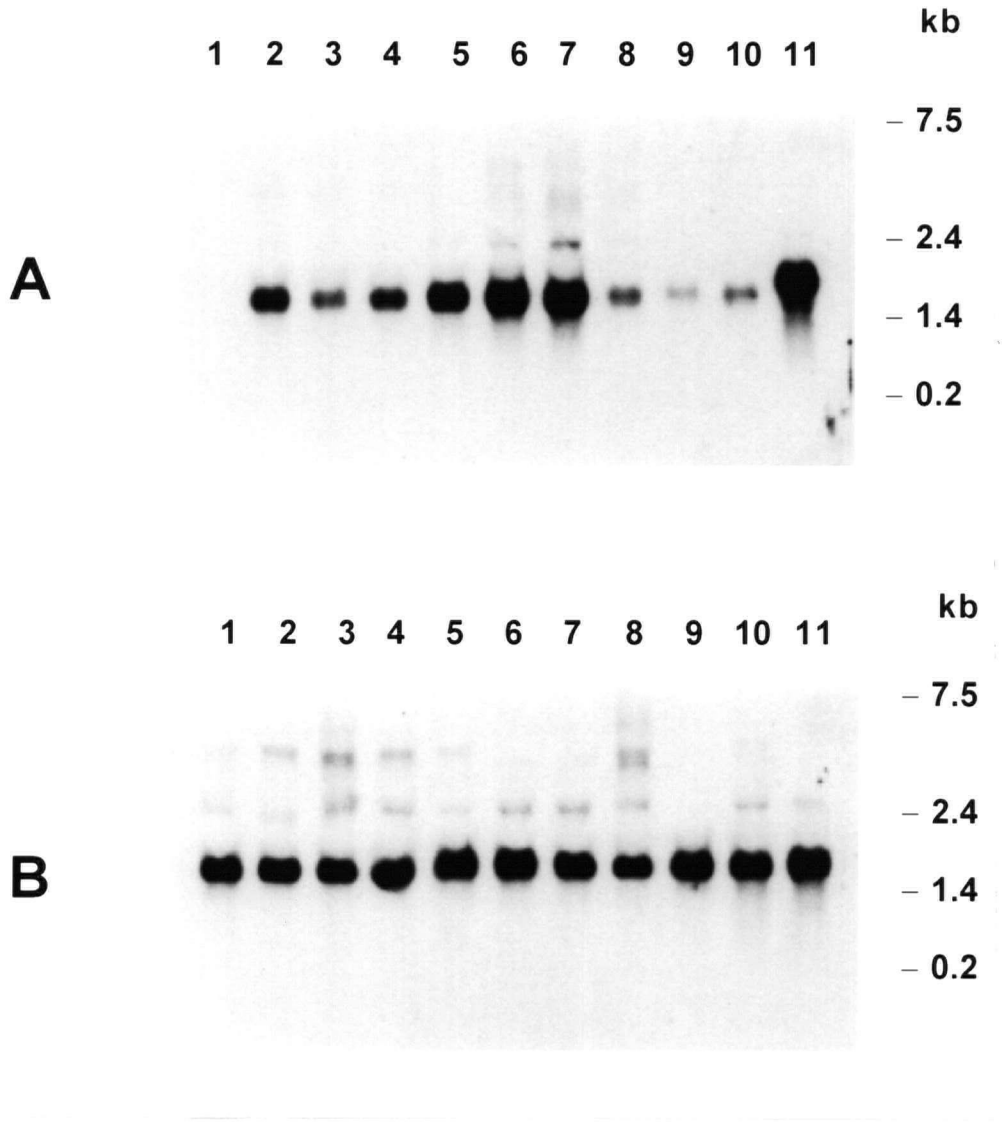

FIGURE 4.6 Representative Northern blot analysis. 2.5 μg of RNA was loaded onto each of two 1.2% agarose gels which were run in parallel and hybridized with DIG labeled APC and β-actin probes, respectively. (A) Analysis of RNA samples from a clone transfected with pNUT vector (no APC insert) (lane 1) and APC producing clones A-15, A-14, A-20, A-8, A-27, A-27a, A-26, A-21, A-12 and A-27b (lane 2 to 11). All these clones were from the first transfection series except A-27a and A-27b, which were amplified clones from A-27. The gel was hybridized with a DIG-labeled APC DNA probe. (B) The same RNA samples with the same amount of loading as in (A), but the gel was hybridized with DIG-labeled β-actin DNA probe.

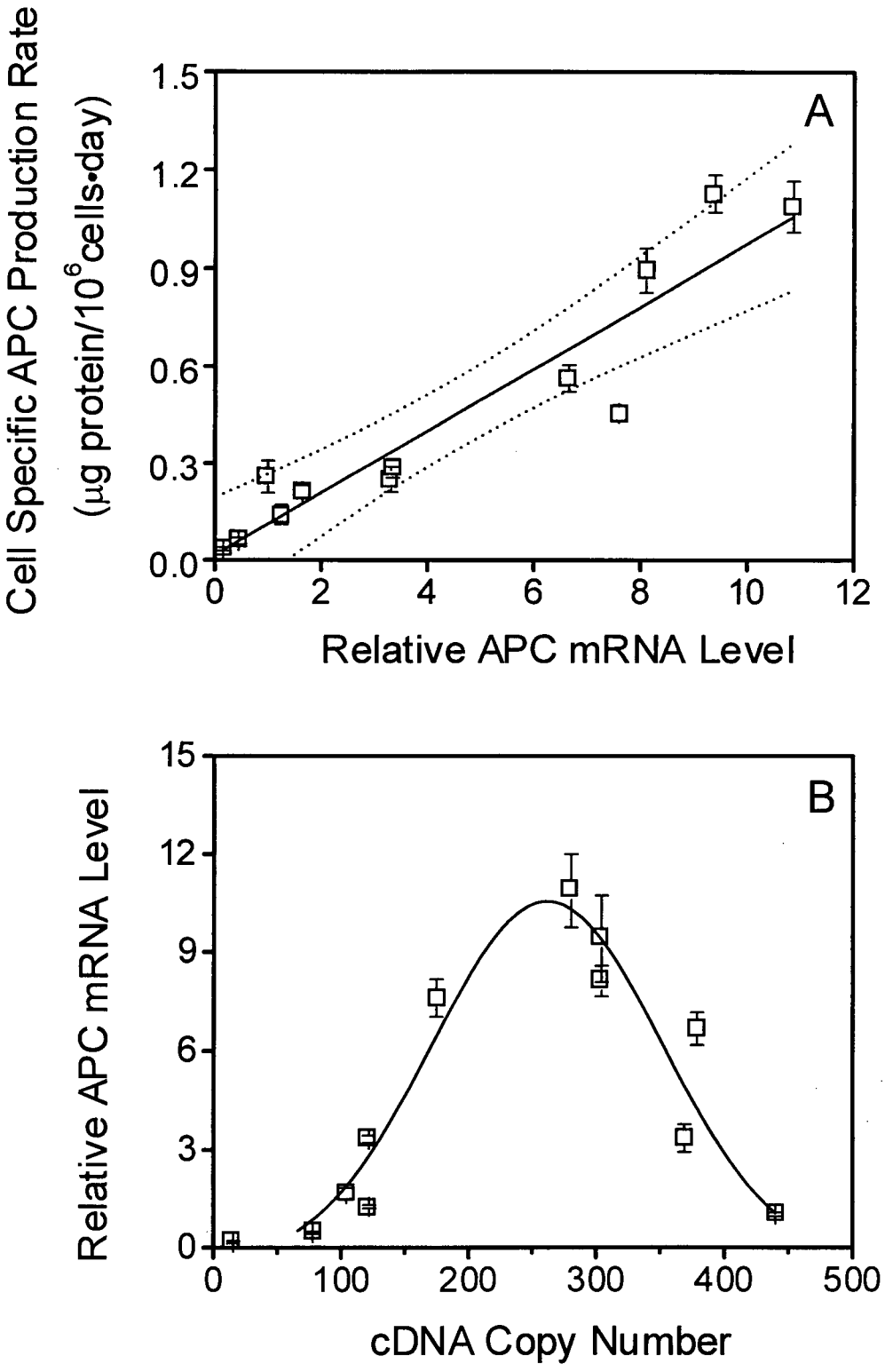

FIGURE 4.7 (A) APC secretion rates of the BHK clones with increasing APC mRNA level. Open squares represent clones A-21, A-12, A-26, A-14, A-20, A-15, A-8, B-1, A-27, A-27a, A-27b and B2 (in orders of increasing relative mRNA level). Linear fit to the data (r - 0.94) with 95% confidence is shown. (B) Relationship between relative APC mRNA level and cDNA copy number in the original transfected or amplified BHK clones.

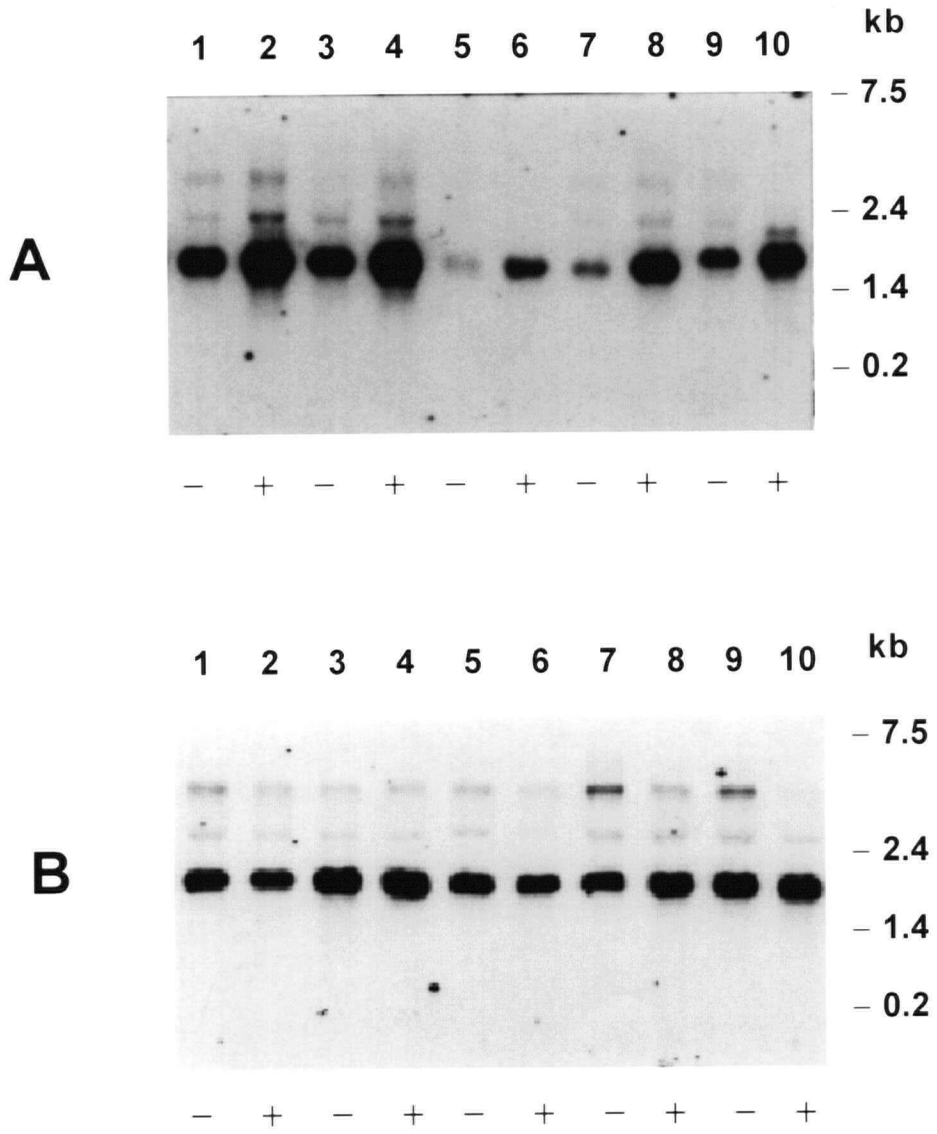

FIGURE 4.8 Northern blot analysis of sodium butyrate treated clones. 2.5 μg of RNA samples extracted from clones without (–) or with (+) 5 mM sodium butyrate treatment were applied on two gels and run in parallel. (A) gel hybridized with DIG-labeled APC probe with RNA samples from clones A-27b (lane 1,2), B-2 (lane 3,4), A-15 (lane 5,6), A-8 (lane 7,8) and A-27a (lane 9,10). (B) gel loaded with the same amount of samples as in (A) but hybridized with DIG-labeled β-actin probe.

TABLE 4.1 Increase of APC mRNA levels and secretion rates by sodium butyrate induction. BHK clones A-15, A-8, A-27a,b and B-2 were cultured for 72 h before sodium butyrate treatment, then the medium was replaced with fresh medium with (+) or without (–) 5 mM sodium butyrate. After culturing for additional 24 h, the medium and cells were collected and analyzed for mRNA levels, APC secretion rates and cell specific growth rates. The data are presented in the ascending order of the non-induced mRNA levels.

Clone No.	Sodium Butyrate Treatment	Cell Growth Rate in 24h Culture (h^{-1})	Relative mRNA Level (Arbitrary Unit)	Fold increase in mRNA Level	APC Secretion Rate (μg protein /10^6cells·day)	Fold increase in APC Secretion Rate	APC Secretion/ mRNA Level (μg protein /10^6cells·day /mRNA)
A-15	–	0.037	1.1		0.3		0.27
	+	0.027	6.5	5.9	0.9	2.7	0.14
A-8	–	0.037	3.3		0.5		0.15
	+	0.027	13.6	3.9	0.9	1.8	0.07
A-27a	–	0.031	8.2		1.4		0.17
	+	0.019	19.2	2.3	2.7	2.0	0.14
A-27b	–	0.035	9.4		1.8		0.19
	+	0.023	40.3	4.3	2.3	1.3	0.06
B-2	–	0.026	10.8		1.8		0.17
	+	0.015	39.9	3.7	2.6	1.5	0.07

sodium butyrate (Table 4.1) as previously reported for cultured myoblast cells (Leibovitch and Kruh, 1979). The mRNA level of the housekeeping gene, β-actin (Figure 4.7), was not affected by sodium butyrate treatment, whereas the APC mRNA levels increased approximately 2 to 6-fold in five treated clones (Table 4.1). This specific induction of a heterologous gene by sodium butyrate without induction of a housekeeping gene was consistent with the report by Dorner et al. (1989). In general, the addition of sodium butyrate treatment increased APC production rates with increasing APC mRNA levels up to 2.7 $\mu g/10^6$cells·day. However, for the high producing clones (A-27b and B-2), despite the 2-fold higher APC mRNA levels achieved by sodium butyrate induction than any other clones, the APC production rate was not increased correspondingly (Table 4.1). A limitation downstream from mRNA appeared to be reached at the highest mRNA levels (Figure 4.9A).

4.2.7 Increased APC mRNA Levels and APC Production Rates by Re-transfection

The second strategy to increase intracellular APC mRNA levels was re-transfection of the APC producing clone 27-4 (Figure 2.2 in Chapter 2). This clone was the highest expressing clone recovered from the transfection series with ZMB3-1058 vector and had been selected in a low methotrexate concentration (40 nM). By re-transfecting 27-4 cells with the pNUT-1058 vector containing a mutant DHFR gene, the resulting clones could then be re-selected at 0.50 mM MTX. The cDNA copy numbers and the mRNA levels of 13 re-transfected clones were analyzed by Southern and Northern blot analysis. Most of the re-transfected clones produced higher APC mRNA levels than the parental 27-4 cells and when combined with the mRNA results from the original transfected clones (Figure

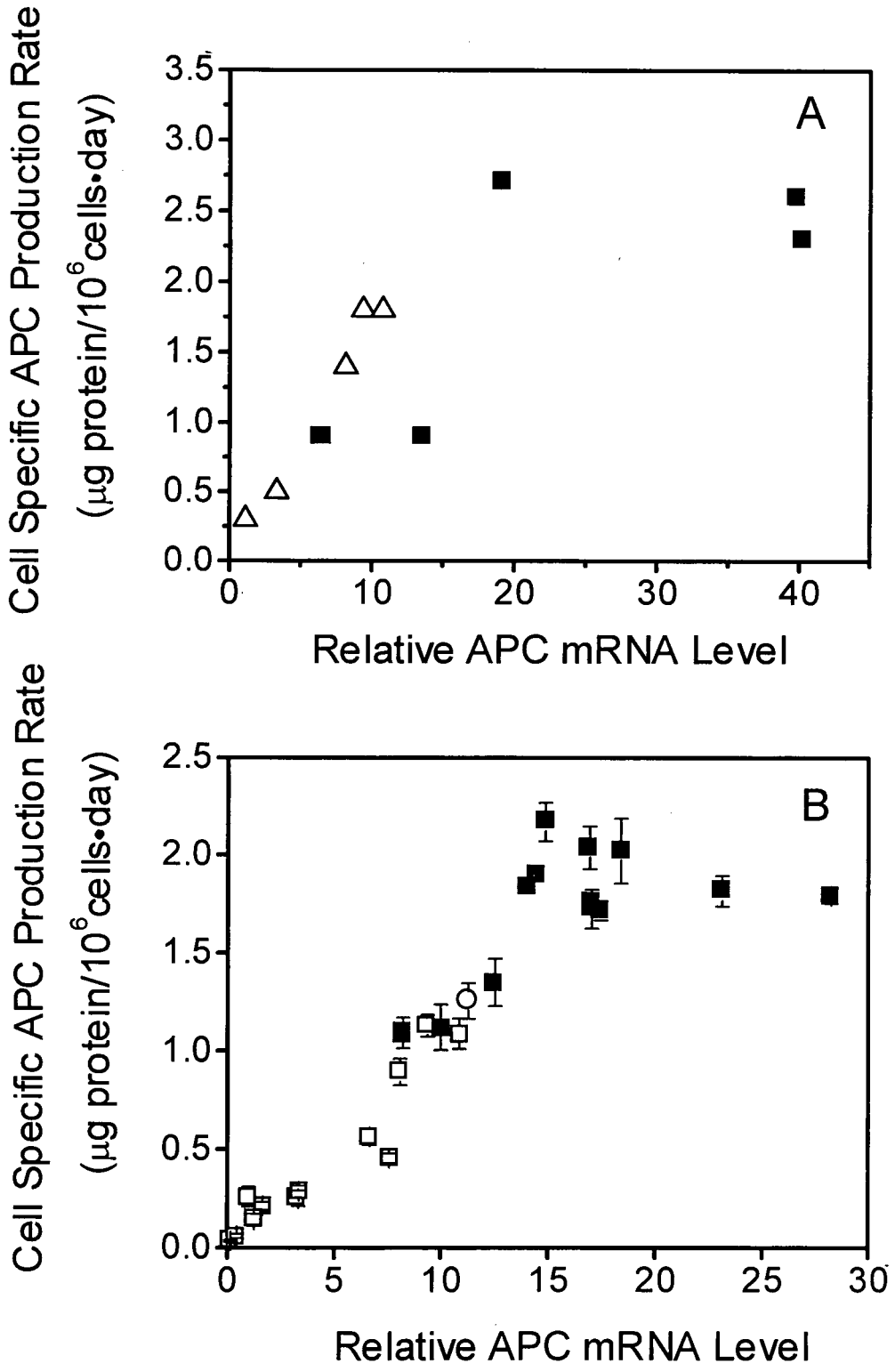

FIGURE 4.9 (A) Relationship between APC mRNA level and APC secretion rates in sodium butyrate treated clones (Table 4.1). The open triangles represent the 5 analyzed clones without sodium butyrate treatment. The solid squares represent the same clones with sodium butyrate treatment. (B) Secretion of APC by the original transfected clones, clone 27-4 and the re-transfected clones at various APC mRNA levels. The original transfected and amplified clones are presented as open squares. The open circle represents clone 27-4 and the solid squares represent the new clones from re-transfection of clone 27-4 with pNUT-1058 vector. The re-transfected clones were named LD1 to LD13 in the sequence of relative APC mRNA levels from low to high.

4.9B), a linear relationship was observed between APC production rate and relative mRNA up to 2.2 μg/10^6cells·day. An apparent saturation in APC production rates was reached for the 2 clones with the greatest APC mRNA levels (Figure 4.9B). The re-transfected clones also contained higher APC cDNA copy numbers than the parental clone 27-4 (Figure 4.10), although there was no clear correlation between production rates and cDNA level.

The possible saturation in APC production was investigated by measuring the intracellular APC content of 8 original or re-transfected clones. These 8 clones had a range of intracellular APC contents from 0.8 to 1.5 pg/cell which were linearly correlated with the relative APC mRNA levels (Figure 4.11A). The cell specific APC production rates increased with increasing intracellular APC concentrations reaching a maximum at an intracellular APC content of approximately 0.8 pg/cell (Figure 4.11B). These results demonstrate an apparent saturation in the APC secretory pathway since increases in the intracellular APC concentrations up to 1.5 pg/cell did not yield increased APC production rates. The secretion rate could also calculated from Figure 4.11B using Equation (3.3) as $k_S = 0.11 \pm 0.007\ h^{-1}$.

The growth rates of the original clones and the re-transfected clones were also investigated. An inverse correlation was observed between cell growth rates and APC production rates (r - 0.93) (Figure 4.12), the clones with higher APC production rates had lower growth rates.

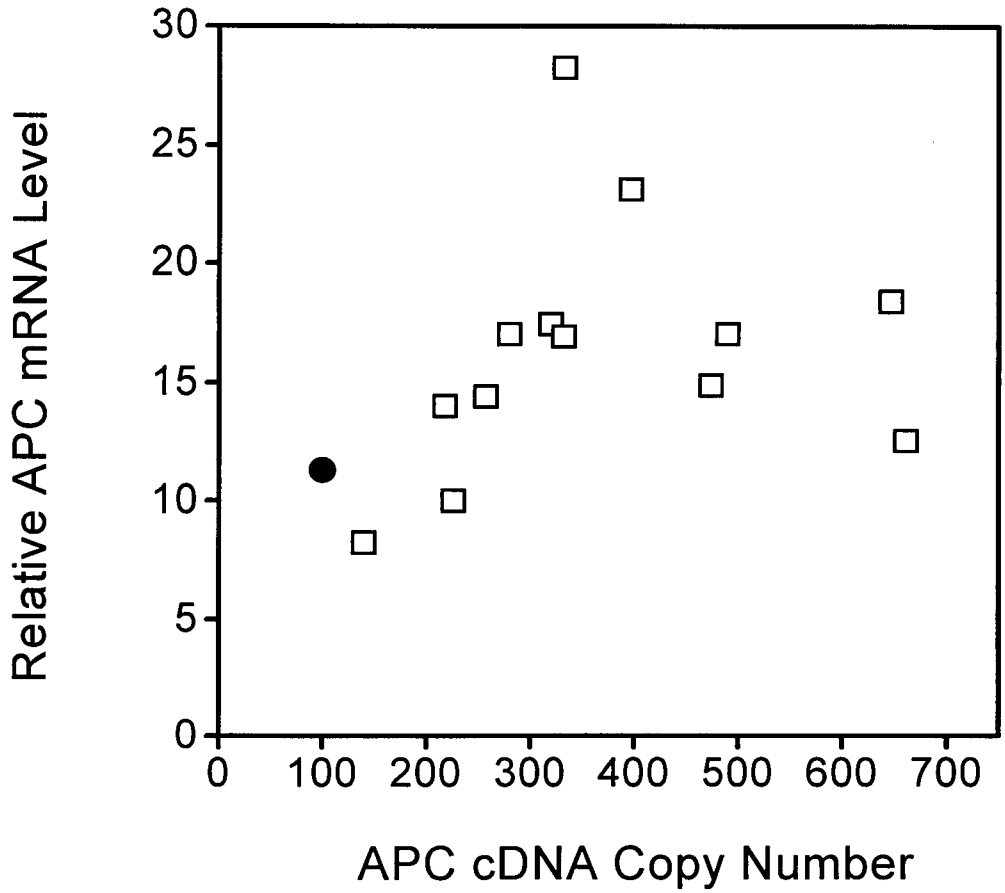

FIGURE 4.10 Relation between APC cDNA copy number and relative mRNA level in re-transfected clones (open squares). The parental cell clone 27-4 (solid circle) is also presented for comparison.

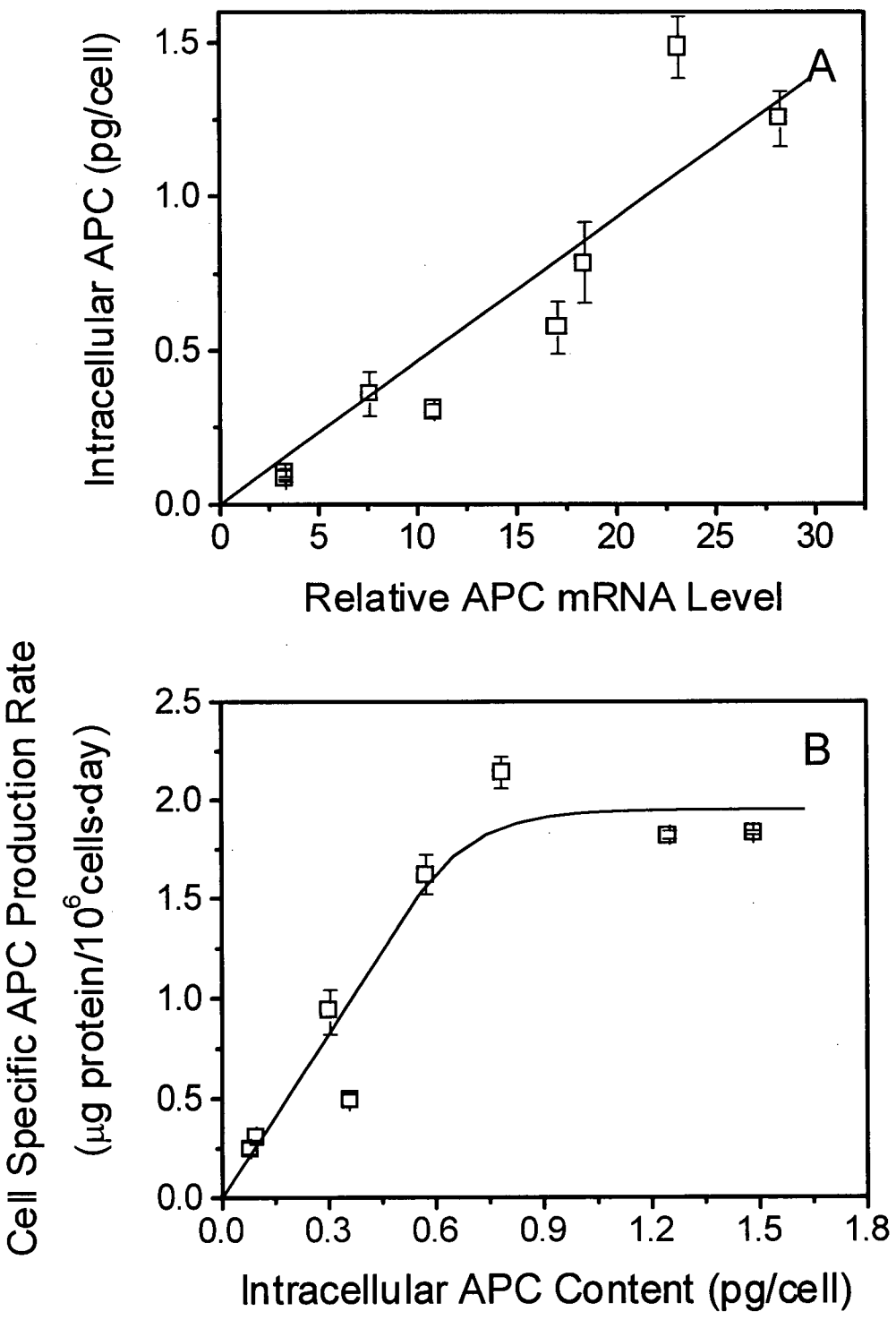

FIGURE 4.11 (A) Relationship between intracellular APC content and relative APC mRNA level. The original transfected clones A-8, A-15, A-27, B-2 and the re-transfected clones LD9, LD11, LD12, LD13 were included in the analysis. (B) Relationship between APC secretion rate and intracellular APC content.

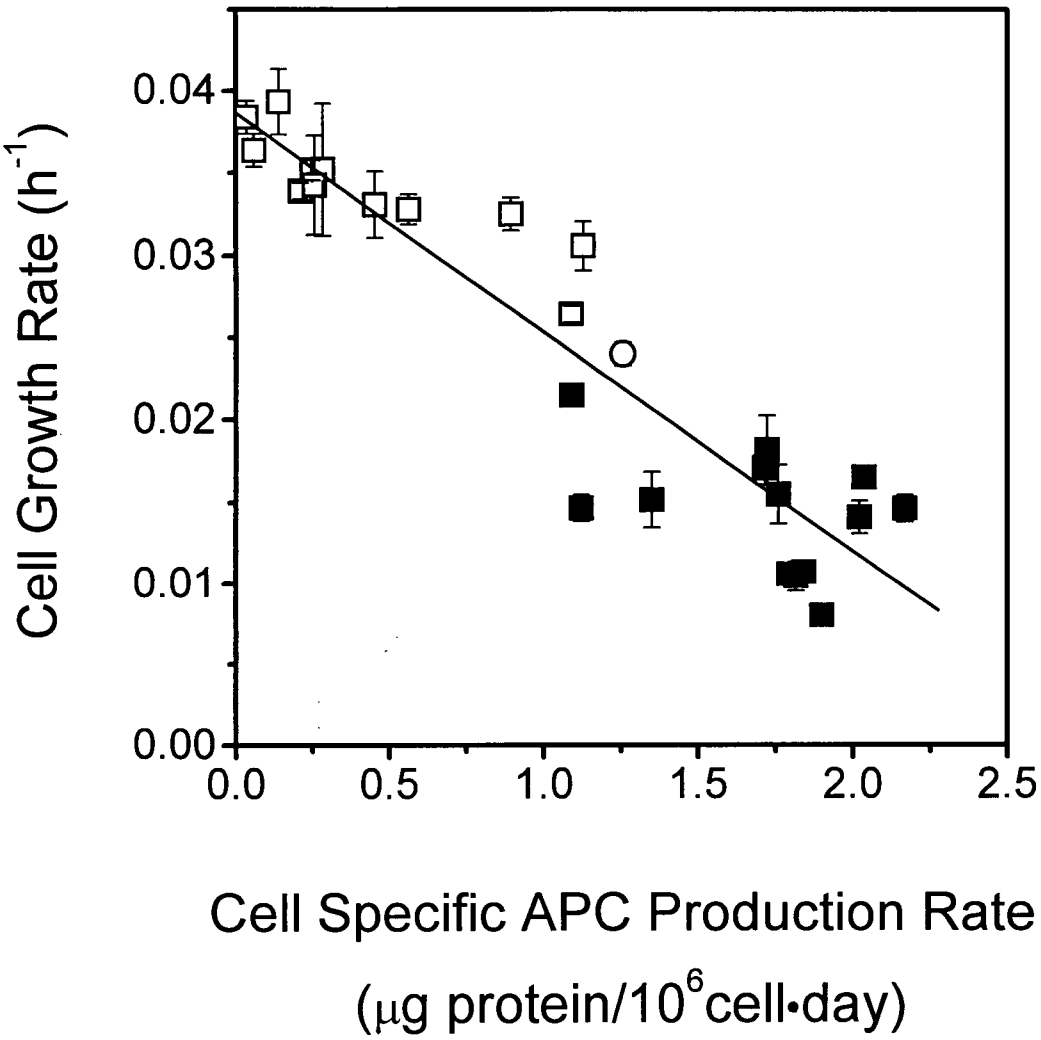

FIGURE 4.12 Relationship between cell specific growth rate and specific APC production rate in all APC producing clones. The original transfected/amplified clones are shown as the open squares. The open circle and the solid squares represent clone 27-4 and the re-transfected clones, respectively.

4.2.8 APC Production in Batch Culture

All of the studies described in previous sections were performed using the exponentially growing cells to reach the quasi-steady state. To investigate the relationship between mRNA level and APC production rate in cell growth phases beside exponential growth, a batch culture in T75 flasks with the cell line 27-4 was performed. The cells grew exponentially for 120 h, followed by a stationary phase from approximately 140 to 190 h, then the cell numbers declined (Figure 4.13A). The percentage dissolved oxygen saturation (%pO_2) levels and the pH values of the culture declined from 18.5 % and pH 7.1 at inoculation, to 14.6 % and 6.7 during the stationary phase (Figure 4.13B). During the decline phase, the pO_2 levels recovered while the pH decreased to 6.5. The glucose concentrations declined rapidly during the exponential phase, ultimately leveling at 3 mM in the decline phase (Figure 4.13C). The lactate concentrations increased during the culture reaching a plateau at approximately 22 mM.

The levels of total RNA, APC mRNA and β-actin mRNA were relatively stable during the lag and exponential growth periods, but rapidly declined once the cells reached the stationary phase and stabilized at a much lower level in the decline phase (Figure 4.14A). The APC concentration produced during the batch culture increased with increasing cell numbers to a maximum in the stationary phase at 5.5 mg/L (Figure 4.14B). As the viable cell number declined, the APC concentrations detected by ELISA decreased to 4 mg/mL by the end of the batch. During the growth phase, while APC concentration increased, the proportion of γ-carboxylated APC decreased and reached a lower percentage (approximately 8% γ-carboxylation) when the APC concentration was at its maximum

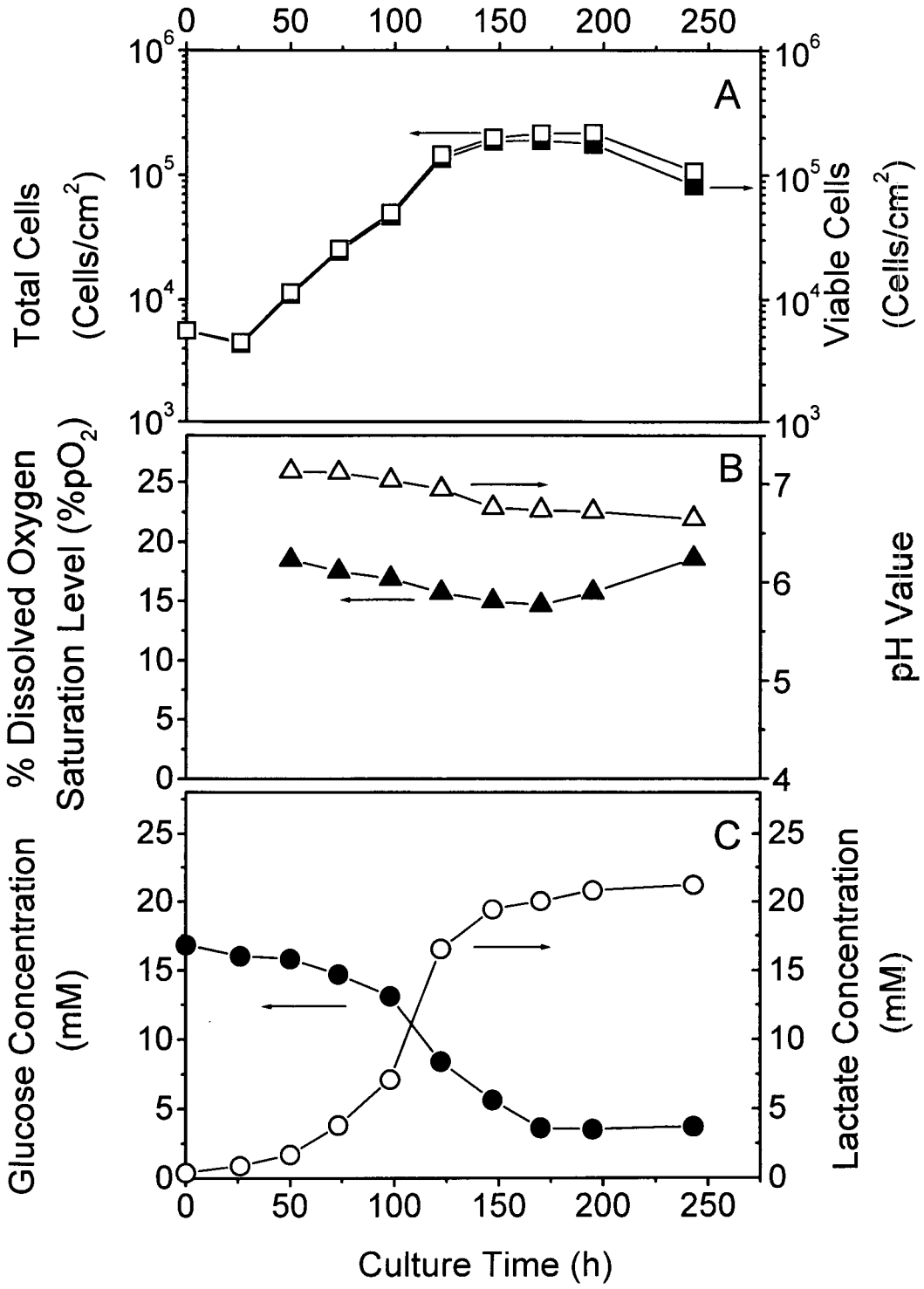

FIGURE 4.13 Batch culture: (A) total (open squares) and viable (solid squares) cell number, (B) dissolved oxygen level (solid triangles) and pH (open triangles), and (C) glucose (solid circles) and lactate (open circles) concentrations.

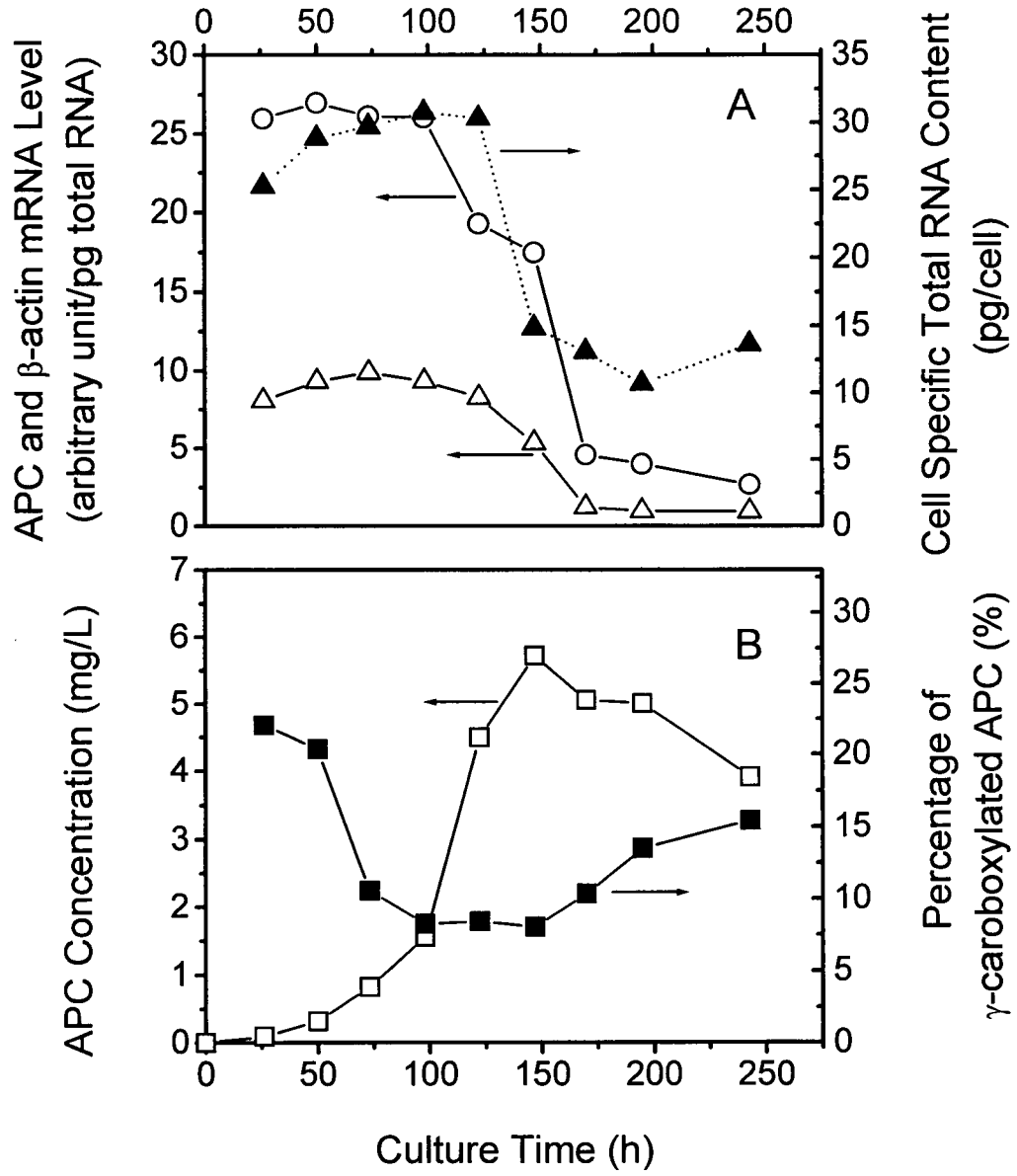

FIGURE 4.14 Batch culture: (A) APC (open circles), β-actin (open triangles) mRNA levels and cell specific total RNA content (solid triangles), (B) APC concentration (open squares) and percentage of γ-carboxylated APC (solid squares).

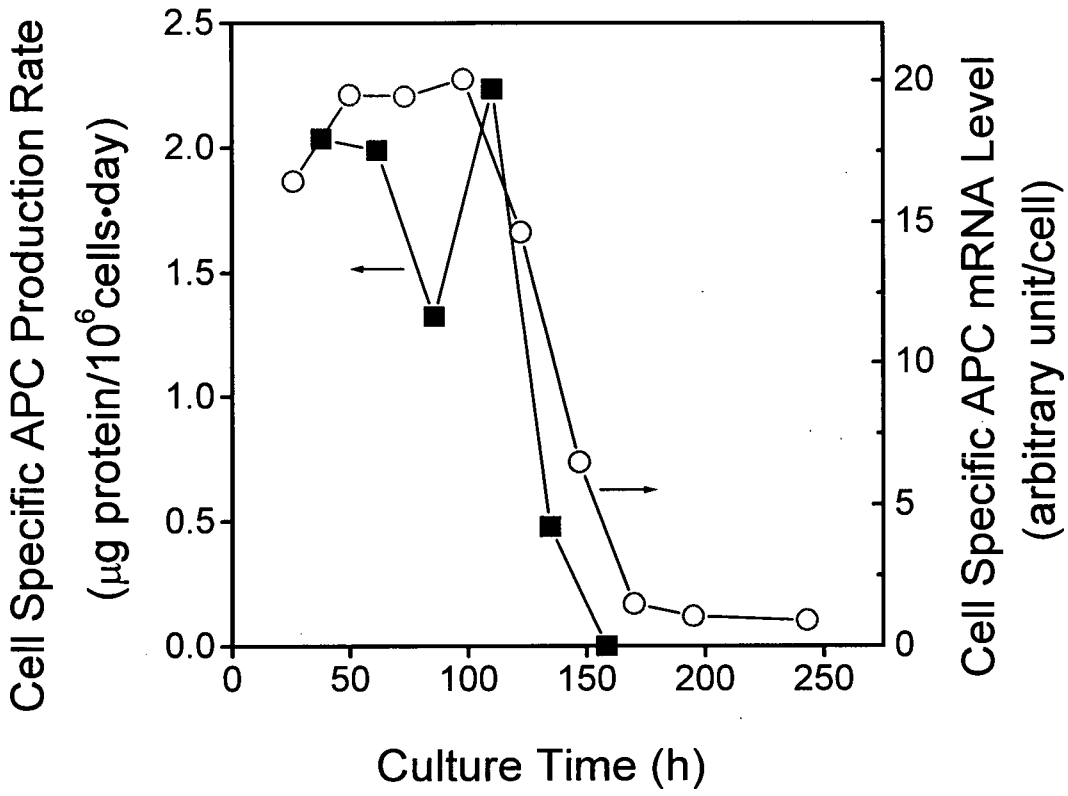

FIGURE 4.15 APC secretion rate (solid squares) and APC mRNA level per cell (open circles) during the batch culture.

(Figure 4.14B). Interestingly, the ratio of γ-carboxylated APC increased when APC level decreased in the decline phase.

The cell specific APC mRNA levels were stable during exponential growth, which demonstrated that the cells were close to steady-state. Cell specific APC mRNA levels declined sharply when cells reached the stationary phase and finally were reduced to a very low level in the decline phase (Figure 4.15). Cell specific APC production rates were closely correlated to the cell specific mRNA levels through the exponential and stationary phases. Although low levels of APC mRNA were detected during the decline phase, no apparent APC production was measured (Figure 4.15). These results indicate that APC mRNA levels limited the rates of APC production at least during the exponential and stationary phases in the batch culture.

4.3 DISCUSSION

The effect of cDNA copy number on the production and post-translational modification of recombinant APC was quantitatively determined. At low cDNA copy number, there was an apparent cooperative effect of increasing cDNA dosage on APC production per copy (Figure 4.3). The cell specific APC production rate increased ~35 fold while the cDNA copies per cell only increased from 50 to 240. Thus, APC production per copy increased by 7 fold over this range. Since the term $k_S \mathcal{E}_P$ in Equation (3.8) is a constant in this production range, this non-constant rate of APC production per cDNA copy is likely due to the variations in transcription rate (k_D) or mRNA turn-over

rate (k_m). An increase of protein production per cDNA copy can also be calculated from the data reported by Pendse et al. (1992) who studied MTX amplified CHO cells producing HbsAg and by Gentry et al. (1987), who studied CHO cells producing transforming growth factor beta. Pendse et al. (1992) argued that the high HbsAg mRNA level observed in the highest expressing clone was due to integration of the amplified HbsAg gene in a transcriptionally active chromosomal position. However, we observed a consistent pattern of increasing protein production per cDNA copy in eight independent clones. This consistency of results from independent clones derived from separate experiments argues strongly for an effect of cDNA copy number in this system, not markedly influenced by the inevitable random events associated with transfection and integration of DNA.

The increasing production of APC per cDNA copy observed below about 250 copies of cDNA/cell (Figure 4.2) could be explained by the influence of heterochromatin on the transcription of APC cDNA which is integrated primarily as tandem repeats. Heterochromatin can inhibit the transcriptional activity of genes integrated within several hundred kilobase pairs of the heterochromatin euchromatin junction (Wilson et al., 1990). For higher cDNA copy numbers, integrating in tandem as we observed, a greater proportion of cDNA would be located away from the negative influence of heterochromatin.

Despite the efforts to increase cDNA copy numbers, the maximum APC production reached was only 2.2 μg/10^6cells·day (Figure 4.9B). Processing of the glycosyl core was reported to be rate limiting for the secretion of protein C by a 293 cell line (McClure et al., 1992). However, the saturation of a step in the secretion pathway would not directly

explain the decline in the cell specific production rates at higher cDNA copy numbers (Figure 4.3). At higher expression rates, intracellular degradation could be responsible for the reduced secretion (Pendse et al., 1992). However, pulse-chase experiments of APC production indicated that clones with low or high copy number had similar secretion rates and low intracellular protein degradation. The average retention half-life of APC in BHK cells was approximately 6 h, which was longer than the 2 h half-life reported by McClure et al. (1992) for their protein C production by 293 cells. This retention time variation is at least partially responsible for the production rate difference (maximum 25 $\mu g/10^6$cells·day in 293 cells versus maximum 2.2 $\mu g/10^6$cells·day in BHK cells) as cell specific protein production rate (q_p) is directly controlled by protein secretion rate (k_S) in Equation (3.3). The retention time difference between protein C in 293 cells and APC in BHK cells is probably due to the modified structure of APC.

Cell lines expressing vitamin K-dependent factors, including APC, produce a mixture of partially and fully γ-carboxylated protein (Yan and Grinnell, 1989). Incomplete γ-carboxylation of vitamin K-dependent factors results in partial biological activity (Zhang et al., 1992; Ratcliffe et al., 1993). It has been argued that γ-carboxylase activity is limiting in these cells and this has been the rationale for cotransfecting γ-carboxylase in recombinant cell lines producing vitamin K-dependent factors. However, overexpression of γ-carboxylase did not increase the carboxylation of factor IX (Rehemtulla et al., 1993). We have investigated the degree of γ-carboxylation for clones expressing from 1.13 to 0.06 μg APC per 10^6 cell per day (Figure 4.5). For the nearly 20-fold lower production rates, if γ-carboxylase activity were the only limit to APC processing then a corresponding

large increase in γ-carboxylation might have been expected. Instead, there was only a 3-fold increase in the proportion of fully γ-carboxylated APC. This result suggests that incomplete modification of protein C is due to a more complex combination of factors than a simple γ-carboxylase limitation.

The dependence of recombinant APC production on the increasing mRNA levels was investigated in 25 transfected, amplified and re-transfected clones (Figure 4.9B). Analysis of the APC mRNA levels of the original 8 clones revealed a similar relationship between mRNA level and cDNA copies (Figure 4.7B) as between APC production rates and cDNA dosage (Figure 4.3). The reduction in APC production rate at higher cDNA dosage was mainly due to the decline of APC mRNA level rather than to an increased intracellular recombinant protein degradation rate as has been reported by Pendse et al. (1992) for HbsAg production. The approximately linear increase in APC production rate with increasing mRNA level indicated that the mRNA level limited the rates of APC production.

Sodium butyrate has a variety of morphological and biochemical effects on cultured mammalian cells (Prasad and Sinha, 1976; Kruh, 1982). The induction of gene expression by sodium butyrate has been used to increase protein production in mammalian cells (Dorner et al., 1989; Palermo et al., 1991; Oh et al., 1993). Although the mechanism of sodium butyrate induction is not certain, it is believed that the hyperacetylation of the chromatin structure at the cDNA integration sites may increase recombinant protein production (Prasad and Sinha, 1976; Boffa et al., 1981; Cuisset et al., 1997). Dorner et al. (1989) reported mRNA induction by sodium butyrate treatment from 1.5 to 19-fold for a number recombinant proteins. In our study, there was a 2- to 6-fold increase in mRNA

levels for the five APC producing clones treated with 5 mM sodium butyrate. Although the mRNA level still limited APC production up to 2.7 μg/10^6cells·day, further induction of mRNA levels by sodium butyrate did not increase APC production rates. This could have been due to saturation in the APC secretion pathway or to the inhibitory effects of sodium butyrate on the cells and secretory pathway. The latter hypothesis is consistent with the 18% to 68% decrease in the production rate to mRNA ratio of all the sodium butyrate treated clones (Table 4.1). Sodium butyrate also inhibited cell growth by 30 to 40% as has been previously reported. Dorner et al. (1989) have reported that the secretion of factor VIII was severely reduced following sodium butyrate treatment. Increased GRP levels in factor VIII were believed to be responsible for the decreased secretion. Nonetheless, there was an indication of secretory pathway saturation at approximately 2.7 μg/10^6cells·day for butyrate treated cells (Figure 4.9A).

Similar saturation results were observed in the re-transfected clones (Figure 4.9B). The APC production rate was limited by mRNA level up to approximately 2.2 μg/10^6cell·day, then an apparent saturation was reached at higher APC mRNA levels where there was no further increase in APC production. The additional expression of APC mRNA levels in the re-transfected clones is probably due to the increase of pNUT-1058 insertion, although there might also have been some amplification of the initial insert, ZMB3-1058. The linear correlation between intracellular APC content and mRNA levels (Figure 4.11A) revealed that the intracellular APC levels were proportionally increased with increasing mRNA. However, above 0.8 pg/cell, increased intracellular APC levels did not yield increased APC production rates, apparently due to saturation of the secretory pathway (Figure 4.11B).

Table 4.2 The intracellular kinetic parameters of recombinant APC production by BHK cells. The parameters presented in the table are k_D: transcription rate, k_m: mRNA turnover rate, μ: cell growth rate, ε_R: transcription efficiency, k_R: translation rate, k_S: secretion rate, which two values are reported in the table as (a) data obtained from intracellular t-PA content and APC production rate, and (b) data from pulse-chase analysis, k_P: intracellular protein degradation rate, and ε_P: translation efficiency. NA: not available. The sample number indicates the number of clones analyzed to generate the results.
*In the range of secretory pathway saturation, and **assuming the cells are still at quasi-steady-state without intracellular APC accumulation.

Parameter	Value ± SD		Sample number	Units
k_D	NA		NA	range of mRNA/cDNA·h
k_m	NA		NA	h^{-1}
μ	0.008 ~ 0.04		26	h^{-1}
ε_R	0.002 ~ 0.1		26	range of mRNA/cDNA
k_R	0.005 ± 0.001		8	pg APC/mRNA·h
k_S	0.11 ± 0.007	(a)	6	h^{-1}
	0.12 ± 0.01	(b)	2	h^{-1}
	0.05*		3	h^{-1}
k_P	0.004 ± 0.004		2	h^{-1}
	0.04 ~ 0.05**		3	h^{-1}
ε_P	0.04 ± 0.01		8	pg APC/mRNA

The secretion rate (k_S) was estimated independently in both pulse-chase experiments and intracellular APC content analysis, with the average values of 0.12 ± 0.01 and 0.11 ± 0.007 h^{-1}, respectively (Table 4.2). These similar results indicate that the measurement of intracellular APC concentration and APC production rate may be an easier approach to accurately estimate the secretion rate of mammalian cells.

The substantial drop in the cell growth rates as APC production increased (Figure 4.12) revealed significant negative consequences from amplified production of this recombinant protein. It is not expected that APC production represents a significant overall metabolic burden for the cells (Gu et al., 1996) since even the maximal APC production rates were less than 1% of total cellular protein production. Also, it is unlikely that the low growth rate is a consequence of expressing an active protease since higher production rates of the protein C zymogen have not been obtained using the same expression system. The negative effect of APC production on the growth rate may be an indirect consequence of APC filling the secretory pathway capacity of cells. Several intracellular factors in the ER may be limiting at high APC production rates. For instance, saturation of the glycosylation system inside the ER could cause incomplete N-linked glycosylation of APC at amino acid position 97. Incomplete glycosylation reduces protein C secretion by 70-75% in 293 cells (Grinnell et al., 1991). The reduction in secretion may also be due to the binding of improperly folded proteins to GRP78, which in turn can cause the retention of the proteins inside the ER until they are re-folded or transported for proteolytic degradation (Dorner et al., 1987, 1988).

When the APC production was saturated at higher mRNA levels, according to Equation 3.2, the excess intracellular APC either caused intracellular accumulation as $\frac{d[P_i]}{dt} > 0$ and/or there was an increase in the intracellular degradation rate k_p (Table 4.2). An accumulation inside the cells would result in dilation of the ER, which has been observed for the secretion of factor VIII by CHO cells (Dorner et al., 1989). In other cases, cells have responded by increased protein degradation rates (e.g. HbsAg, Pendse et al., 1992)

The results reported in this chapter underline the importance of selecting appropriate strategies to amplify mammalian cell recombinant production. For example, efforts to increase the cDNA copy number or the mRNA levels (by increasing k_D or reducing k_m) would be appropriate for clones with a non-saturated secretory pathway. On the other hand, it could be useful to increase levels of secretory processing proteins such as PDI or to reduce the levels of GRP 78 (Tuite and Freeman, 1994) to increase the production rate (q_p) in clones not limited by mRNA levels.

The batch culture results revealed a growth related APC production profile. During the exponential growth phase, the cell specific mRNA levels remained high and consequently, the production rates of APC were relatively high. Entry into the stationary phase was correlated with a decrease in the mRNA for β-actin and recombinant APC as well as total RNA (likely due to the decrease in the major extractable component, rRNA). A similar total RNA decrease was reported by Dalili and Ollis (1990) in the analysis of a batch hybridoma cell culture by flow cytometry. The rapid decrease in the APC mRNA (decreased *[mRNA]*) and cellular rRNA (decreased k_R) explain the rapid decrease in the

APC production rate as the cells entered the stationary phase. The change in the RNA levels between the exponential and stationary phases underlined the importance of consistently using exponentially growing cells for our studies comparing different clones.

Since incomplete γ-carboxylation reduces APC anticoagulant activity (Zhang et al., 1992), it is essential to monitor APC γ-carboxylation as well as maximize the amount of APC produced. The quality of the APC varied during the batch culture as the ratio of γ-carboxylated APC decreased from 22% in the early exponential phase to 8% in the stationary phase (Figure 4.14B). Changes in recombinant protein quality have also been reported by Curling et al. (1990) for γ-interferon production where the non-glycosylated γ-interferon increased 30% during 195 h in a batch culture and by Sugiura and Maruyama (1992) who reported 46% less γ-carboxylated protein C in a larger culture (2 L vs. 125 mL).

In conclusion, the analysis of APC production in many clones as well as in batch culture suggested that at most lower expression rates the mRNA levels limited APC production, indicating transcriptional rather than secretory pathway limitations (Pendse et al., 1992; Schroder and Friedl, 1997). Treatment with sodium butyrate or re-transfection did yield clones with decreased APC production rate per mRNA. Analysis of the intracellular APC content suggested that this decrease was due to secretory pathway limitations.

CHAPTER 5

LIMITATIONS TO THE AMPLIFICATION AND STABILITY OF HUMAN TISSUE-TYPE PLASMINOGEN ACTIVATOR EXPRESSION BY CHINESE HAMSTER OVARY CELLS

5.1 INTRODUCTION

Although gene amplification has been widely studied, only a few reports attempted to address the production stability after amplification, and in even fewer cases, to define the maximum stable protein production rates that could be achieved by amplification. With the aim to understand these two issues, t-PA production was chosen in this study since it allows comparison of our results with those obtained by several other groups. CHO cell growth rates and cell specific t-PA production rates were closely monitored during stepwise amplification and subcloning in increasing MTX concentrations. These approaches were to analyze the amplification kinetics and to investigate the limitations to the maximum t-PA production rate that could be achieved in the presence of selective pressure. Moreover, stability of t-PA expression without MTX selection was also studied in serum-containing and serum-free cell cultures, and subcloning in different culture conditions was performed in an attempt to acquire high and stable t-PA producing clones. Taken together, these investigations provided the rationale for developing a bulk amplification strategy to shorten the usually tedious and labor-intensive amplification work, and finally leading to selection of a reasonably high and stable clone for recombinant protein production.

5.2 RESULTS

5.2.1 Amplification of CHO Cell t-PA production

The MTX amplification of three out of the four initial clones increased their cell specific t-PA production by 5- to 17-fold, from the basal levels of 500 and 600 U/10^6cells·day to 2,600 and 10,600 U/10^6cells·day, respectively (SI12-5 and SI9-24 in Figure 5.1), while the cell specific t-PA production rates of the fourth (SI12-7) decreased 4-fold from 1,500 to 400 U/10^6cells·day. A replicate amplification of the SI12-5 clone was performed with a more detailed analysis of the cell growth and t-PA production rate. A high growth rate was maintained during the selection in 0.04 μM MTX, but this decreased dramatically after transfer to 0.2 μM MTX (Figure 5.2). The decrease and variability in cell growth rates indicated significant selection pressure. After each subsequent MTX concentration increase, the cell specific growth rates declined sharply as the cells adapted to the new level of selection. The criterion for transferring the cells to a 5-fold higher MTX concentration was that their growth rates had recovered to 0.02 h^{-1} or above. The amplified population growth rate usually recovered within 10 to 20 days (Figure 5.2).

As the MTX concentration was increased, the cell specific t-PA production rates of the cell population increased in a fluctuating pattern gradually for MTX concentration increases up to 1 μM MTX (Figure 5.3). At 5 μM MTX, a rapid increase in cell specific

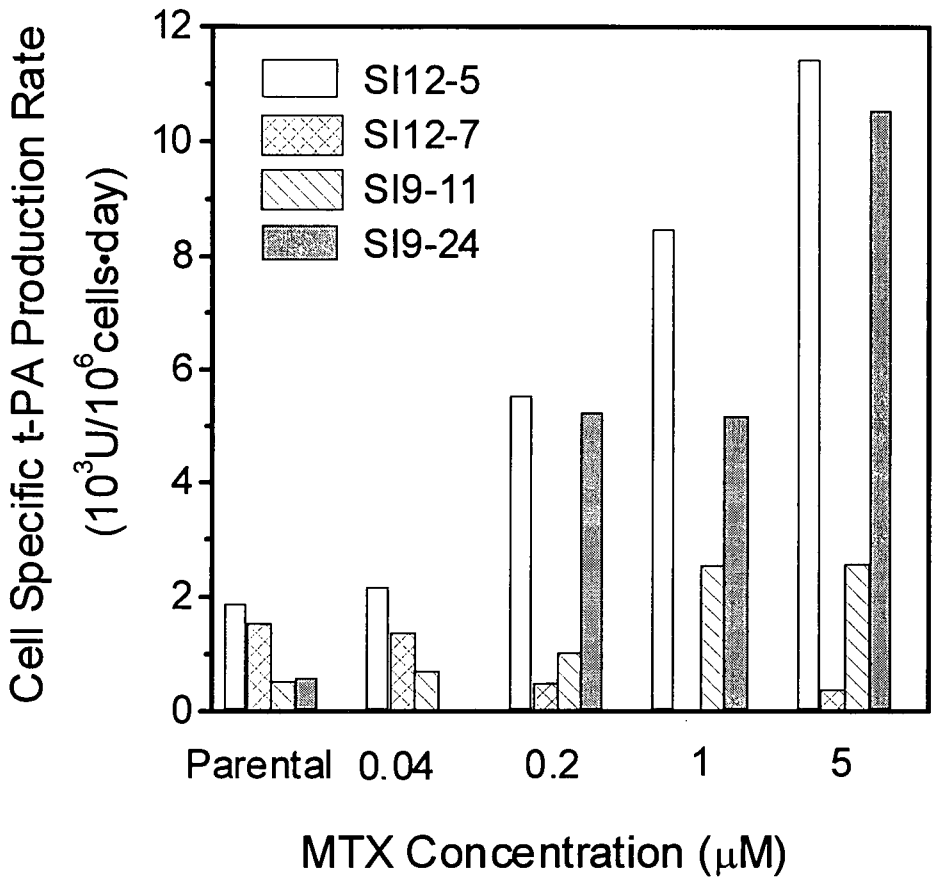

FIGURE 5.1 Four parental t-PA producing cell lines, SI9-11, SI9-24, SI12-5 and SI12-7 were amplified with increasing MTX concentrations from 0.04 to 5 μM. The culture duration in each MTX concentration was approximately one month.

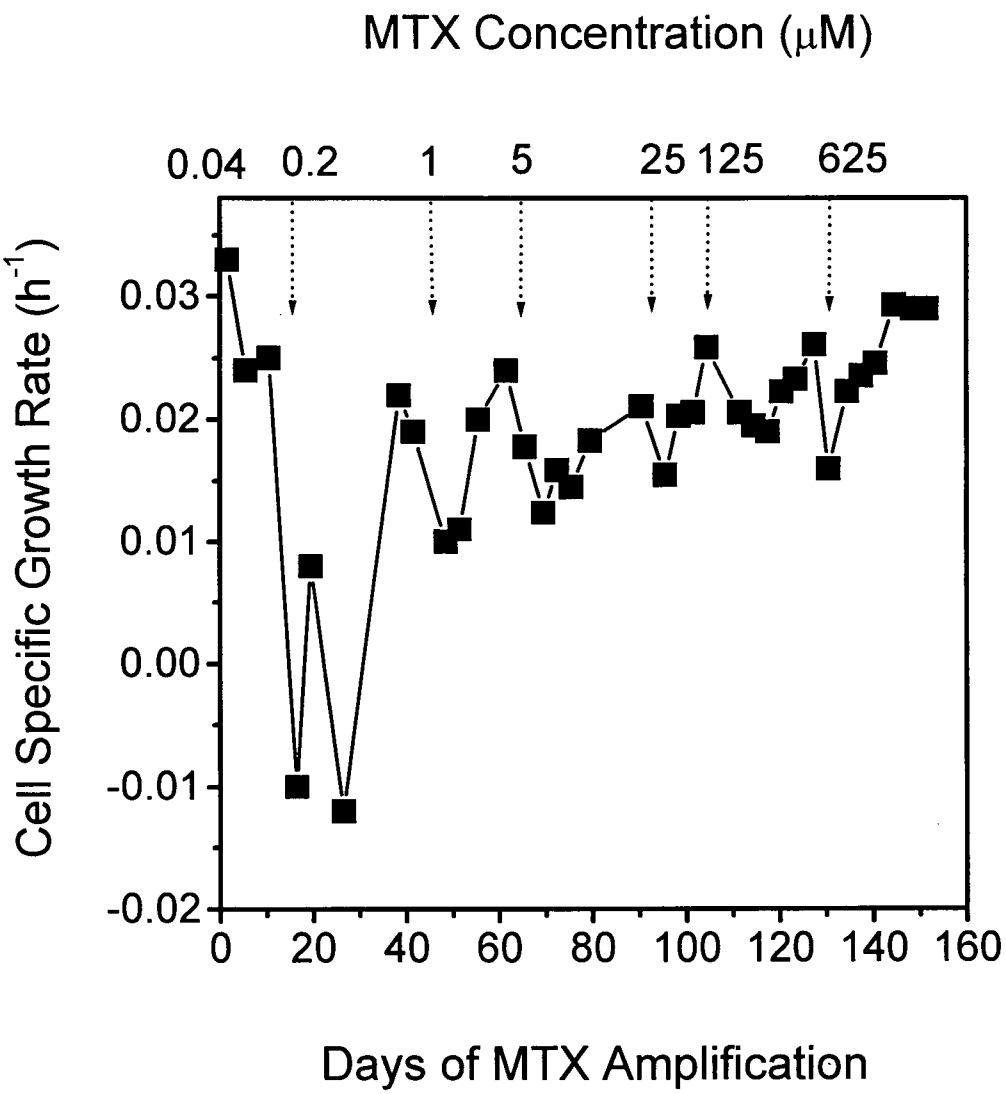

FIGURE 5.2 The specific growth rates during the replicate SI12-5 amplification. The vertical dashed arrows indicate the times in which MTX levels were increased.

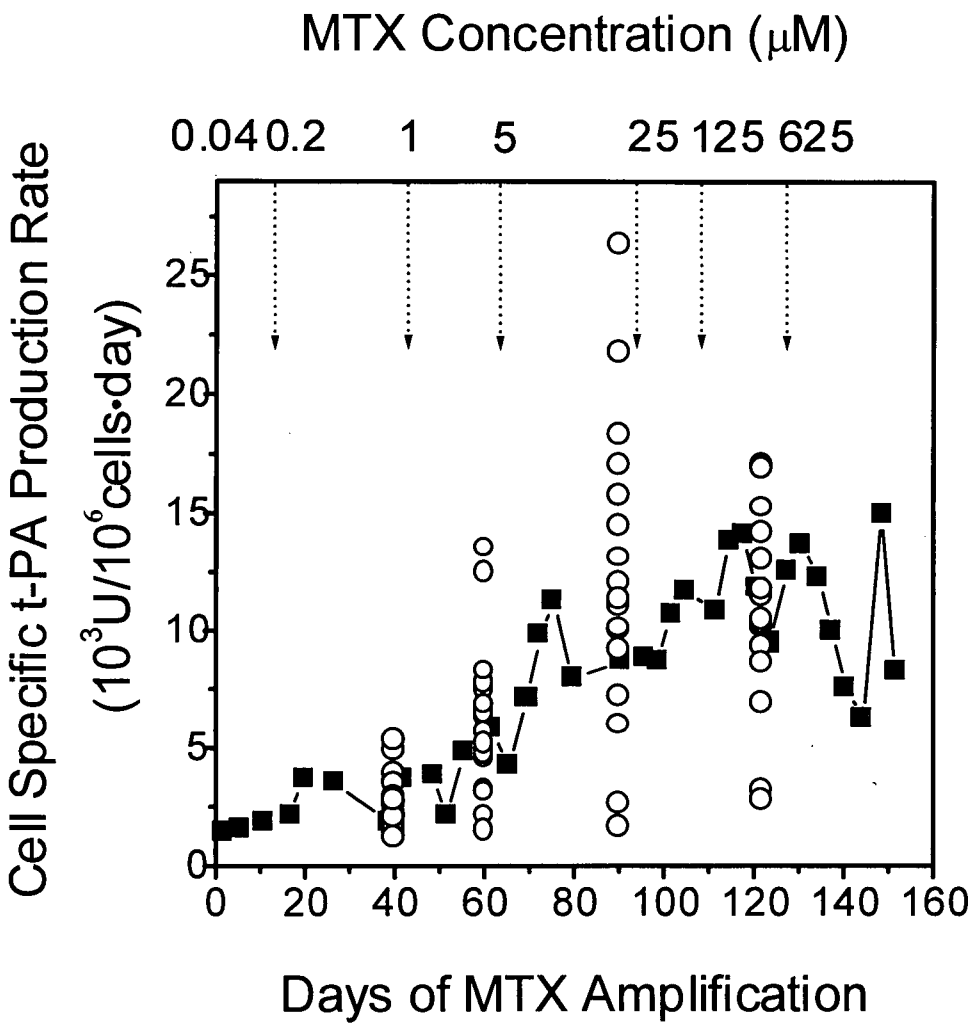

FIGURE 5.3 The t-PA production rates (solid squares) during the replicate SI12-5 amplification. The vertical dashed arrows indicate the times in which MTX levels were increased. The bulk amplified cells were subcloned at 0.2, 1, 5 and 125 μM MTX and the cell specific t-PA production rates of the resulting subclones are shown as the open circles.

t-PA production rate from 4,000 to 11,000 U/10^6cells·day was obtained. Further amplification at 25, 125 and 625 μM MTX yielded a bulk population having a t-PA production rate as high as 15,000 U/10^6cells·day. However, this higher t-PA production rate was not stably maintained. The production rate was more unstable at 125 and 625 μM MTX while no significant additional increase in the t-PA expression was measured.

The average cDNA copy numbers (Figures 5.4A and 5.4B) of the SI12-5 cell population increased from 50 copies per cell to 160 copies per cell, when the t-PA production rates reached 11,000 U/10^6cells·day at 5 μM MTX (Figure 5.3). Interestingly, the highest cDNA copy number of approximately 400 was observed at 25 μM MTX, but the cell specific t-PA production rate at this MTX level (maximally 12,000 U/10^6cells·day) was not significantly higher. At higher MTX concentrations, the average cDNA copy number declined, ultimately reaching 140 copies per cell at 625 μM MTX.

Limiting dilution of the cells was used to analyze the heterogeneity of the bulk amplified populations at 0.2, 1, 5 and 125 μM MTX (Figure 5.3). The clonal distribution at 0.2 μM MTX showed a range of cell specific t-PA production rates from 1,100 to 4,700 U/10^6cells·day, with a mean of 2,500 U/10^6cells·day compared to 2,800 U/10^6cells·day for the bulk amplified cells at the same MTX level (Table 5.1). The range of clonal production rates increased with increasing MTX concentrations up to 5 μM, where t-PA production rate ranged from 1,600 to 26,000 U/10^6cell·day. Thus, the bulk amplified cell populations were highly heterogeneous.

The integration of transfected t-PA cDNA in chromosomes was localized by FISH at three MTX selection levels (Figure 5.5), 1 μM, 125 μM, and 625 μM. The t-PA

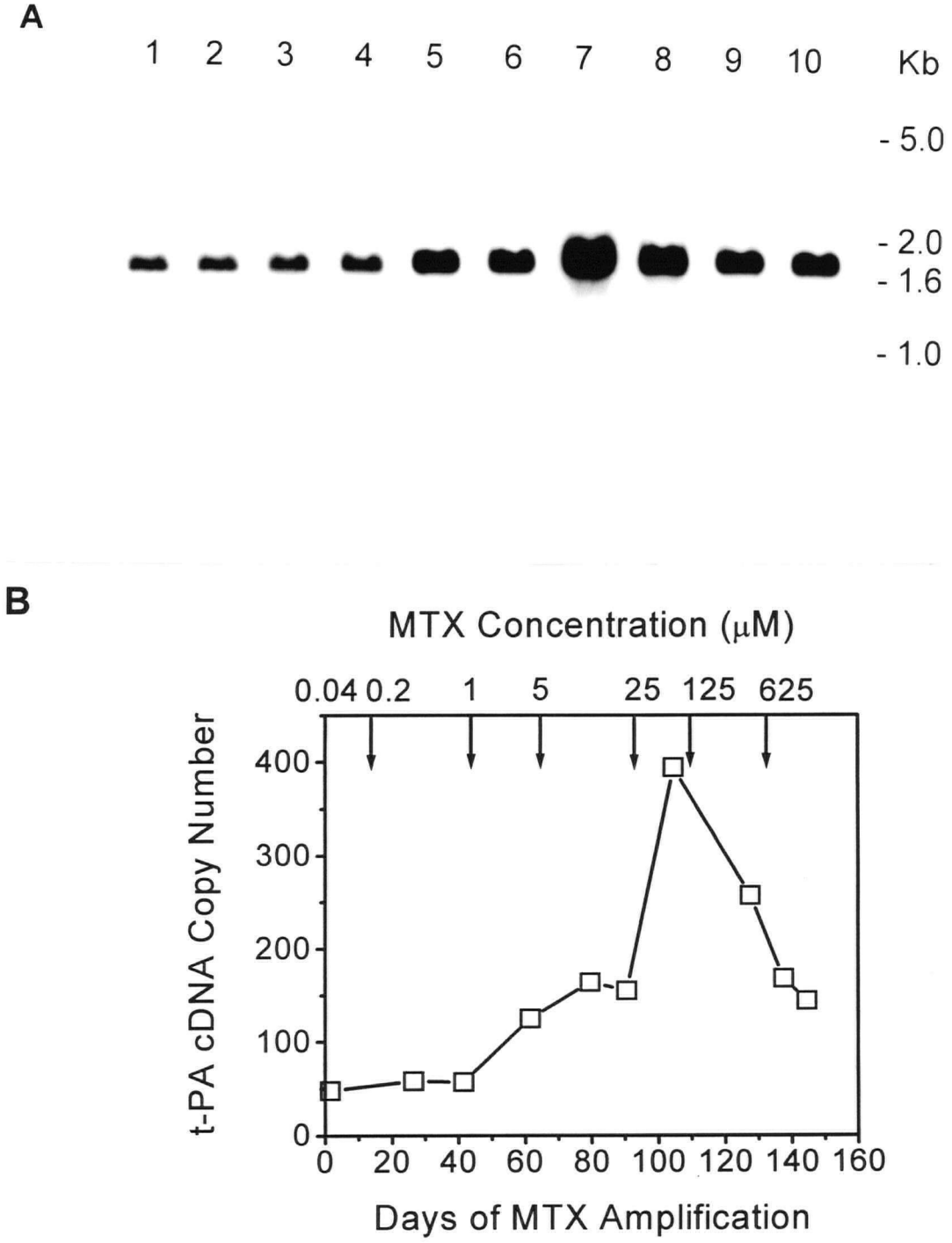

FIGURE 5.4 (A) Southern blot analysis of genomic DNA isolated from SI12-5 cells during the replicate amplification. DNA loaded in Lane 1: day 0 (no MTX); Lanes 2 and 3: days 15 and 30 (0.2 μM MTX); Lane 4: day 50 (1 μM MTX); Lanes 5 and 6: days 64 and 79 (5 μM MTX); Lane 7: day 93 (25 μM MTX); Lane 8: day 116 (125 μM MTX); Lanes 9 and 10: days 129 and 136 (625 μM MTX). Each lane of the agarose gel (1.2%) was loaded with 2 μg of genomic DNA. The material was transferred to a membrane and hybridized with a DIG-labeled t-PA DNA probe. (B) The calculated t-PA cDNA copy numbers during the replicate amplification. The vertical dashed arrows indicate the times in which MTX levels were increased.

TABLE 5.1 Cell specific t-PA production rates (A) and cell specific growth rates (B) of the amplified bulk populations and subclones shown in Figure 5.3.

A

MTX Concentration (μM)	Cell Specific t-PA Production Rates ($U/10^6$cells·day)		
	Bulk Amplified Cells	Subclones	
		Mean	Range
0.2	2800	2500	1100 - 4700
1	5800	5300	1260 - 11610
5	8600	12200	1600 - 26300
125	11800	10700	2700 - 17000

B

MTX Concentration (μM)	Cell Specific Growth Rate (h^{-1})		
	Bulk Amplified Cells	Subclones	
		Mean	Range
0.2	0.020	0.019	0.014 - 0.028
1	0.019	0.017	0.008 - 0.023
5	0.018	0.015	0.003 - 0.026
125	0.022	0.023	0.014 - 0.032

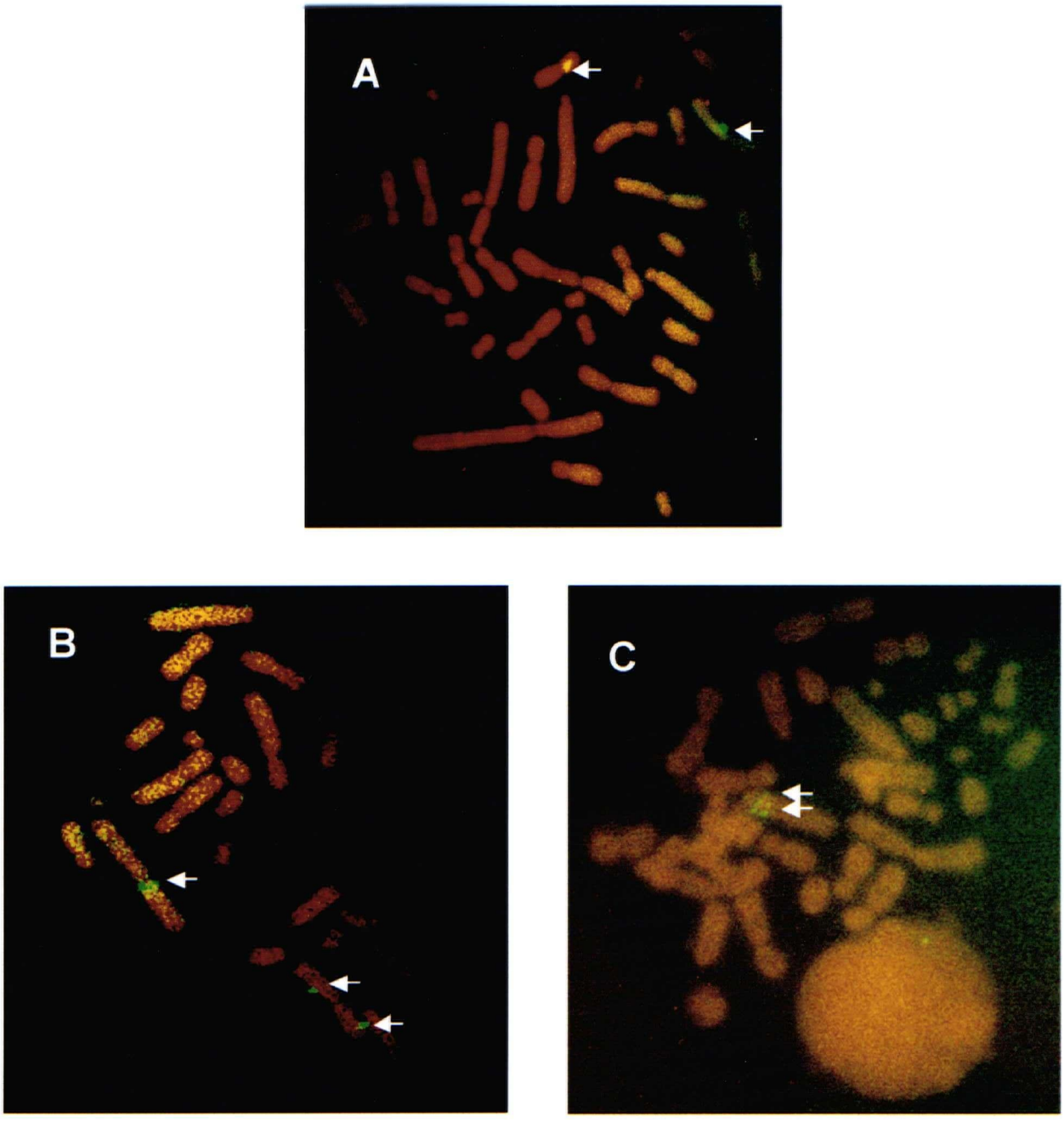

FIGURE 5.5 FISH analysis of the replicate SI12-5 amplification. SI12-5 cells analyzed at some MTX selection levels as (A) 1 μM (day 64 in Figure 5.3) (B) 125 μM (day 110) and (C) 625 μM (day 145).

cDNA integrated as small cDNA clusters whose numbers increased with increasing cDNA copy number up to 3~4 clusters at 125 μM MTX (Figure 5.5B), when the average t-PA cDNA copy number was close to the maximum (approximately 400 copies). Each cluster possibly contained more than 100 t-PA cDNA copies as shown in Figure 5.5A (approximately 250 cDNA copies in 2 clusters), which implying integration in tandem repeats. All t-PA cDNA clusters localized in chromosomes, no transfected genes were observed in small circular DNA.

Interestingly, high t-PA producing clones were maintained and recovered from these bulk amplified populations despite the presence of many low producing cells. The cell growth rates of the clones were evaluated to assess whether low producing clones would have higher growth rates. Instead, these rates were randomly distributed over a wide range, from 0.003 to 0.032 h^{-1} (Table 5.1), without a correlation between t-PA production rate and cell growth rate, as illustrated by the values obtained for the 0.2 μM MTX subclones (Figure 5.6). Overall, the mean t-PA production rate and cell growth rates of the subclones correlated with the values for the corresponding bulk cell populations (Table 5.1).

5.2.2 Stability of t-PA Production in MTX Amplified Cells

Two clones isolated from the SI9-24 cell bulk amplification at 1 μM MTX (SI9-24.16 and SI9-24.17) and two isolated at 5 μM MTX (SI9-24.m and SI9-24.r) were cultured for another 89 days, in the presence or absence of the cloning MTX levels (Figure 5.6). When cultured in MTX, the two lower producers, SI9-24.16 and SI9-24.m, were

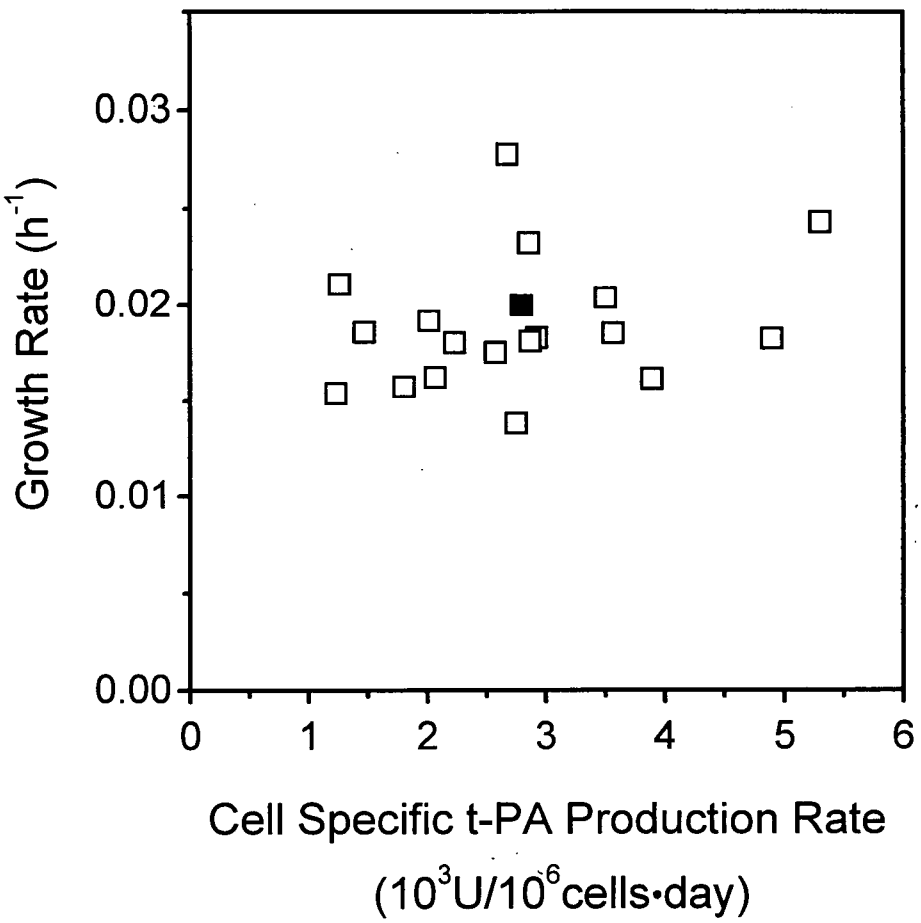

FIGURE 5.6 The cell specific t-PA production rates and cell specific growth rates of the clonal subpopulations (open squares) obtained from bulk amplified SI12-5 cells. The cells were selected and cloned at 0.2 μM MTX on day 30. The solid square represents the t-PA production rate and cell specific growth rate of the bulk population from which the clones were derived.

relatively stable. The SI9-24.17 and SI9-24.r cells, which both originally produced greater than 10,000 U/10^6cells·day, lost 35% and 40% of their t-PA production rates, respectively. In the absence of MTX, the t-PA production rate of all four clones decreased by more than 60% within the first 50 days, and all tended toward a more stable rate around 1,500 U/10^6cells·day at 89 days.

In an effort to isolate more stably expressing clones, the SI9-24.17 cells were cloned again after 108 days of culture in the absence of MTX. These new clones showed a range of t-PA production rates from 270 to 3,500 U/10^6cells·day (Figure 5.7B). Three of the high producing subclones were cultured without MTX for another 116 days and had lost from 30 to 60% of their t-PA production rate by the end of the culture. However, the slower decrease in t-PA production rate of these 3 clones compared to their parental cells (Figure 5.7A) appears to reflect a stabilization in the t-PA production rate.

To compare these rates of production rate decay more quantitatively, a first order equation was formulated:

$$\frac{dq_p}{dt} = -k_a q_p \qquad (5.1)$$

where q_p is the average cell specific t-PA production rate (U/10^6cells·day), t is the time (day), and k_a is the cell specific t-PA production decay rate (day^{-1}). The k_a for the cells in MTX and the cells after adaptation to MTX-free culture were similar, while in the period after transfer from MTX-containing to MTX-free medium, the decay constant was approximately an order of magnitude higher (Table 5.2).

The decline of t-PA production rate observed for the SI9-24.17 and SI9-24.m cells following transfer to MTX-free medium was accompanied by a decrease of the t-PA

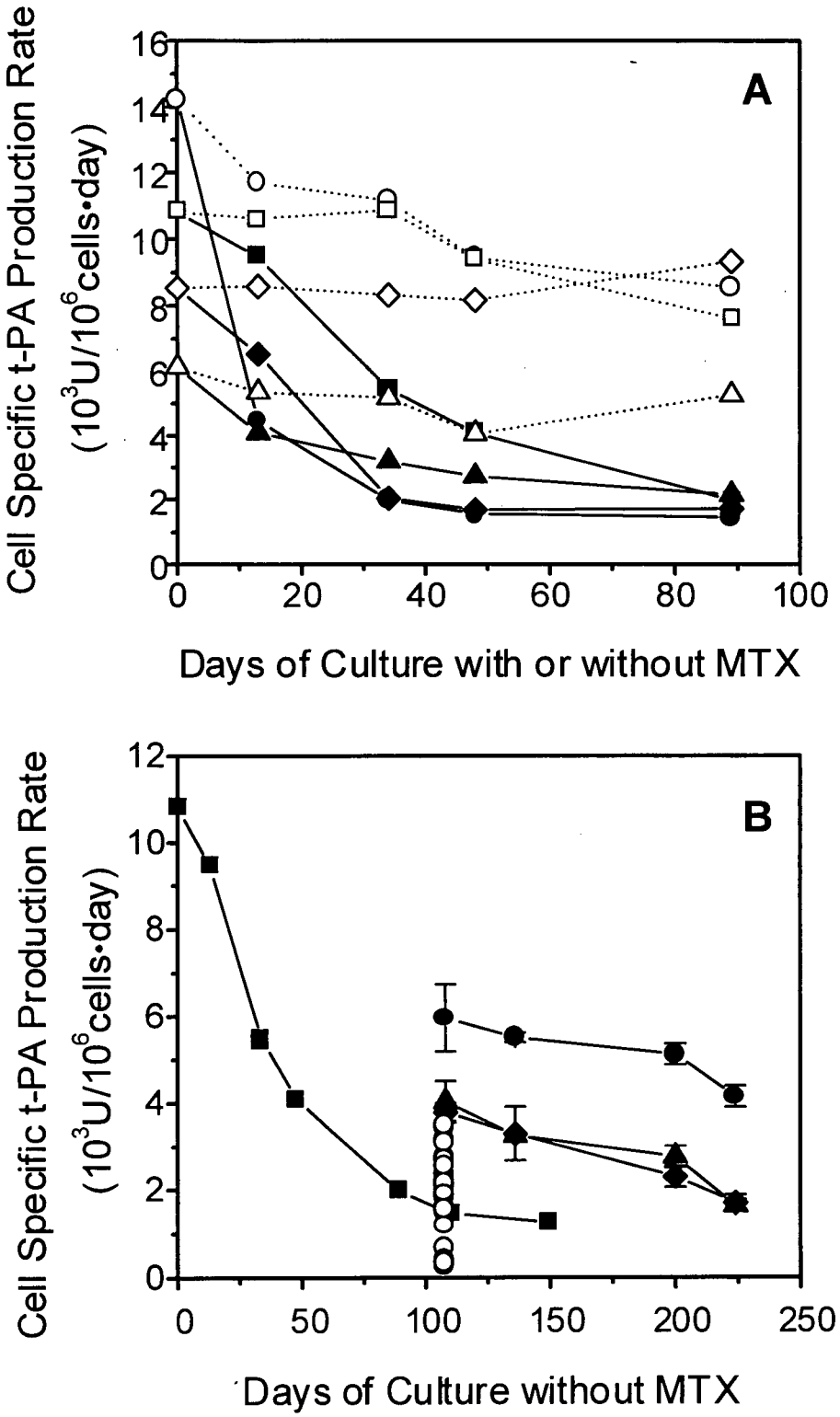

FIGURE 5.7 The stability of SI9-24 subclones cultured in the presence and absence of MTX. (A) Cells cloned in 1 μM MTX (SI9-24.16, solid triangles and SI9-24.17, solid squares) and 5 μM MTX (SI9-24.m, solid diamonds and SI9-24.r, solid circles) were transferred to MTX-free culture (solid lines). The same clones cultured in their cloning MTX concentrations are shown as the open symbols and dotted lines. (B) Clone SI9-24.17 was subcloned after 108 days without MTX (28 subclones are represented by open circle symbols on day 108) and three of these subclones were further cultured without MTX (C17.5, solid triangles, C17.11, solid diamonds, and C17.21, solid circles).

TABLE 5.2 Summary of the kinetics of cell specific t-PA production rate decrease with or without MTX selection.

Initial MTX Concentration (μM)	Analyzed MTX Concentration (μM)	Clones Analyzed	Average k_a (d^{-1})
1 or 5	1 or 5	4	0.003 ± 0.002
1 or 5	0	6	0.03 ± 0.02
0	0	8	0.005 ± 0.002

The first row includes 4 clones in MTX, where the average k_a was calculated based on the period of 90 days in Figure 5.7A. The second row includes the same 4 clones (90 days in Figure 5.7A) without MTX as well as the SI12-5.23 cells (148 days in Figure 5.9). The third row includes 8 clones, 3 of them were SI9-24 derived clones without MTX (116 days in Figure 5.7B), the rest 5 clones were derived from SI12-5.23 in serum-free culture (144 days in Figure 5.9).

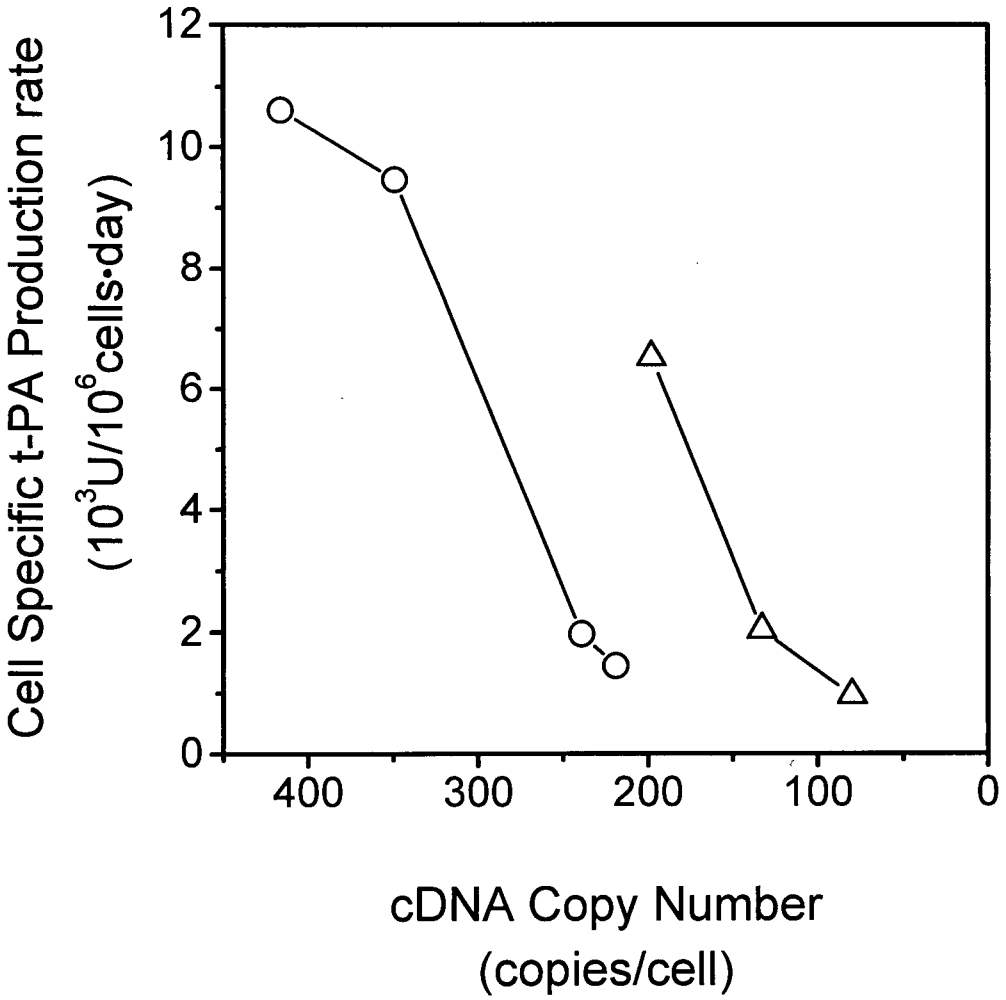

FIGURE 5.8 Decrease of cell specific t-PA production rates with decreasing cDNA copy number in the absence of MTX for SI9-24.17 (open circles) and SI9-24.m (open triangles).

cDNA copy number (Figure 5.8). However, while the t-PA production rates both decreased by approximately 7-fold, the t-PA cDNA copy numbers declined by only 1.9- and 2.5-fold, respectively. This decreasing expression per cDNA copy number would indicate that cDNA copies responsible for high expression were more prone to being lost. Upon adaptation of these cells to serum-free culture over 20 days, SI9-24 derived clones lost t-PA expression rapidly to below 250 U/10^6cell·day. Because of this phenomenon, subsequent clone selection was always performed after adaptation of the cell populations to serum-free medium.

The stability of the t-PA production by independently derived SI12-5 cells was also investigated. The highest t-PA producing subclone, SI12-5.23, isolated at 5 μM MTX (Figure 5.3) was adapted at the same time to serum-free and MTX-free medium. The t-PA production rate declined from 15,000 U/10^6cells·day to approximately 6,000 U/10^6cells·day (60% loss) within 54 days of culture in both serum-free (Figure 5.9, solid line) and 10% FBS serum-containing cultures (Figure 5.9, dotted line). This indicated that the removal of the MTX selective pressure and not the adaptation to serum-free conditions was responsible for the instability and decline in t-PA production rate. The t-PA production rates subsequently stabilized at approximately 6,000 U/10^6cells·day, for 60 days in serum-free medium. The SI12-5.23 cells were then re-cloned after 121 days, yielding 9 subclones with t-PA production rates varying from 2,000 to 11,500 U/10^6cells·day (Figure 5.9). Five of the subclones were cultured for another 144 days and again, a progressive decline in t-PA production rates was observed. However, further cultivation of the 23SFM1 subclone cells yielded a stable and relatively high level t-PA production (approximately 7,000 U/10^6cells·day), which was maintained for over 250 days

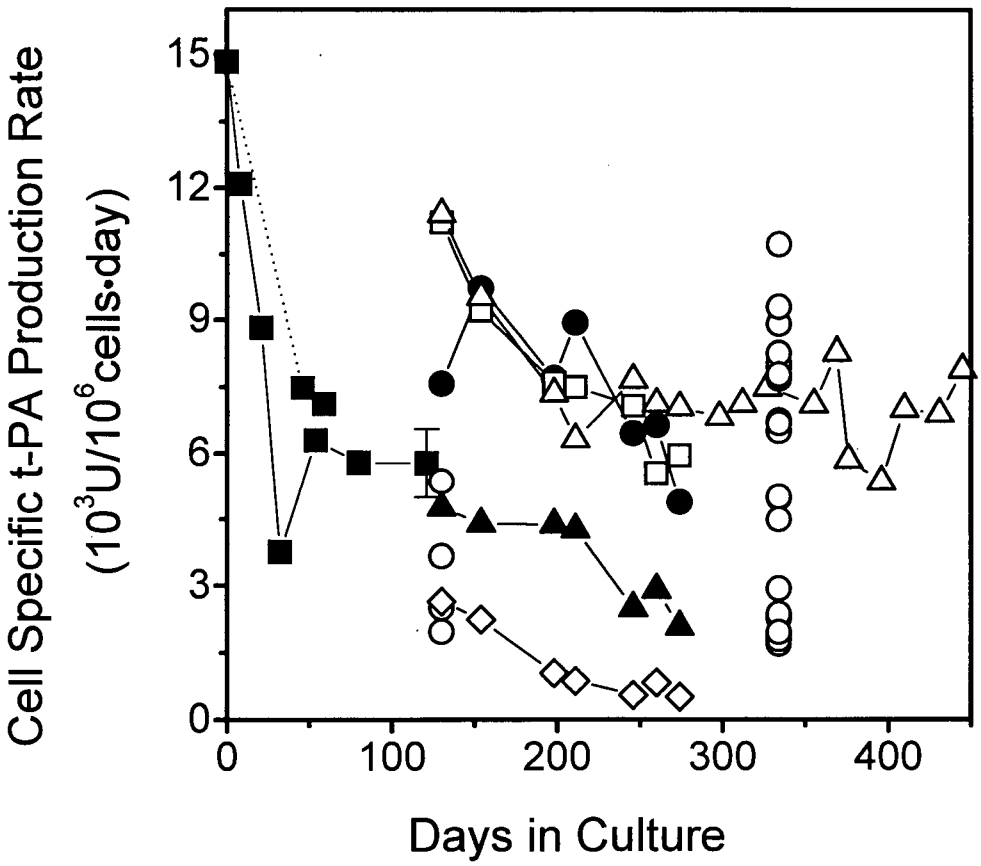

FIGURE 5.9 The SI12-5.23 cells (solid square symbols) were transferred to MTX-free medium on day 0 and adapted to serum-free medium within the first 21 days of this culture. A parallel culture of these cells in MTX-free IMDM/10% FBS medium is shown using the same symbols and dotted lines. After 130 days of serum-free culture, the SI12-5.23 cells were subcloned and 5 of the resulting clones were further cultured for an additional 150 or more days (23SFM1, open triangles; 23SFM2, open squares; 23SFM3, solid circles; 23SFM4, solid triangles; 23SFM5, open diamonds). An additional subcloning of 23SFM1 cells was performed and these subclones are prepared by the open circles on day 340.

in serum-free medium. Interestingly, this result was obtained despite a limiting dilution which indicated that this cell population was approximately as heterogeneous with respect to t-PA production rate at day 340 as its parental population was at day 121 (Figure 5.9). The average stability kinetics are tabulated in Table 5.2 for the comparison of cell cultures in the presence of MTX, in the transition state from MTX to MTX-free, or in the MTX-free state.

5.3 DISCUSSION

Amplification of cDNA has been a common strategy for increasing recombinant protein production in mammalian cells. However, cDNA amplification is a labor intensive task and clonal specific protein production rates are often unstable when the selective pressure is removed. The amplification and stability of t-PA expression in this study illustrate recommendations for efficient amplification and cloning in order to obtain a high production rate and stable production cell line.

The considerable time and labor required for MTX selection has motivated the development of alternative methods to more rapidly obtain high t-PA production rate. For instance, high copy electroporation (Barsoum, 1990) transfects more cDNA into the cells, allowing rapid selection of higher producing cells and thereby eliminating the need for amplification. Using this method, CHO clones with a maximum t-PA production rate of 21 $\mu g/10^6$cells·day were obtained within 1 month after electroporation (Barsoum, 1990).

High copy number transfection can be expected to reduce the duration and labor of amplification by more rapidly isolating relatively high producing cells.

Rather than subcloning and amplifying multiple subclones at each MTX level as reported by others (Michel et al., 1985; Zettlmeissl et al., 1987), bulk amplification was chosen as a less labor intensive method to generate high producing clones. After each of the 5-fold MTX concentration increases above 0.2 μM, a sharp decrease in growth rate followed by a recovery over approximately 10 days was observed. Although a recent report (Kim et al., 1998a) described a continuous decrease in CHO cell growth rates with increasing MTX levels, we observed no significant effects of increasing MTX concentrations on the maximum cell specific growth rate at each MTX level. The good correlations in cell specific growth rates and t-PA production (r - 0.88 and 0.98, respectively) between the mean clonal values and the corresponding bulk amplification data (Table 5.1) indicated that the cell population in the mixed bulk amplified cells was well-represented by the subclones. This result verified the significance of using the cell clonal approach for characterizing the heterogeneous cell populations in amplified cells as reported by other groups (Sinacore et al., 1995; Kim et al., 1998a).

The cell specific t-PA production rate increase during the amplification was correlated (r - 0.87) with the average change in cDNA copies (Figure 5.3 and 5.4B) before reaching 25 μM MTX. At 25 μM MTX, the additional t-PA cDNA copies were apparently transcriptionally less active. These results indicate that the maximum t-PA production rate that could be achieved is limited by simply increasing cDNA copies. Using FISH analysis of cDNA in MTX selected cells, Wurm and co-workers reported increased heterogeneity of *c-myc* or CD4IgG integration upon amplification (Pallavicini et

al., 1990; Wurm et al., 1992; Wurm and Petropoulos, 1994). They also demonstrated that these integrated amplicons, which existed in 40-60% of the amplified CHO cell populations were genetically unstable. The different locations of integrated t-PA cDNA clusters in our FISH analyses at various MTX levels supported their conclusion, and showed that the unstable t-PA amplicons may undergo frequent re-arrangement both during the amplification and in MTX-free medium, resulting in the observed high t-PA production variations. However, the dissociation between DHFR and t-PA cDNA at high MTX selection could also contribute to these production rate variations (Kaufman et al., 1985).

The rapid 5 to 10-fold t-PA expression decrease in both serum-containing and serum-free cultures within the first 50 days without MTX was similar to that observed in the reports of Weidle et al. (1988) and Sinacore et al. (1994), as their t-PA production rate declined from 37 to 10 $\mu g/10^6$cells·day or the production levels of a recombinant protein decreased from 6 to 1 $\mu g/10^6$cells·day by CHO cells, respectively. Our study as well as these two reports also observed a final stabilized recombinant protein production rate after approximately 50 days without MTX. Apparently, the average decrease in the rate of t-PA production rate, as presented by the production rate decay rate k_a, was approximately 10-fold faster for the cells being transferred from MTX-containing to MTX-free culture than for their counterparts maintained in the MTX-containing culture but without significant change in specific growth rate (Table 5.2). These results are consistent to a recent report (Kim et al., 1998b) that a significant decrease in antibody production rate but not cell growth rate was observed for the CHO cell clones cultivated from MTX to MTX-free medium for 8 weeks. Interestingly, while high producing clones generally had cell

specific production rate loss in the absence of MTX, the production stability was more controversial when the t-PA production rate was lower than 10 μg/10^6cells·day. Kaufman et al. (1985) observed no production rate decrease in two relatively high producing clones (q_P = 2 and 5 μg/10^6cells·day, respectively) after 30 and 38 cell doublings in the absence of MTX, whereas other low producing clones suffered great production rate loss (up to 6-fold) during the same period of time. Similar stability trends were observed by Kim et al (1998b) on the studies of chimeric antibody production by CHO cells, and based on the observation that high producing clones stabilized at higher production rate levels, they suggested that this relationship could be used to predict the clonal stability after MTX amplification. However, we did not observe such an apparent trend between amplified and stabilized expression levels; instead, the final stable t-PA production rates seemed to be unpredictable from the clones we have analyzed.

Clones with low t-PA production rates of between 1,100 and 2,700 U/10^6cells·day were frequently isolated from the amplified populations. However, the growth rates of the subclones were found to not correlate with the t-PA production rates (Figure 5.6), and the low producers did not come to dominate the populations, at least up to 5 μM MTX. These results were consistent with the reports that higher production rates of recombinant CD4IgG were not correlated with lower population growth rates (Wurm et al., 1992).

Goeddel et al. (1989) reported the highest production rate of 18 μg/10^6cells·day without MTX selection (Table 5.3), but the stability of this production level was not reported. Those cells could have been recently transferred to MTX-free medium, such as the day 130 cells (Figure 5.9) producing 12,000 U/10^6cells·day (~ 20 μg/10^6cells·day). The unstable t-PA production up to ~43 μg/10^6cells·day and stable production up to

TABLE 5.3 Summary of reported high recombinant t-PA production rate by CHO cells.

References	Production Rates* ($\mu g/10^6$cells·day)	Reported Stable Expression (days)	Culture MTX Selection (μM)	Medium Serum (%)
*Kaufman et al. (1985)	10	NA	0.05	10
	5	38	0	10
Weidle et al. (1988)	36	NA	5	NA
	10	40	0	NA
Goeddel et al. (1989)	50	NA	10	NA
	18	NA	0	NA
Barsoum (1990)	45	NA	0.15	10
	NA	NA	0	NA
*This work	43	<15	5	10
	20	<20	0	0
	12	250	0	0

NA - not available

*Rates converted to $\mu g/10^6$cells·day using ratio of 600 U/μg

~12 μg/10^6cells·day observed in this work appears to be confirmed by t-PA literature data (Table 5.3). The limitation in stable production rate is not likely due to a cytotoxic effect or metabolic burden (Gu et al., 1996; Morrison et al., 1997) of t-PA production, since no growth inhibition or decrease in viability was observed for the high producing clones. The mechanism responsible for the limitation to stable t-PA production may involve saturation of the secretory pathway (Pendse et al., 1992; Schroder and Fridel, 1997), or instability of high copy number t-PA cDNA (Weidle et al., 1988).

Southern blot analysis of the t-PA producing cells revealed that the decline of cell specific t-PA production rate was related to the loss of cDNA copies. Interestingly, preferential loss of transcriptionally active cDNA copies indicates that the transcriptionally active t-PA cDNA copies were less stable. The loss of copy number may be due to the loss of double minute chromosomes that have been associated with the loss of DHFR in unstable amplified cells (Brown et al., 1981; Kaufman et al., 1979), whereas stable amplified cells usually had DHFR gene integrated in homogeneous staining regions (HSRs). Kaufman et al. (1981) reported that extended culture for at least 30 cell doublings in the presence of MTX could obtain amplified CHO cell clones with more stable DHFR genes, likely due to the integration of DHFR genes in DMs to the HSR of chromosomes. However, our results showed that extended culture for more than 50 days in MTX did not stabilize t-PA producing clones in the cultures without MTX (Figure 5.7), which may due to the fact that no t-PA cDNA has ever been observed localizing in DMs (Kaufman et al., 1985; Weidle et al., 1988), hence, extended culture could not increase t-PA copies in HSR and had no effect on expression stability.

Regulatory agencies require two clonings of production cell lines (Kittle and Pimentel, 1997). A third limiting dilution (day 340, Figure 5.9) revealed a mixed population of high and low producing cells. Thus, production cells may often be heterogeneous; however, the t-PA production levels of this mixed population was stable for 8 months. A similar stable co-existence in mixed populations of high and low recombinant antibody producing transfectomas was also reported by Bae et al. (1995). Within these populations, both higher and lower producing subpopulations appear to co-exist due to the absence of a growth advantage for low producing cells. A similar conclusion was reported by Wurm et al. (1992) from the stable production of CD4IgG in a perfusion culture for 100 days, despite of the heterogeneous CHO cell populations. These results contrast with reports (Chuck and Palsson, 1992; Kromenaker and Sirenc, 1994) of higher growth rate, low producing hybridoma populations which limit stable long-term production of monoclonal antibodies. Morrison et al. (1997) reported a similar loss of a recombinant membrane protein production. In this case, high producing cells had lower growth rates, and based on this fact, a segregated model was proposed to describe the conversion of producers to nonproducers in the mixed cell population. However, although this model successfully illustrated the instability of growth-associated CHO cell production, it could not apply to non-growth associated protein expression such as t-PA in this study.

In conclusion, the bulk amplification was a valid strategy to obtain cell populations with high cell specific t-PA production rates. However, the maximum unstable and stable t-PA production rates that could be achieved were limited to 43 and 12 $\mu g/10^6 cells \cdot day$, respectively. These differing limitations are consistent with our analysis of previous

literature reports (Table 5.3). Thus, when establishing stable recombinant protein producing clones, it appears important to recognize that such difference may exist and thereby reduce delays due to fruitless attempts to amplify above the stable t-PA production range. Our results also provide some implications for amplification and isolation of stable production cell clones. Because of the potential for rapid loss of cDNA upon transfer to MTX-free medium (and sometimes to serum-free medium), it can be recommended that cells be adapted to MTX-free, serum-free medium before recloning to establish candidate cell lines for high and stable t-PA production. Apparently, these stable clones could be suitable for long-term (i.e. 6 months) perfusion culture. This study also indicated that clones with higher stability could be obtained from the subcloning of stabilized cell population in MTX-free culture, and stable or unstable clones could also be isolated by subcloning. Analysis of the intracellular factors limiting t-PA production should provide more insights into the difference between the stable and unstable ranges of cell specific t-PA production rates.

CHAPTER 6

TRANSCRIPTIONAL LIMITATION TO THE RATES OF RECOMBINANT HUMAN TISSUE PLASMINOGEN ACTIVATOR PRODUCTION BY CHINESE HAMSTER OVARY CELLS

6.1 INTRODUCTION

All of the limitation studies of recombinant mammalian cells described in the literature and our studies for APC produced recombinant proteins in a range between 0.03 to 10 $\mu g/10^6$cells·day (Chapter 4 and Pendse et al., 1992; Schroder and Friedl, 1997). In this chapter, we investigated the limitations to CHO cell production of t-PA, a protein previously reported to be produced in the amount of 50 $\mu g/10^6$cells·day. However, although high t-PA production rates have been reached, the maximum reported stable t-PA production rate has only been 12 $\mu g/10^6$cells·day (Table 5.3).

In this work, CHO cell clones with a range of t-PA production rates from low and high were obtained by stepwise methotrexate selection. The intracellular factors which limited production rate were investigated to determine if the maximum production rate for these cells was achieved. Based on the results and a structured mathematical model described in Chapter 3, we provide an analysis of the limiting factors to help in the selection of strategies to optimize recombinant protein production. Possible limitations, including cDNA copy number, mRNA levels and secretion rates were analyzed. Further investigation of the localization of transfected t-PA cDNA, t-PA intracellular residence

time and mRNA half-life were also performed in the stable clones with the attempt to reveal the intracellular step which limits stable level of recombinant t-PA production.

6.2 RESULTS

6.2.1 t-PA cDNA Copy Numbers and Specific t-PA Production Rates

The t-PA production by CHO cells was amplified by MTX selection up to 5 μM by the methods described in Chapter 5. This population was cloned in the presence of 5 μM MTX. Clone SI12-5.23, with t-PA production rate approximately 24,000 U/10^6cells·day, was cultured for 57 cell doublings in the absence of MTX and the t-PA production rate declined rapidly within the first 50 h and then more slowly to 7,000 U/10^6cells·day (Figure 6.1). These SI12-5.23 cells were then subcloned to obtain 24 clones with t-PA production rates from 300 to 25,000 U/10^6cells·day (Figure 6.1). These clones were used for all the following analysis.

The wide range of cell specific t-PA production rates had no apparent correlation with cell specific growth rates of 0.03 ± 0.004 h^{-1} (Figure 6.2). The cDNA copy numbers of these clones were estimated by Southern blot analysis (Figure 6.3). Up to approximately 200 cDNA copies, t-PA production rates were very low at 800 U/10^6cells·day, but these production rates increased to 25,000 U/10^6cells·day at a t-PA

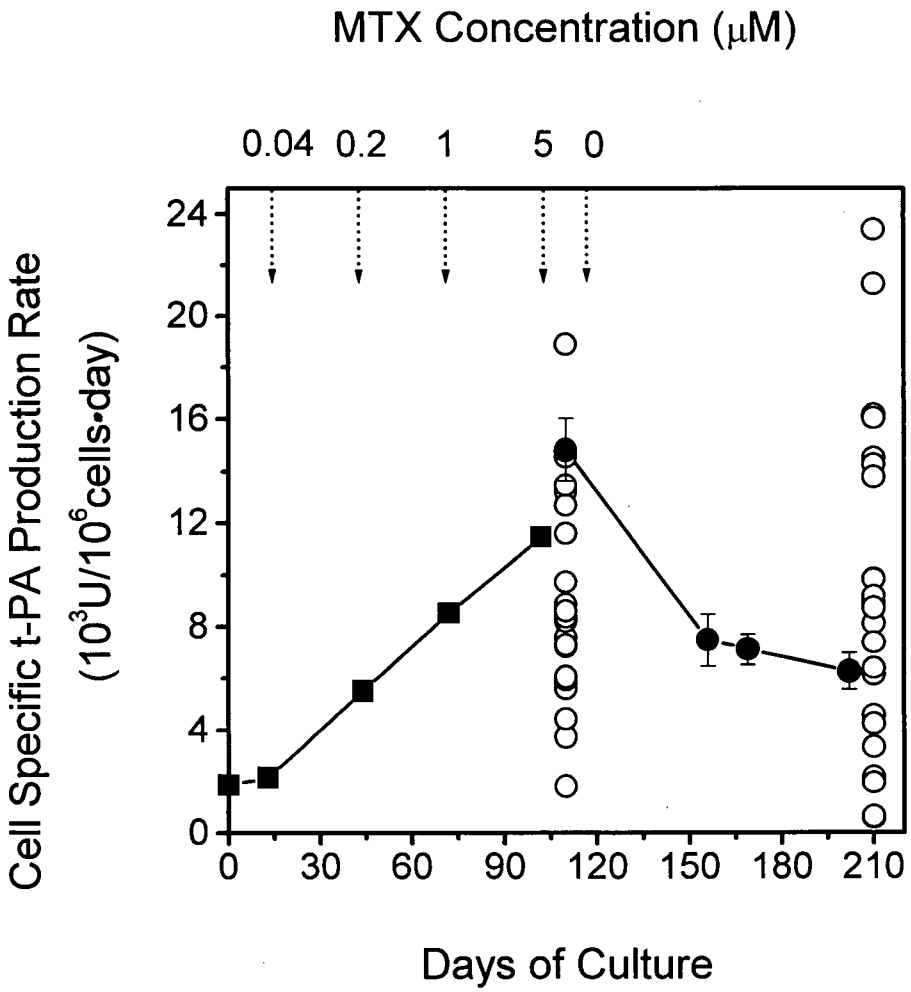

FIGURE 6.1 Generation of 24 t-PA producing CHO clones. SI12-5 cells were first amplified by step-wised increase of MTX concentrations (indicated by the dash arrows) from 0.04 to 5 μM (solid squares). A limiting dilution cloning was performed on day 110 at 5 μM MTX (open circles on day 110). Several clones including SI12-5.23 (solid circles) were cultivated in the absence of MTX (after day 110) for 100 more days when another limiting dilution was performed (the second set of open circles, performed on day 210), these 24 clones were subjected to the following analysis in this chapter.

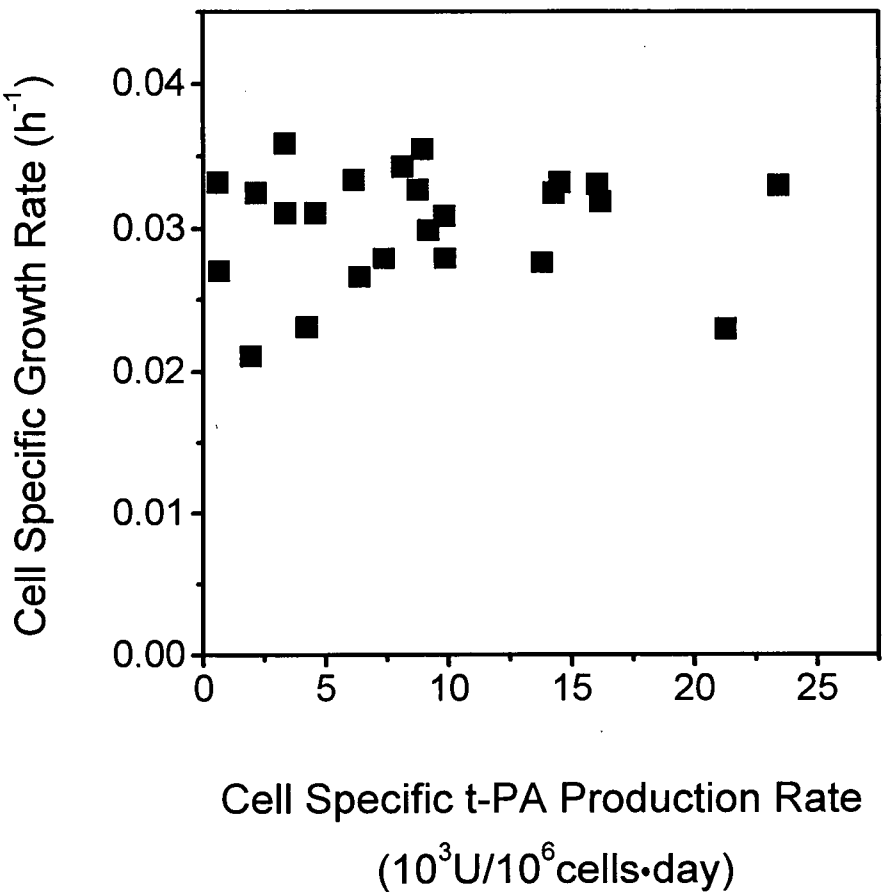

FIGURE 6.2 Relationship between cell growth rate and average cell specific t-PA production rate.

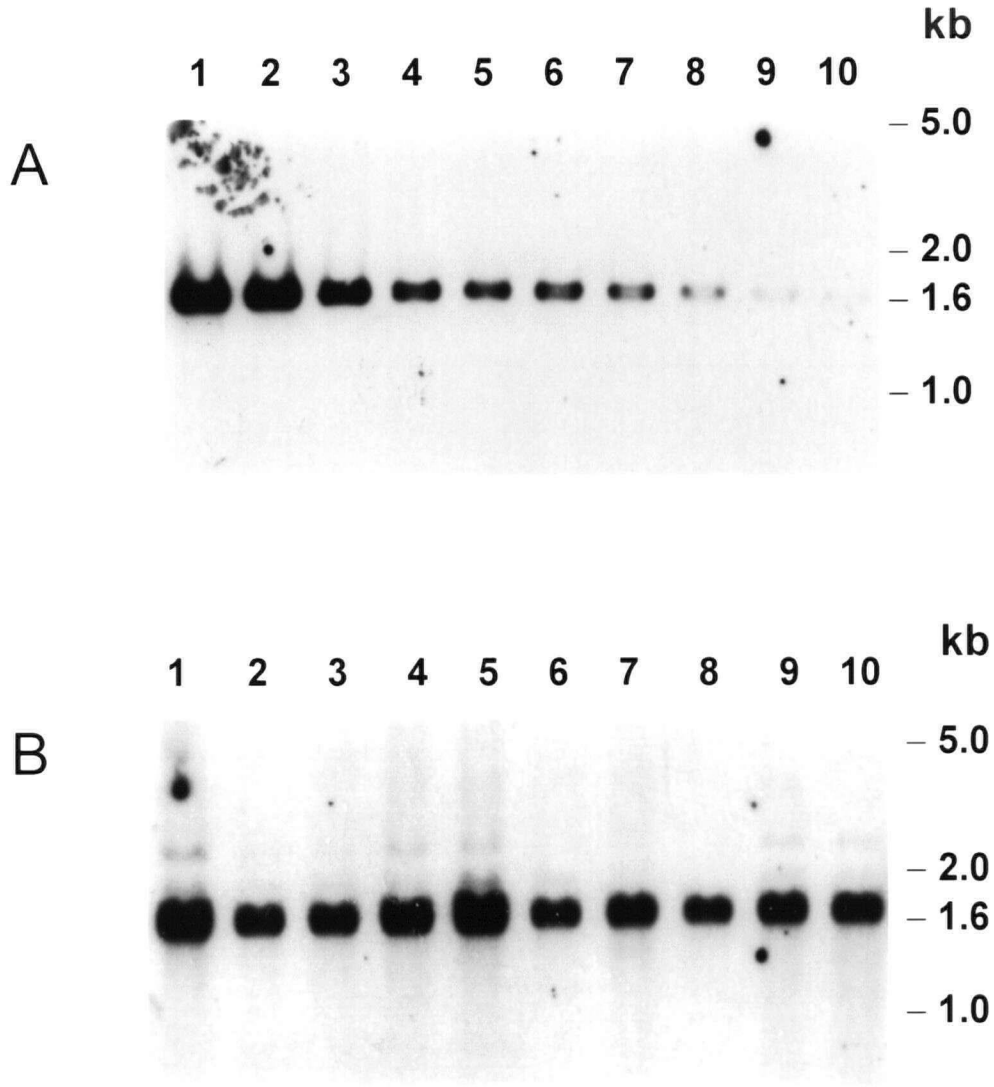

FIGURE 6.3 Representative Southern blot analysis of genomic DNA isolated from different clones. (A) Different amounts of plasmid pSL-11 were used as the standards for t-PA quantitation. Lanes 1-10: 1 ng, 750, 500, 250, 100, 75, 50, 25, 10 and 5 pg of *Bgl*II digested pSL-11. A standard plot was generated from the densitometry of the bands, and the t-PA cDNA copy number was calculated by interpolating the standard curve. (B) The genomic DNA isolated from each clone was restriction digested with *Bgl*II and loaded at 2 μg per lane then hybridized with dig-labeled t-PA DNA probe after transferring onto the nylon membrane. Lanes 1-10: Clones SI12-5.23.1 to SI12-5.23.10.

copy number of 340 (Figure 6.4). At higher than 340 cDNA copies, the t-PA production rates were more randomly distributed, but the clones with maximum cell specific production rates generally declined with increasing cDNA copy numbers.

The cleavage of genomic DNA by *Kpn1*, which only cut the transfected vector pSL11 once, was performed to determine if the t-PA cDNA integration occurred in tandem repeats (Figure 6.5). A predominant DNA fragment approximately 8 kb long was generally observed as the linear conformation of the integrated vector in all the analyzed clones. This result revealed that most t-PA amplicons were in tandem repeats. Minor bands with smaller DNA fragments were also observed which may be due to linear or circular conformations of the t-PA vector and also due to head-to-head or tail-to-tail integration arrangement as reported (Handeli et al., 1989; Riggs and Bates, 1989).

Further investigation using fluorescence *in-situ* hybridization (FISH) was aimed to study the difference in chromosomal integration of t-PA cDNAs between high and low producing clones (Figure 6.6). Up to 9 t-PA cDNA clusters were observed in the 8 clones analyzed by FISH (Figure 6.7). Although clones with higher copy number had the tendency to have more integration sites, the number of clusters were not closely correlated with cDNA copy number (r - 0.7) (Figure 6.7A), and had no apparent correlation with cell specific t-PA production rate (Figure 6.7B).

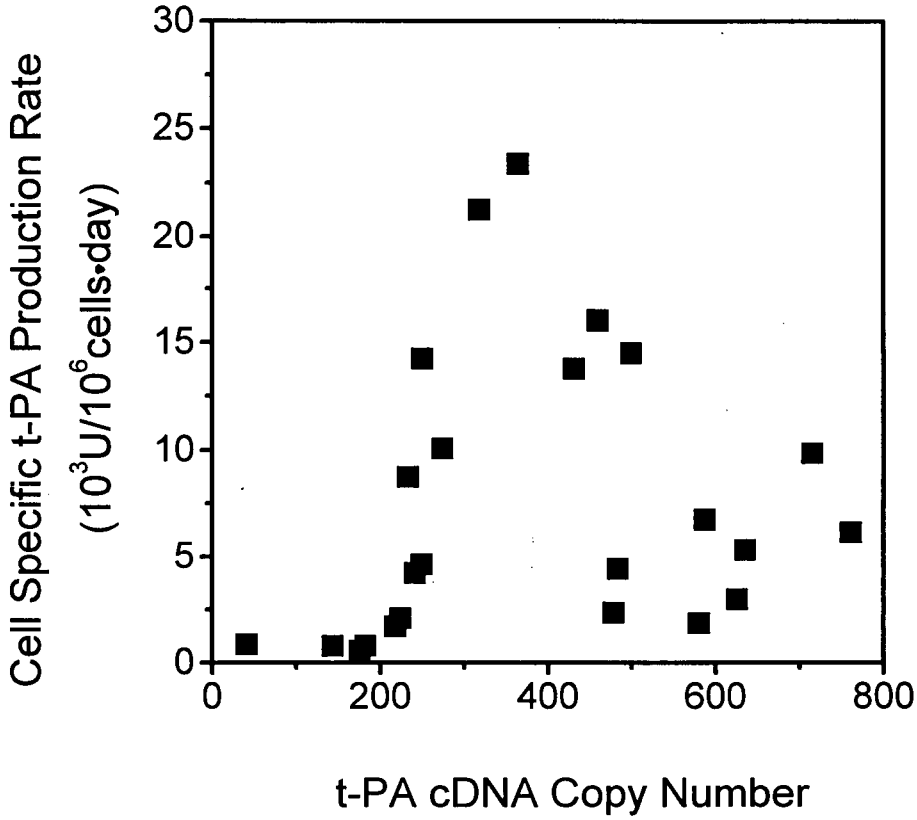

FIGURE 6.4 Relationship between cell specific t-PA production rate and t-PA cDNA copy number.

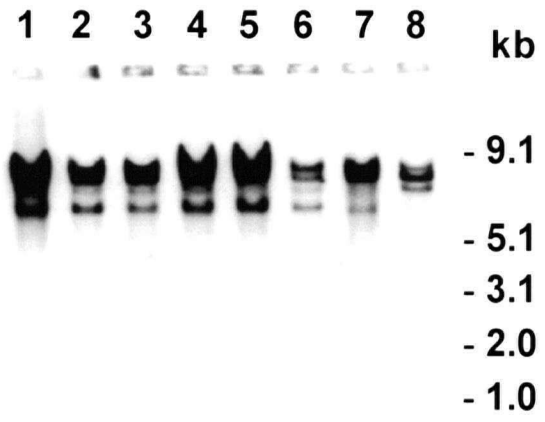

FIGURE 6.5 Representative Southern blot analysis of genomic DNA digested with restriction enzyme *Kpn*I. The genomic DNA isolated from each clone was restriction digested and loaded at 2 μg per lane similar as described in Figure 2. Lanes 1-8: Clones SI12-5.23.1 to SI12-5.23.8.

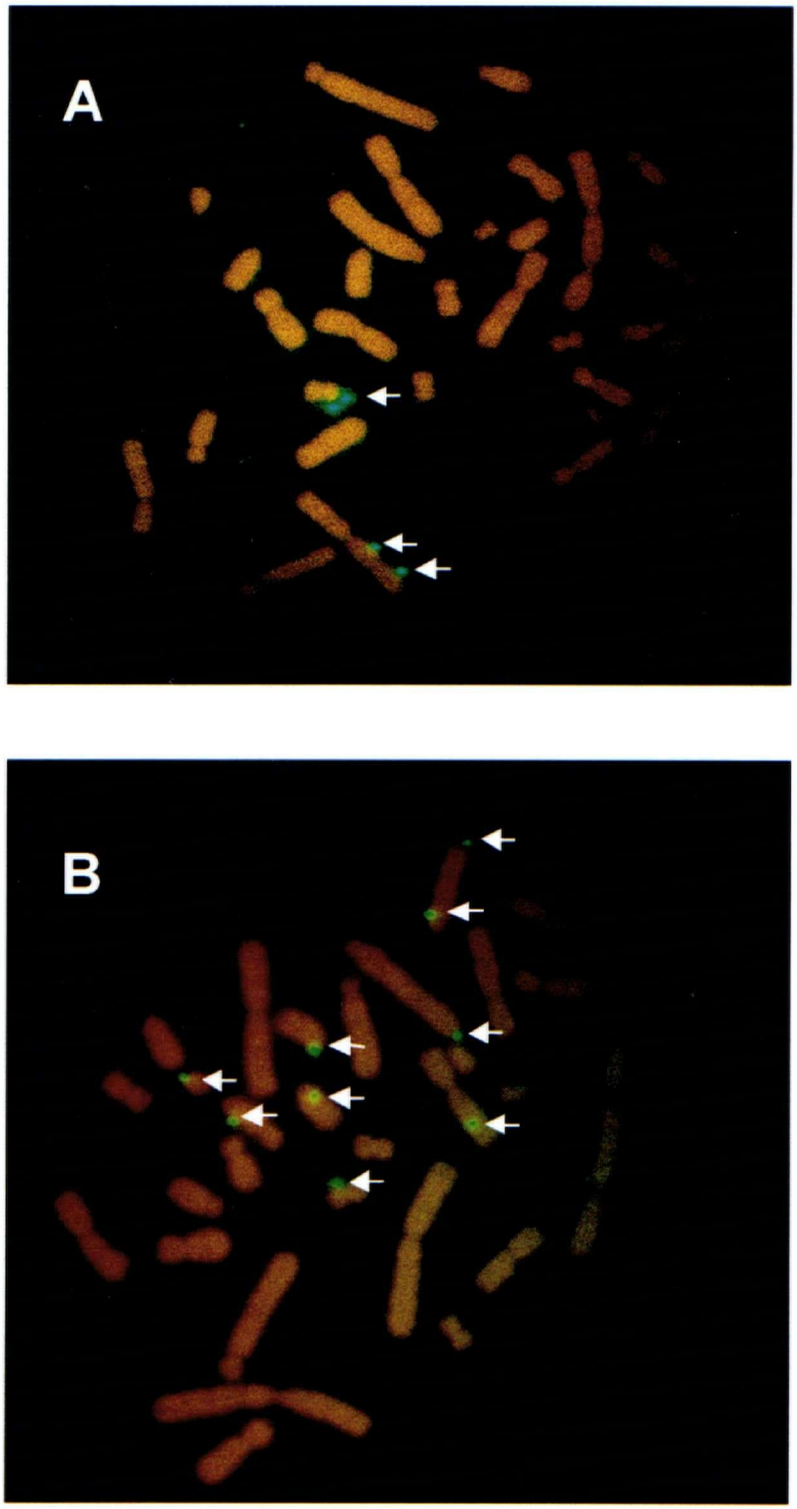

FIGURE 6.6 Fluorescence *in-situ* hybridization analysis. The chromosomes shown here were from (A) clone SI12-5.23.6, which contained approximately 250 t-PA cDNA copies and (B) SI12-5.23.22, which contained approximately 480 t-PA cDNA copies. The arrows indicate the locations of integrated t-PA cDNA.

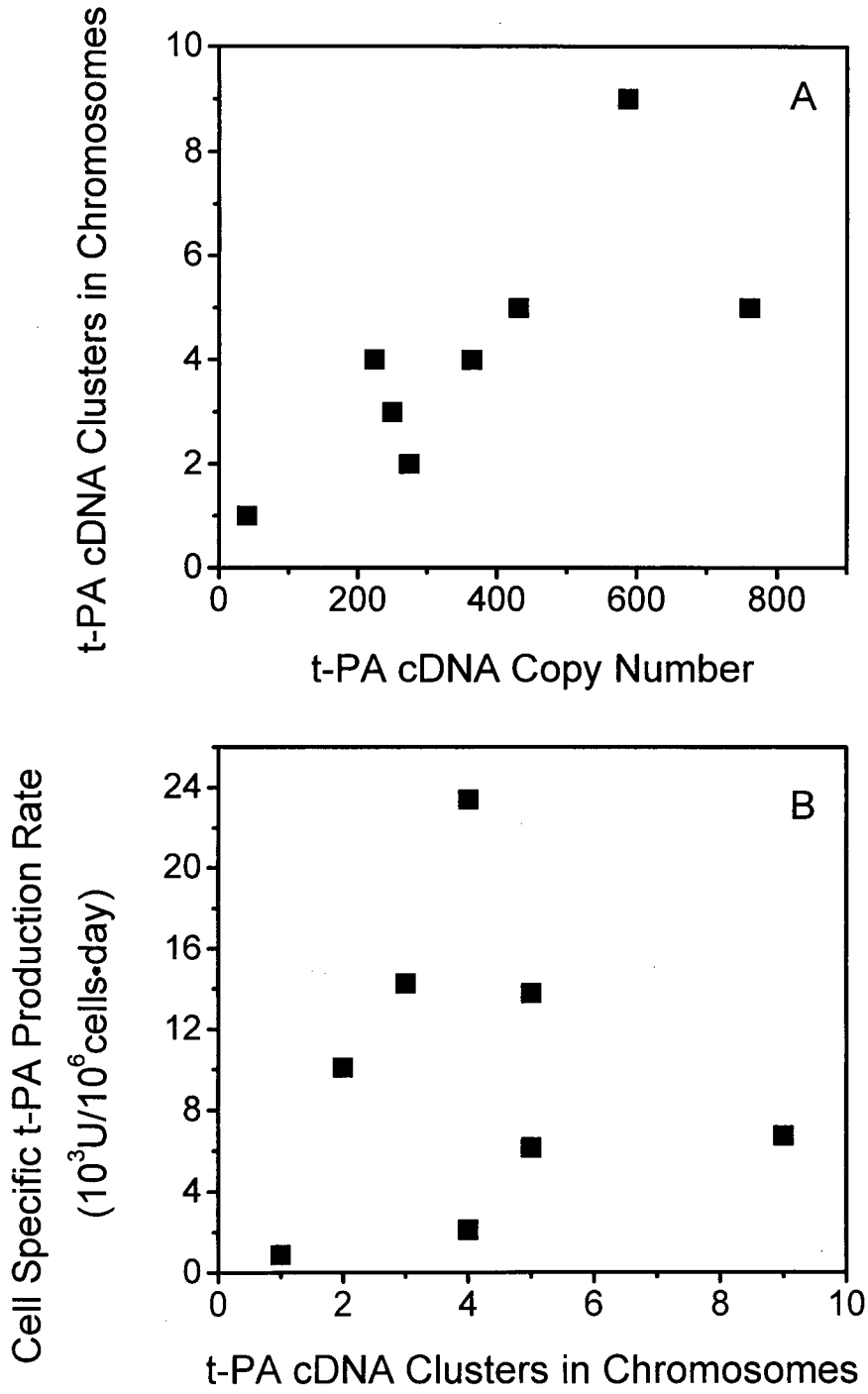

FIGURE 6.7 (A) Relationship between integrated t-PA cDNA clusters in host cell chromosomes and average t-PA cDNA copy number per cell in eight analyzed clones. (B) Relationship between average cell specific t-PA production rate and number of t-PA cDNA clusters in host cell chromosomes.

6.2.2 Dependence of t-PA Production Rates on mRNA Levels

Northern blot analysis was performed on t-PA mRNA using β-actin mRNA to normalize the loading (Figure 6.8). A pattern similar to Figure 4 was observed between relative t-PA mRNA level and cDNA copy number (Figure 6.9A). The linear relation (r - 0.94) between production rates and mRNA levels (Figure 6.9B) indicated that t-PA mRNA levels limited cell specific t-PA production rates. A duplicated analysis was performed after two weeks and the highest t-PA expression was reduced from 25,000 (solid symbols, Figure 6.9B) to 16,000 U/10^6cells·day (open symbols, Figure 6.9B). Although the high t-PA production rates of over 16,000 U/10^6cells·day only seemed to be transiently obtained, the limitation of t-PA production by mRNA levels existed even in the unstable high expression range (Figure 6.9B). To confirm the result that secretory pathway capacity did not limit t-PA production rate, the following analyses of intracellular t-PA contents and t-PA intracellular retention time were performed.

6.2.3 Intracellular t-PA Content

To test the secretion efficiency of t-PA, an ELISA assay was developed to determine the intracellular content. For t-PA production rate up to 36 μg/10^6cells·day, a linear correlation was observed between intracellular t-PA level and relative mRNA level (r - 0.97, Figure 6.10A) as well as between t-PA production rates and intracellular t-PA content (r - 0.98, Figure 6.10B). These results confirmed that the t-PA secretory pathway capacity was not limiting, even for cells expressing t-PA in the unstable range of

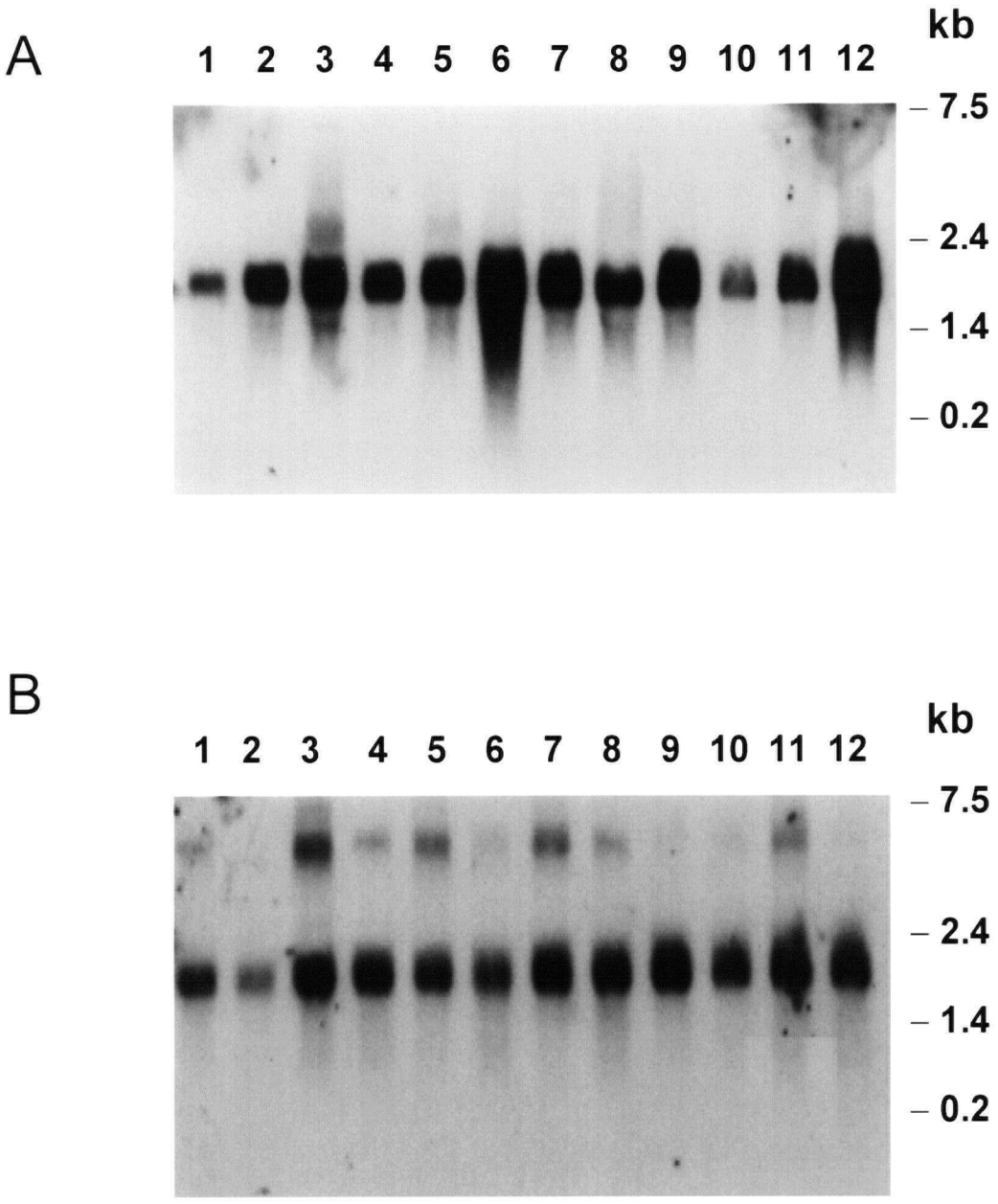

FIGURE 6.8 Northern blot analysis of t-PA mRNA. Same amount (5 μg) of total RNA from individual cell line was loaded in two separated gels. One was hybridized with the t-PA DIG-DNA probe (A), the other was hybridized with β-actin dig-DNA probe (B). Clones SI12-5.23.1 to SI12-5.23.12 are shown.

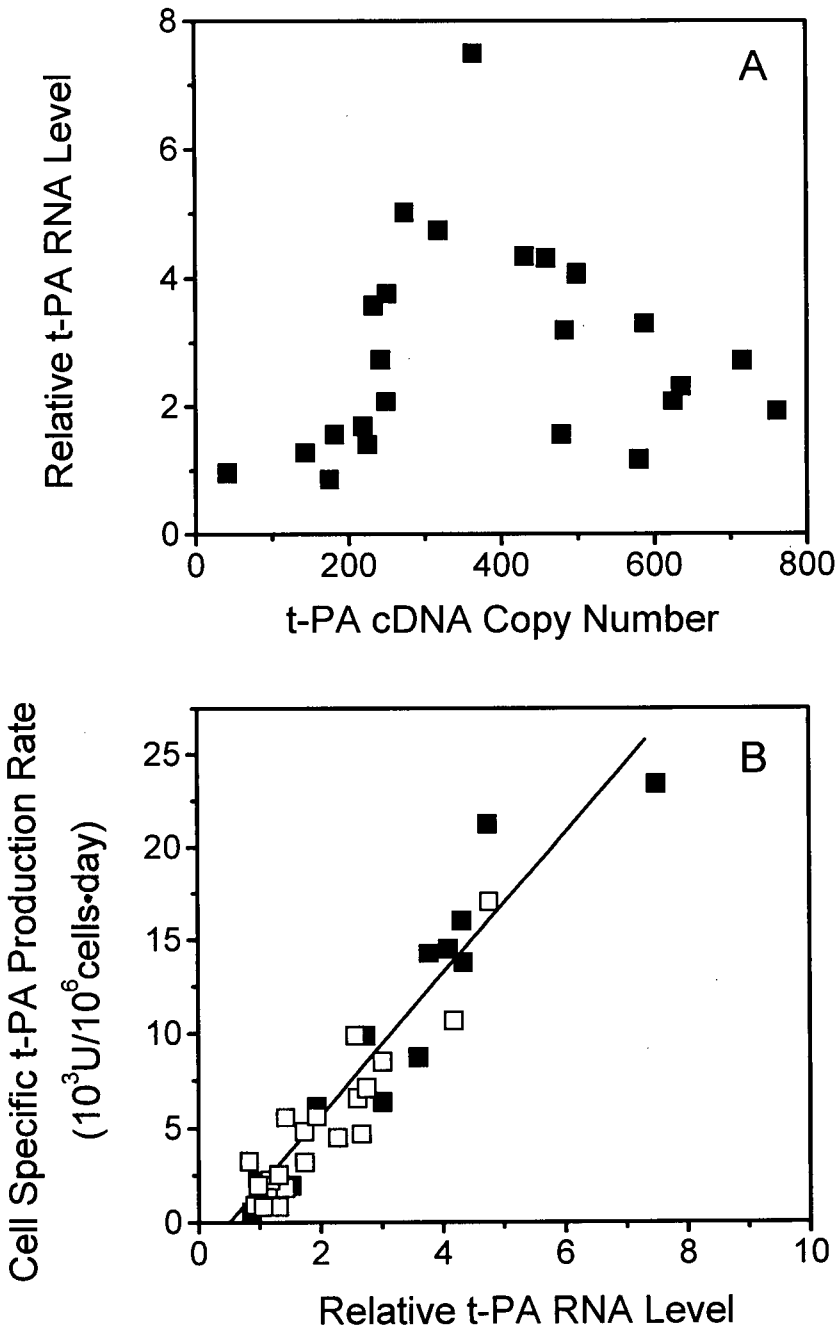

FIGURE 6.9 (A) Relationship between relative mRNA level and cDNA copy number of SI12-5.23 derived clones. (B) Correlation between cell specific t-PA production rate and relative mRNA level of SI12-5.23 derived clones. Two sets of data are presented in this figure. The solid squares represent the first data set which the 13 clones were analyzed right after limiting dilution cloning. The open squares represent the second data set which including more clones (24) were analyzed two weeks after the first data set.

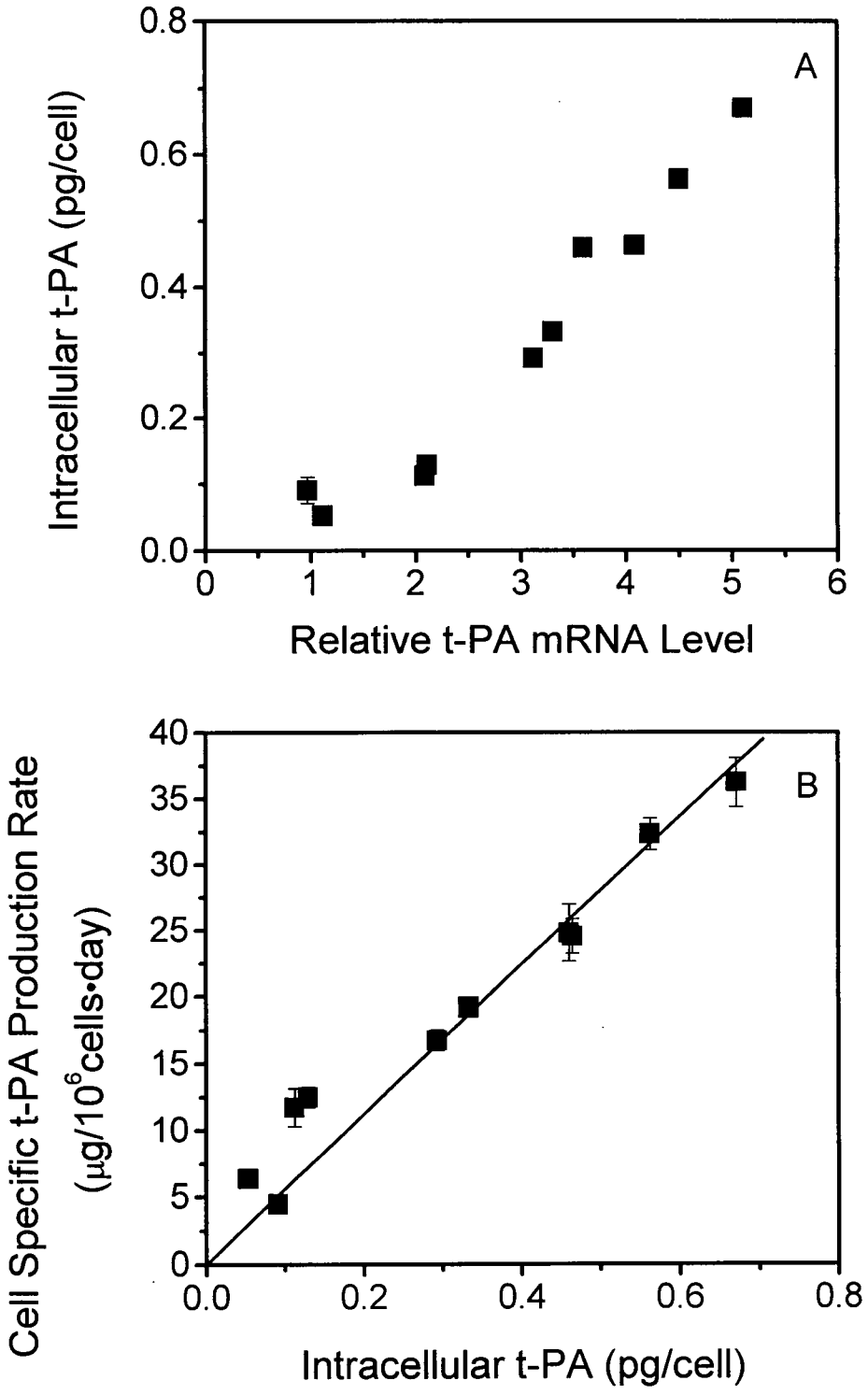

FIGURE 6.10 Correlations between (A) intracellular t-PA content and relative mRNA level and (B) cell specific t-PA production rate and intracellular t-PA content.

production levels. Based on the production rates in Figure 6.10B and using Equation 3.3, the t-PA secretion rate was calculated to be $k_S = 2.25 \pm 0.35$ h^{-1}.

6.2.4 t-PA Cellular Residence Time

The intracellular residence time of t-PA was determined by pulse-chase analysis (e.g., Figure 6.11A) to confirm that the secretion rates (k_S) of t-PA was not reduced at higher production rate. The maximum intracellular t-PA concentration was obtained after 30 min of chase. The intracellular t-PA rapidly decreased within the following 60 min and almost all intracellular t-PA was secreted within 120 min. This intracellular decline pattern was consistent with the increase of secreted t-PA in the medium (e.g., Figure 6.11B), and all t-PA producing clones secreted over 90% of labeled t-PA within 120 min (Figure 6.12).

The t-PA protein residence time inside the cell was calculated assuming negligible intracellular degradation ($k_P \sim 0$), and negligible dilution by cell growth ($k_S >> \mu = 0.03$ h^{-1}). In this case, Equation 3.2 can be simplified to

$$\frac{d[P_i]}{dt} = -k_S[P_i] \qquad (6.1)$$

Estimating from the decrease between 30 to 90 min during the chase (Figure 6.11B), the t-PA secretion rate (k_S) for individual clones ranged from 0.91 to 2.21 h^{-1} with an average k_S value of 1.63 ± 0.52 h^{-1} and an average retention half-life of 30 ± 10 min.

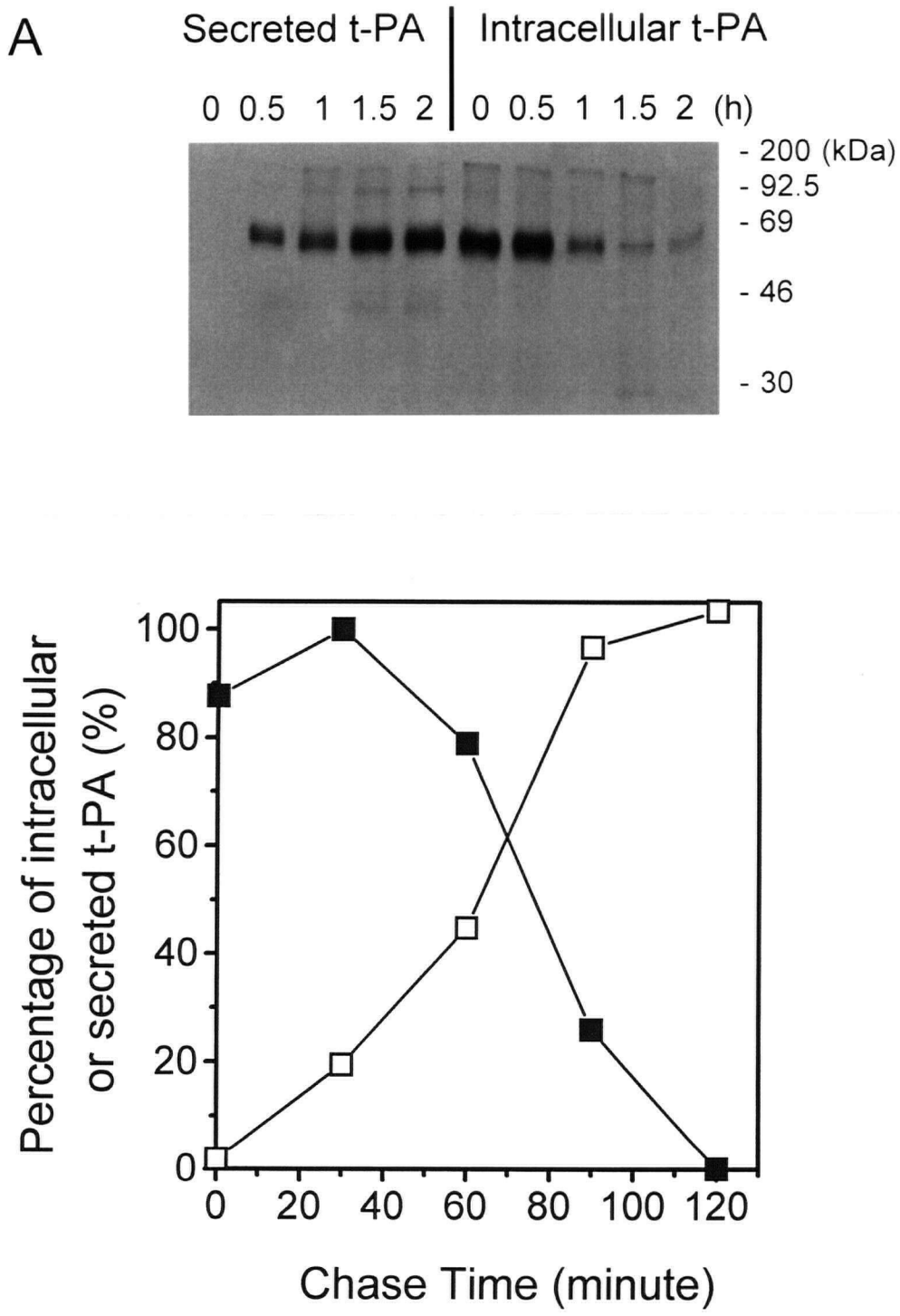

FIGURE 6.11 Pulse-chase analysis of t-PA secretion. A range of t-PA producing clones were pulsed with ^{35}S-methionine then chased with cold methionine for 0, 30, 60, 90 and 120 min. Representative intracellular and secreted t-PA of clone SI12-5.23.6 on a 10% SDS-acrylamide gel are shown in (A). (B) The time course of intracellular t-PA decrease and t-PA secretion of clone SI12-5.23.6.

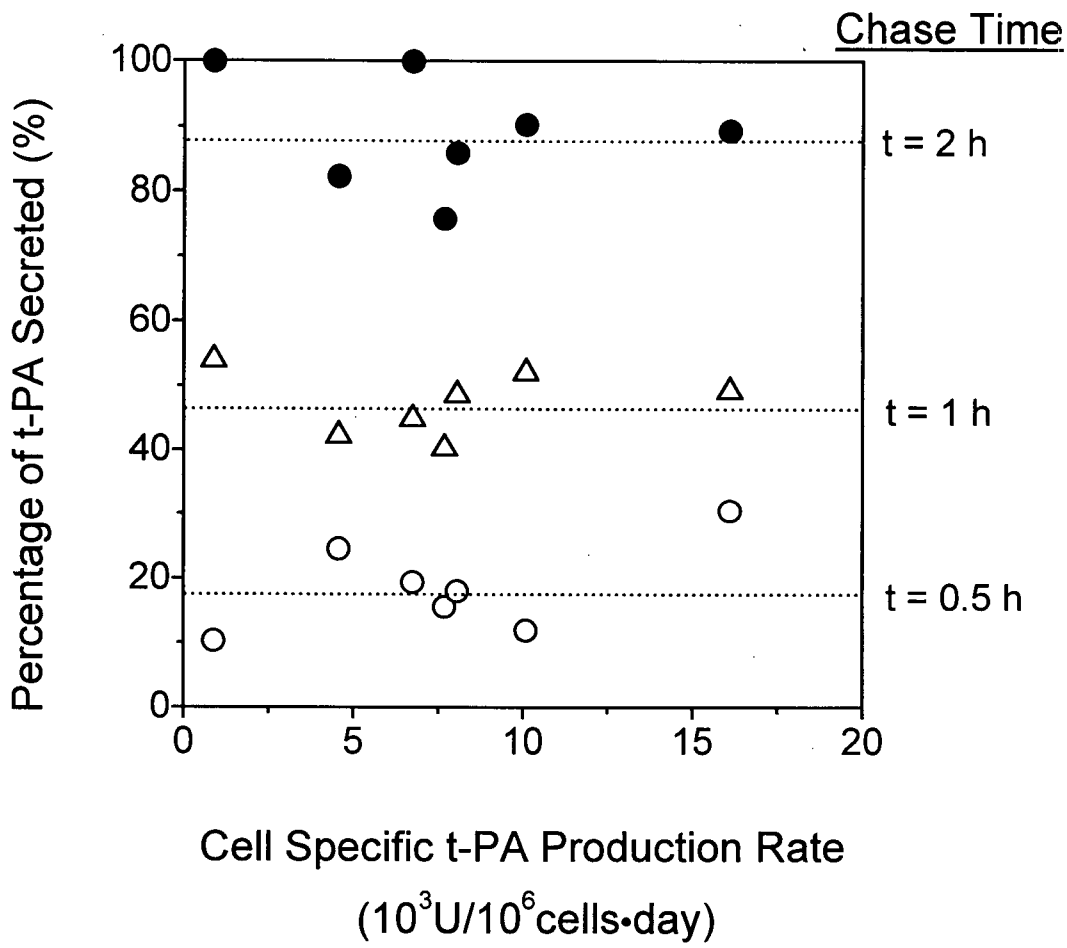

FIGURE 6.12 Percentage t-PA secreted at various chase time for eight SI12-5.23 derived clones.

This k_S value is close to the k_S of 2.25 h^{-1} estimated from the Figure 6.10 data, despite the completely distinct approaches.

6.2.5 t-PA Percentage of Total Protein Production

The percentage of t-PA out of the total protein synthesized or secreted were determined in two representative clones, SI12-5.23.3 and SI12-5.23.9, which produced t-PA at 870 and 16,100 U/10^6cells·day, respectively. Pulse-chase samples labeled with [^{35}S]-methionine were used to measure the radioactivity in t-PA versus total protein, from supernatants or cell extracts. For clones SI12-5.23.3 and SI12-5.23.9, the synthesized t-PA accounted for 0.18 and 3.2% of total synthesized proteins, and the secreted t-PA represented 26 and 87% of total secreted proteins, respectively (Table 6.1). These results show that at high expression levels t-PA was the predominant secreted protein in recombinant CHO cells, but only represented a small fraction of the total synthesized proteins.

6.2.6 t-PA mRNA Half-life Analysis

Since all of the above results supported the role of mRNA as the limiting factor in t-PA production rate, the stability of mRNA (k_m) was investigated to see if mRNA stability was decreased in the range of unstable t-PA production rate. The t-PA mRNA half-lives of a range of clones were measured in the 10 h following blocking transcription

TABLE 6.1 t-PA Percentage in Cellular Protein Production

Clone	Production Rate ($\mu g/10^6$cells·day)	t-PA/total protein × 100%	t-PA/secreted protein × 100%
SI12-5.23.3	1.5	0.18%	26%
SI12-5.23.9	26.8	3.2%	87%

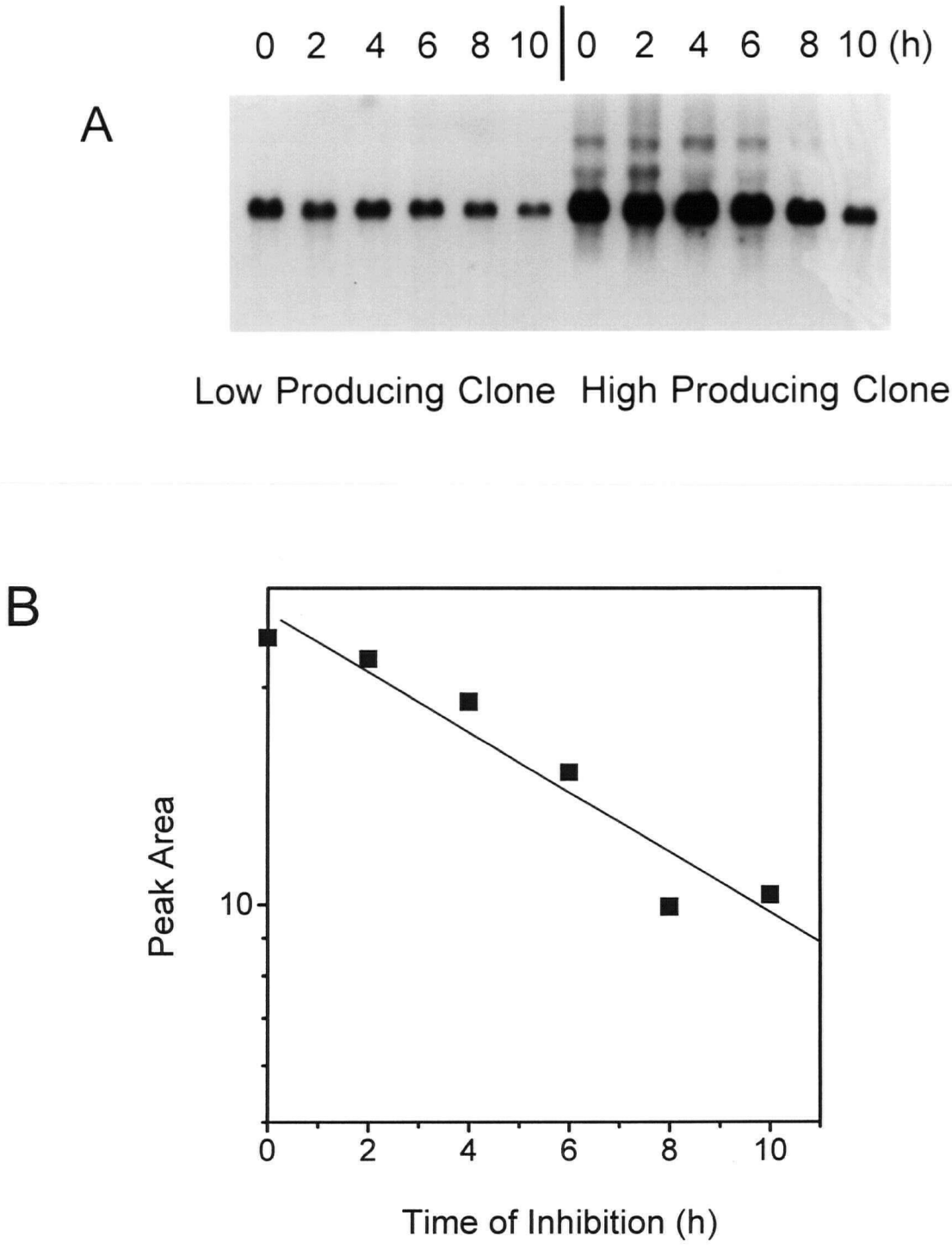

FIGURE 6.13 Decline in the t-PA mRNA levels following actinomycin D inhibition. (A) Two representative clones, the lower producer SI12-5.23.3 and the higher producer, SI12-5.23.9. (B) The first-order mRNA decay of SI12-5.23.3.

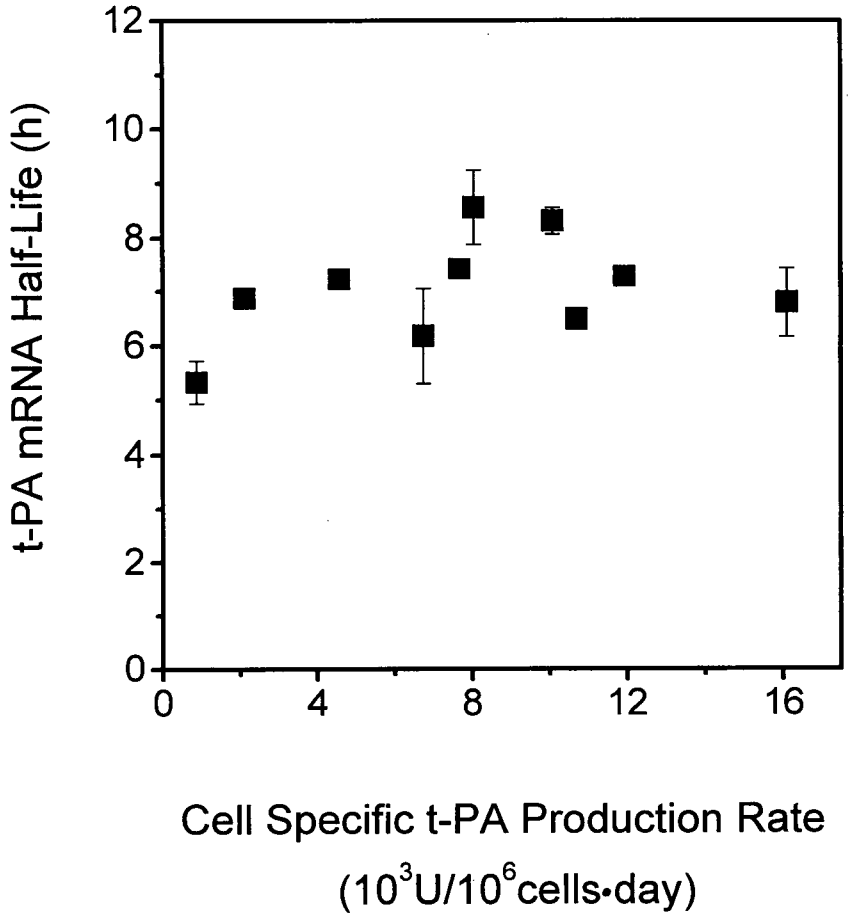

FIGURE 6.14 Comparison of cell specific t-PA production rate and t-PA mRNA half-life. The t-PA mRNA half-lives for eight SI12-5.23 derived cell clones were determined. A duplicated experiment was carried out for five of these clones (error bars represent standard deviations).

(k_D) using actinomycin D (Figure 6.13). The average k_m was 0.1 ± 0.01 h^{-1}, corresponding to mRNA half-lives of approximately 7 ± 2 h (Figure 6.14). Thus the levels of t-PA mRNA did not appear to be regulated by variable half-lives.

6.2.7 t-PA Production in Batch Culture

Since all of the analyses described above were conducted with exponentially growing cells in T flasks, batch cultures were performed to analyze the relationship between mRNA level and t-PA production rates in other batch phases besides the exponential growth. The serum-free adapted SI12-5.23 cell population used was from a cell bank approximately 60 days after serum-free adaptation (solid squares, Figure 5.9). The t-PA production rate of these cells was stable for at least another 60 days (Figure 5.9). Despite the better pH control in the reactor (Figure 6.15 II-B), the cell concentration, viability and glucose consumption in both the reactor and spinner vessels were very similar (Figure 6.15 I-B, II-A), whereas the maximum t-PA concentration was higher in the spinner culture (Figure 6.15 I-A). The cells grew exponentially for 5 days, then were in the stationary phase for approximately 24 h, followed by a rapid decline in both viable cell concentration and viability (Figure 6.15 I-B). The glucose concentrations declined rapidly during the exponential phase, then were maintained at a lower level of between 1 and 2 mM in the stationary and decline phases (Figure 6.15 II-B).

The cell specific t-PA production rates correlated with the mRNA levels during the lag and exponential growth periods (Figure 6.16), but rapidly declined once the cells reached the late exponential phase in the reactor (Figure 6.16B) and the stationary phase in

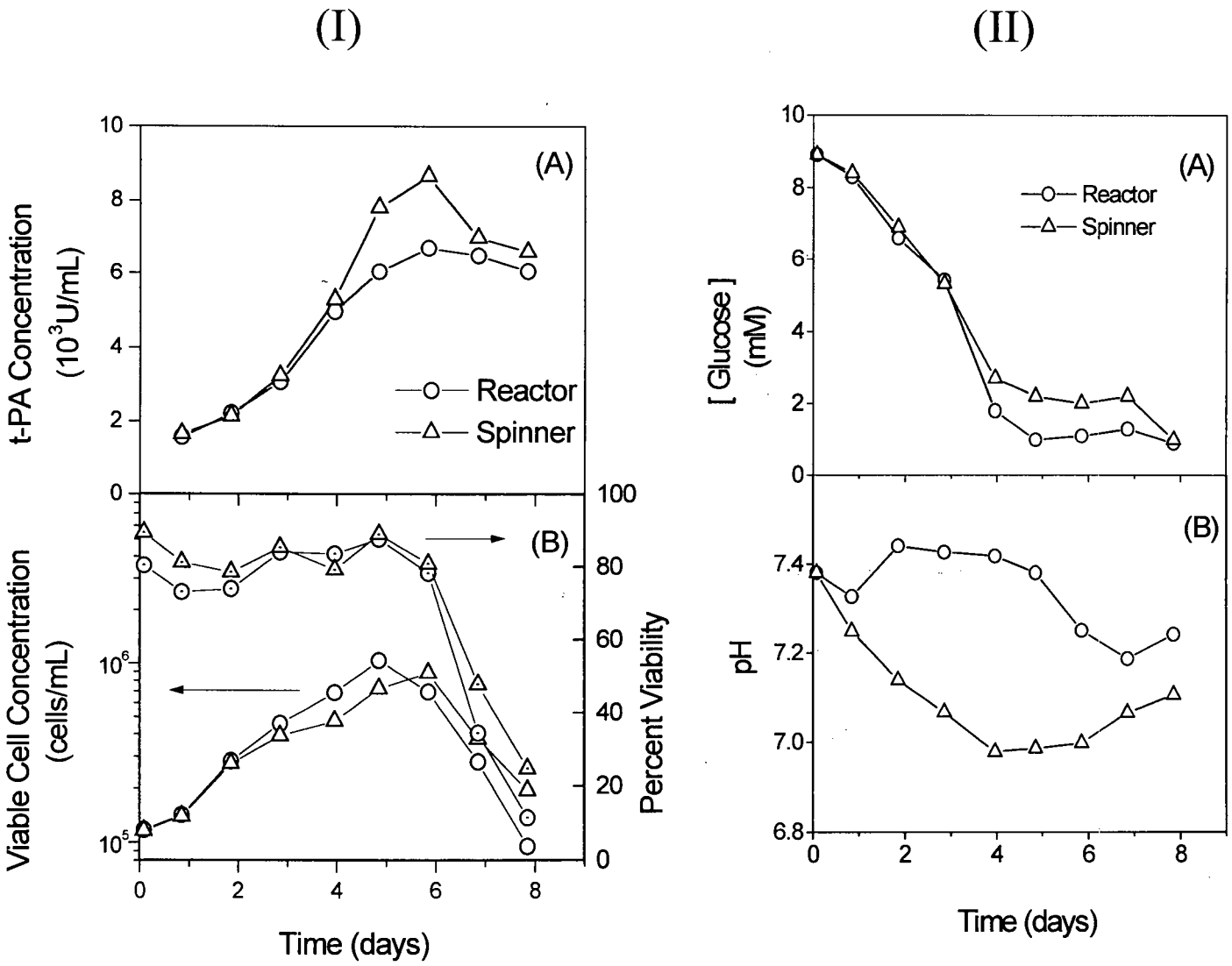

FIGURE 6.15 (I) t-PA Production and cell growth of SI12-5.23 cells in the serum-free viable culture experiments. The triangles represent the change of t-PA concentrations (A), cell concentrations (B, left) and cell viability (B, right) in the spinner culture without pH control. The circles represent the same parameters in the reactor culture with pH control.
(II) Glucose concentration and pH profiles. The change of (A) glucose concentrations and (B) pH values during the SI12-5.23 batch experiment in the reactor with pH control (triangles) and in the spinner without pH control (circles) are shown.

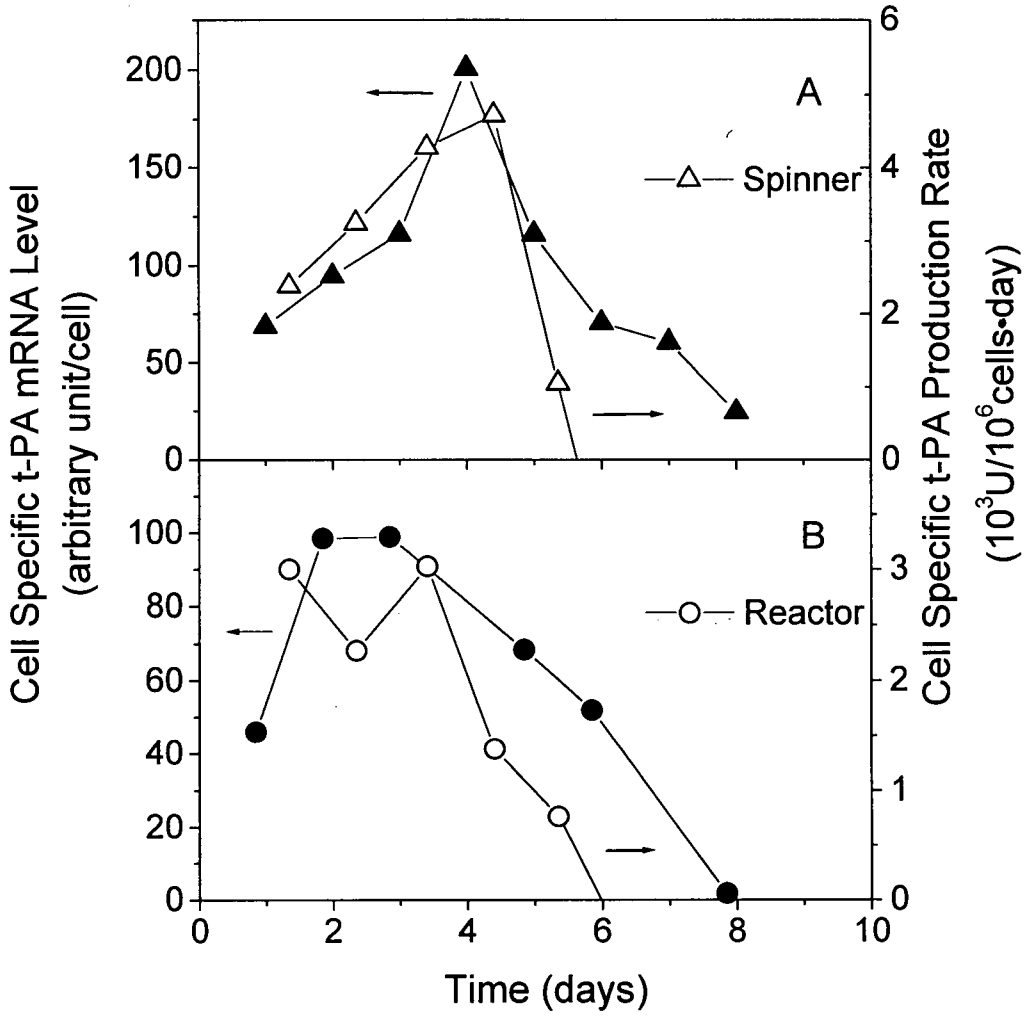

FIGURE 6.16 Cell specific t-PA production rate and t-PA mRNA level of SI12-5.23 cells during serum-free batch culture. (A) Batch culture in spinner without pH control. The filled triangles represent the cell specific mRNA level and the open triangles represent the cell specific t-PA production rate. (B) Batch culture in bioreactor with pH control. The filled circles represent the cell specific mRNA level and the open circles represent the cell specific t-PA production rates.

the spinner (Figure 6.16A). No apparent t-PA production was observed after 6 days in both batch cultures. Interestingly, although t-PA mRNA levels also declined in parallel with the decreasing production rate, cellular t-PA mRNA expression did not completely cease until day 8 (Figure 6.16). Similar to what we observed in APC batch culture, the mRNA levels and cell specific t-PA production rates were relatively stable in the exponential phase, indicating a quasi-steady-state.

6.2.8 Cell Apoptosis Analysis

To investigate whether increased apoptosis may limit t-PA production of high producing cells, cell apoptosis analysis was performed on three representative cell populations, untransfected CHO cells (DHFR$^-$), low producing SI12-5.23.3 cells (q_p = 900 U/10^{6}cells·day), and high producing SI12-5.23.11 (q_p = 16,000 U/10^{6}cells·day) (Figure 6.17). A shift toward the higher FITC-dUTP fluorescence indicated higher cell numbers undergoing apoptosis. As shown in Figure 6.17, both t-PA producing cells had higher apoptosis rates than the untransfected CHO cells, and the high producing clone seemed to have more distinguishable apoptosis pattern than the low producing clones. However, this difference was marginal compared to the reported cell apoptosis analysis (Sgonc et al., 1994) in which drug treatment was used to accelerate cell death.

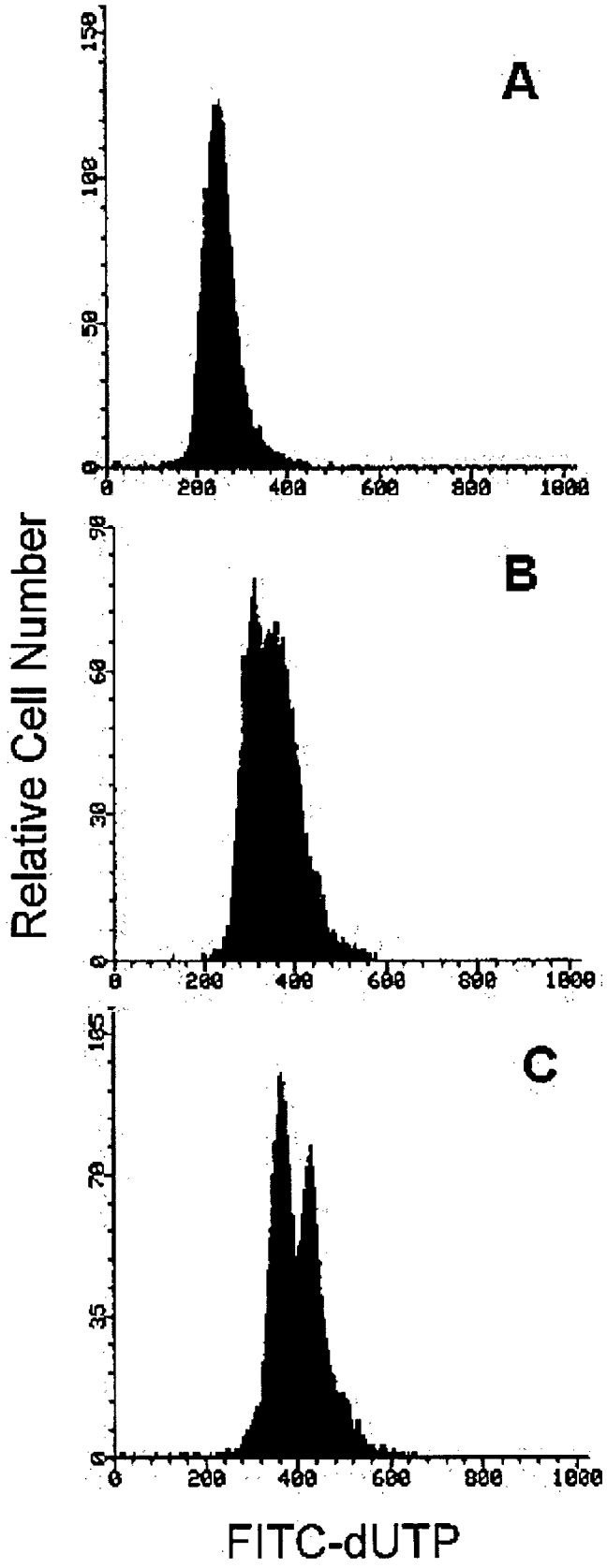

FIGURE 6.17 Apoptosis analysis of SI12-5.23 Clones. (A) Control untransfected CHO cells. (B) Low producing SI12-5.23 cells. (C) High producing SI12-5.23.11 cells.

6.3 DISCUSSION

Secretory pathway saturation has been reported to limit the maximum recombinant protein expression rates of HbsAg at 10 μg/10^6cells·day (Pendse et al., 1992), hATIII at 7.4 μg/10^6cells·day (Schroder and Friedl, 1997) and APC at 2.1 μg/10^6cells·day (Chapter 4). At the maximum production rates of these proteins, the secretion rates were decreased and intracellular recombinant protein levels increased. In this work, despite higher t-PA production rates, up to 42 μg/10^6cells·day, there were no indications of secretory pathway saturation limiting production.

The half-life of t-PA retention was only 30 ± 10 min, comparable to the rapid secretion of albumin from rat hepatoma cells (Strous and Lodish, 1980), with a half-life of 23-30 min. Longer retention half-lives have been reported for HbsAg in CHO cells (approximately 14 h) (Pendse et al., 1992), protein C in 293 cells (approximately 2 h) (McClure et al., 1992) and monoclonal antibodies in hybridoma cells (1~1.5 h) (Choi et al., 1971; Baumal and Scharff, 1973). The high t-PA secretion rates are consistent with the need for t-PA production within minutes *in vivo* in response to fibrin formation by endothelial cells (Kooistra et al., 1994). Although t-PA only represented up to 3.2% of the total synthesized proteins (close to the 5% reported by Kaufman et al, 1985), it was the major secreted protein (up to 87%, Table 6.1). Schroder and Friedl (1997) suggested an intracellular hATIII threshold concentration between 0.5 and 2.1 pg/cell for the secretory pathway to become limiting for their production rates between 2.2 and 7.4 μg/10^6cells·day. In our studies, the maximum t-PA and APC intracellular contents were 0.7 and 1.5 pg/cell,

at maximum production rates of 36 and 1.8 μg/10^6cells·day, respectively (Figure 6.10 and Figure 4.10). For such different proteins, the similar reported maximum intracellular recombinant protein contents imply that a general intracellular recombinant protein processing/secretion saturation concentration may exist at around 1 pg/cell for mammalian cells. Proteins with longer intracellular retention time (i.e. lower secretion rate) would therefore be predicted to saturate this concentration at lower maximum cell specific production rate. Measurement of the recombinant protein secretion rate and the intracellular protein concentration provide an easy estimate of the maximum production rate using the following equation:

$$q_p^{max} = k_s[P_i^{max}] \qquad (6.2)$$

where q_p^{max} is the predicted maximum cell specific protein production rate, k_s is the protein secretion rate, and $[P_i^{max}]$ is the intracellular recombinant protein secretory pathway saturation concentration (approximately 1 pg/cell) Using this equation, the estimated maximum production rates would be 2.6 μg/10^6cells·day for APC and 54 μg/10^6cells·day for t-PA (based on k_s= 0.11 and 2.25 h^{-1} in Tables 4.2 and 6.2), respectively. These estimated results (Table 6.3) are impressively similar to the reported maximum production rates of APC (2.2 μg/10^6cells·day, Figure 4.11B) and t-PA (50 μg/10^6cells·day, Table 1.2 and Goeddel et al., 1989), and suggest Equation 6.2 may provide a valid estimate of the maximum cell specific rate for mammalian recombinant protein production. Since BHK and CHO cells generally have similar maximum recombinant protein production rates (Table 1.3), the maximum APC and t-PA production

TABLE 6.2 Intracellular parameter values for t-PA production in CHO cells at steady-state with standard deviations. The parameters presented in the table are: transcription rate k_D, calculated from Equation 3.4; mRNA turnover rate k_m, from Figure 6.14; cell growth rate μ, average of data in Figure 6.2; range of transcription efficiency ε_R, calculated from Equation 3.5; translation rate k_R, calculated from Equation 3.9; secretion rate k_S, calculated (a) from Figure 6.10B and (b) Figure 6.12 data; intracellular protein degradation rate k_P, calculated from Figure 6.11, and transcription efficiency ε_P, calculated from Equation 3.7. mRNA levels are relative.

Parameter	Value ± SD	Sample number	Units
k_D	0.0004 ~ 0.0031	24	range of mRNA/cDNA/h
k_m	0.1 ± 0.01	10	h^{-1}
μ	0.03 ± 0.004	24	h^{-1}
ε_R	0.0016 ~ 0.02	24	range of mRNA/cDNA
k_R	0.22 ± 0.07	9	pg t-PA/mRNA/h
k_S	2.25 ± 0.35 (a)	9	h^{-1}
	1.63 ± 0.52 (b)	8	h^{-1}
k_P	0.01 ± 0.01	8	h^{-1}
ε_P	0.1 ± 0.02	9	pg t-PA/mRNA

TABLE 6.3 Comparison of estimated maximum recombinant protein production rates to reported results. The estimated productivities were calculated using Equation 6.2. q_p^{max} is the predicted maximum productivity, k_s is the protein secretion rate. $[P_i^{max}]$ is the intracellular recombinant protein secretory pathway saturation concentration (approximately 1 pg/cell). The ATIII results were calculated from the report of Schröder and Friedl (1997).

Recombinant protein	Average k_s (h^{-1})	q_p^{max} ($\mu g/10^6$cells·day)	Reported q_p^{max} ($\mu g/10^6$cells·day)
ATIII	0.32	7.7	7.4
APC	0.11	2.6	2.2
t-PA	2.25	54	50*

* Goeddel et al., (1989)

rates is not likely due to the different cell types used for production. The longer retention time of some recombinant proteins may be due to selective binding to secretion processing proteins in the ER. Dorner et al. (1987) reported that different recombinant proteins had different binding affinity to the chaperone protein GRP78. The secretion of wild-type t-PA and vWF were not influenced by the elevated GRP78 levels, whereas the secretions of factor VIII and unglycosylated mutant t-PA were severely retarded by GRP78.

Since for all 24 t-PA producing clones, the t-PA mRNA levels and production rates were correlated, it was concluded that the mRNA levels and not the secretory pathway limited t-PA production. Under this condition, the translation efficiency ($\mathcal{E}_P$) and the apparent secretion rate (k_S) were constants (Table 6.2), indicating all translational and post-translational steps were not limiting, even in the unstable t-PA production rate range from 7,000 up to 25,000 U/10^6cells·day (12 up to 42 μg/10^6cells·day).

At the lower rates of expression, production of t-PA appeared to require a minimum mRNA level (approximately 1 in Figure 6.9B), perhaps due to translation blocking at low mRNA levels in which case mRNA are associated with messenger ribonucleoprotein particles (mRNPs) and are not recruited to ribosomes (Wolffe and Meric, 1996). This threshold $[mRNA]_T$ requirement could be included in Equation 3.2 to account for this inactive t-PA mRNA by adding one term:

$$\frac{d[P_i]}{dt} = k_R([mRNA] - [mRNA]_T) - k_S[P_i] - k_P[P_i] - \mu[P_i] \qquad (6.3)$$

The translation rate k_R in Table 6.2 was calculated from the steady-state form of this equation.

The highly variable transcriptional efficiency ($\mathcal{E}_R$) (Table 6.2) could be due to variations in the transcription rates (k_D) and/or the mRNA turnover rates (k_m). However, the narrow range of mRNA turnover rates ($k_m = 0.1 \pm 0.01$ h^{-1}) of all the analyzed clones demonstrated that the clonal variations in t-PA production rates were due to differences in the transcription rates.

Although the transcription rates are dependent on the site of integration, two general trends between cDNA copy number and cell specific protein production rate have been observed. The cooperative increase of t-PA production rates with increasing cDNA copy numbers at lower copy number (less than 300 copies) is similar to APC production rates (Figure 4.2). This cooperative pattern may be due to the decreased negative influence (Wilson et al., 1990) of heterochromatin on the transcriptional activity of integrated genes at increasing cDNA copy numbers (Figure 6.4). Hendricks et al. (1989) reported a t-PA production rate increase with increasing copy numbers up to 10 $\mu g/10^6$cells·day at 40 copies in myeloma cells, whereas Jalanko et al. (1990) reported no correlation between copy numbers (up to 30) and cell specific t-PA production rates (up to 11 $\mu g/10^6$cells·day) in CHO cells. These contradictory results may due to the cooperative pattern at the lower t-PA cDNA copy number, which could generate conflicting results if only a few clones were analyzed in this region.

Amplification to higher cDNA copy numbers eventually yielded decreasing t-PA production rates (Figure 6.4), these results are similar to the relationship between APC cDNA copy number and cell specific APC production rate (Figure 4.2). Recent studies have reported cosuppression of multiple copies of heterologous genes in fungi (Cogoni et

al., 1996), plants (Joergensen, 1995; Matzke and Matzke, 1995) and *Drosophila* (Dorer and Henikoff, 1994; Pal-Bhadra et al., 1997). Although cosuppression has not previously been reported in cultured mammalian cells, the decreases in BHK cell APC expression and CHO cell t-PA expression at higher cDNA copy number is consistent with reports of cosuppression in other systems. This cosuppression could limit t-PA expression by limiting the transcription rates (Equation 3.5).

FISH analysis showed cDNA integration in the chromosome and no double minute chromosomes, which was in agreement with the observations by Wiedle et al. (1988) and Koehler et al. (1995). Although amplified up to 760 t-PA cDNA copies, only up to 9 integration sites were observed by FISH analysis. These integration site copy numbers are similar to the Robins et al. (1981b) report of up to 100 copies of plasmid DNA incorporated into a single chromosomal site in rat liver cells. The approximately vector sized t-PA tandem repeats (Figure 6.5 and 6.6) are consistent with our APC results, but much smaller than the large amplicons (larger than 200 kb) described by Looney and Hamlin (1987).

Although mRNA levels limited all 24 analyzed clones in the exponential growth phase, batch cultures revealed that cell specific t-PA production rate in the decline phase was not well correlated with the mRNA level (Figure 6.16). Low levels of t-PA mRNA remained at the end of batch cultivation when t-PA production had ended. These results implied that other factors, such as secretory pathway proteins or energy requirements, may become limiting when cells are in the decline phase. This shift in intracellular limitation was very likely due to the deficiency of essential nutrients (i.e. glucose or glutamine). These results imply that in batch cultures, the limitations to recombinant protein

production could be controlled by manipulating the levels of essential nutrients in the medium.

Instability of recombinant protein production can also reduce long-term process yields. Since t-PA production was not growth-associated (Figure 6.2), the instability of high t-PA producing cells could not be explained by the structured model proposed by Morrison et al. (1997). This is due to the fact that the low recombinant protein producing cells had a growth advantage that lead them eventually dominate the cell population in long-term culture. One possible mechanism to explain this non-growth-associated instability is that the high producing cells may have higher apoptosis rates, which reduce their numbers over time. Although the death of CHO K1 cells has been shown to be mainly due to necrosis (Singh et al. 1994), CHO DUKX cells in protein-free batch culture demonstrated apoptotic morphology and nuclease-mediated DNA cleavage (Moore et al., 1995). Several factors, such as nutrient limitation, the hydrodynamic environment, and dissolved oxygen level, may influence the rate of cell apoptosis (Al-Rubeai and Singh, 1998).

Our preliminary analysis results revealed that apoptosis rates may be increased for high t-PA producing cells (Figure 6.17). However, these results were not conclusive since the high producing clone had only a small increase in apoptosis (compared to high rates of drug-induced apoptosis; Sgonc et al., 1994). Nevertheless, it has to be noted that a slightly elevated rate of apoptosis could explain the gradual loss of t-PA production rate over 50 days. Further studies would be required to confirm the significance of this apoptosis mechanism in controlling maximum recombinant production stability.

CHAPTER 7

CONCLUSIONS

Mammalian cell recombinant protein production is complex and involves many intracellular steps. We developed a structured mathematical model to assist the experimental analysis of intracellular limitations. Taking APC and t-PA together, many of the rates (7 out of 10) were constant (Table 7.1). The k_s^{APC}, μ^{BHK}, and k_s^{tPA} did vary and these results are summarized in Table 7.2. The k_D was likely the most variable parameter, apparently dependent on the site of integration. The integrated cDNA copies in both cases were mainly in vector-sized tandem repeats and for t-PA producing CHO cells, up to 9 integration clusters were observed. Nonetheless, two patterns emerged from both the APC and t-PA results up to 240 or 300 copies, respectively. The k_D of both APC and t-PA increased in a nonlinear cooperative trend as the cDNA copy number was increased. At higher cDNA copy numbers, the k_D and the q_p were decreased, likely due to cosuppression at higher copy numbers. This appears to be the first report of cosuppression for mammalian cell lines (Bingham, 1997).

The growth rates of APC producing BHK cells were decreased at increasing q_p. The t-PA producing CHO cells had no such q_p dependence even though they produced 20-fold more recombinant protein. The translational rates and protein degradation rates

TABLE 7.1 Comparison of intracellular parameter values for APC and t-PA productions in BHK and CHO cells at quasi-steady-state with standard deviations. The parameters presented in the table are: transcription rate k_D; mRNA turnover rate k_m; cell growth rate μ; translation rate k_R; secretion rate k_S; and intracellular protein degradation rate k_P. The mRNA levels are relative. This table combines Tables 4.2 and 6.2. *The parameters in the secretory pathway saturation range. (a) k_S data from intracellular protein content. (b) k_S data from pulse-chase method.

Parameter	APC Value ± SD	t-PA Value ± SD	Units
k_D	NA	0.0004 ~ 0.0031	range of mRNA/cDNA/h
k_m	NA	0.1 ± 0.01	h^{-1}
μ	0.008 ~ 0.04	0.03 ± 0.004	h^{-1}
k_R	0.005 ± 0.001	0.22 ± 0.07	pg t-PA/mRNA/h
k_S	0.11 ± 0.03 (a)	2.25 ± 0.35 (a)	h^{-1}
	0.12 ± 0.03 (b)	1.63 ± 0.52 (b)	h^{-1}
	0.05*		h^{-1}
k_P	0.004 ± 0.004	0.01 ± 0.01	h^{-1}

Table 7.2 Summary of intracellular factors influencing recombinant protein production rates for APC by BHK cells and t-PA by CHO cells.

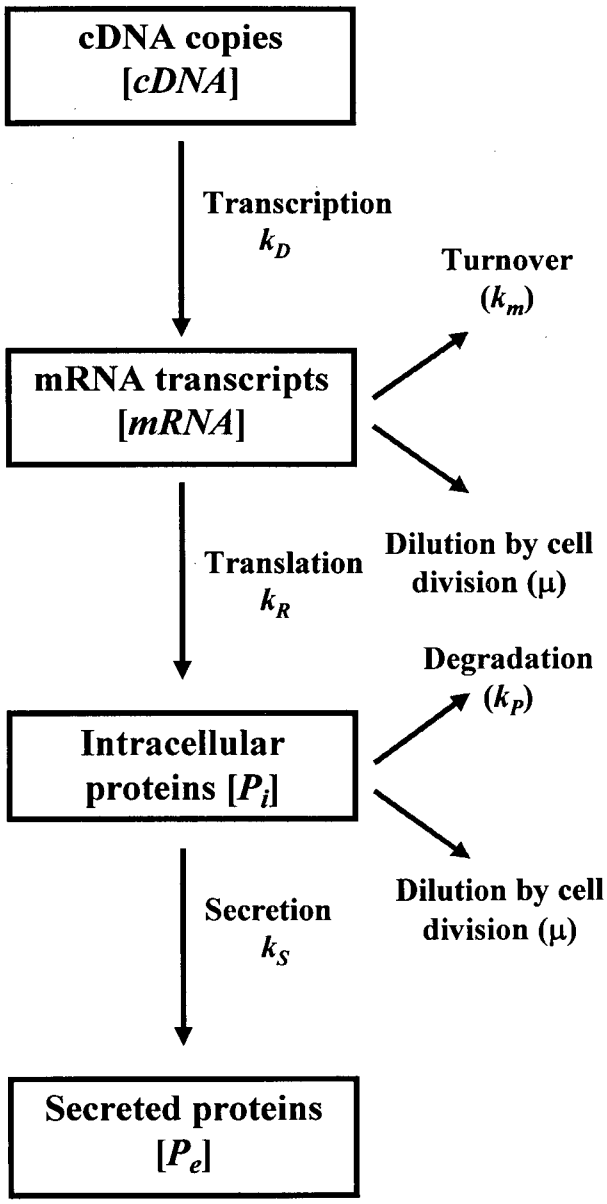

CLONAL PARAMETER VARIABILITY

- $[cDNA^{APC}]$ up to 660 copies/cell
- $[cDNA^{tPA}]$ up to 780 copies/cell

- k_D^{APC} increased up to 240 $cDNA^{APC}$, decreased above 240
- k_D^{tPA} increased up to 300 $cDNA^{tPA}$, decreased above 340
- Maximum q_p^{tPA} limited by maximum k_D^{tPA} (even in the range of unstable q_p^{tPA})

- k_m^{tPA} constant

- k_R^{APC} and k_R^{tPA} constant

- k_p^{APC} increased when secretory pathway saturated
- k_p^{tPA} constant

- $[APC_i] \leq 0.8$ pg/cell, except when secretory pathway saturated at $0.8 \leq [APC_i] \leq 1.5$
- Unsaturated $[tPA_i] \leq 0.7$ pg/cell (saturation not detected)

- μ^{BHK} decreased as q_p^{APC} increased
- μ^{CHO} constant as q_p^{tPA} increased

- k_S^{tPA} constant
- at saturation, k_s^{APC} decreased and $[APC_i]$ increased
- Maximum q_p^{APC} limited at saturated $[APC_i]$

were constant for all APC or t-PA clones, as were the t-PA mRNA turnover rates. At the maximum APC production rate, a saturation of the secretory pathway was detected. Surprisingly, the 20-fold higher cell specific t-PA production rate was limited by transcription rates and not apparently by the secretory pathway. These distinctive limitation patterns were confirmed by pulse-chase and intracellular protein analysis. APC producing BHK cells had higher intracellular APC accumulations due to the 20-fold lower secretion rate for APC from BHK cells compared to t-PA from CHO cells (0.11 ± 0.007 versus 2.25 ± 0.35 h^{-1}) (Table 7.1). This difference in recombinant protein retention half-lives may be responsible for the differences in maximum expression levels. It is hypothesized that a threshold intracellular secretory protein level may exist that limits secretion of many proteins at approximately 1 pg/cell. The results for ATIII (Shroder andd Friedl, 1997) support this conclusion. Other recombinant proteins and cells would need to be investigated to determine how much this threshold concentration is protein or cell-type specific.

Although some kinetic parameters could be directly compared between APC and t-PA (Table 7.2), it should be noted that due to the difficulty in quantifying exact APC or t-PA mRNA transcript numbers, the mRNA levels described in this report are in different arbitrary units. Therefore, the high transcription rate (k_D) and translation rate (k_R) shown for APC should not be taken to imply that APC had higher transcription or translation rates than t-PA. Although both proteins seem to have similar mRNA levels judging from their amount relative to β-actin mRNA (Figures 4.6 and 6.8), it is still premature to make any conclusion since many factors could influence the absolute mRNA levels, such as the

amount of DIG molecules in each probe, the exposure time to the film, and the levels of β-actin expression in different cell types.

Many groups have reported clonal variations in recombinant protein secretory pathway. Table 7.3 compares our own results to literature results from Table 1.4. Identification of intracellular limitations provides a basis for selecting appropriate strategies for increasing recombinant expression, depending on whether transcription or secretion limits protein production. When transcription rate limits protein production, further amplification of cDNA or using more powerful promoters can increase mRNA levels and production rates. At secretion limited rates, engineering the concentrations of secretory processing proteins may increase the recombinant protein production rates (Dorner et al., 1988; Lee et al., 1993; Robinson et al., 1994). Thus, it is important to analyze if secretion is limiting, i.e. k_S decreased at the highest production rate obtained. The secretion rate (k_S) can either be measured directly by pulse-chase analysis or calculated using Equation 3.3 from the intracellular t-PA content and the cell specific production rate. The second approach is much simpler and less labor-intensive approach than the pulse-chase method. Alone, the comparison of secretion rates and intracellular protein levels detected secretory pathway limitations for hATIII (Schroder and Friedl, 1997) and APC (Figure 4.11). In the case of t-PA, the constant secretion rate, even in the unstable range of production (Figure 6.10), indicates a transcription level limitation as discussed above.

Batch culture analysis revealed that for both APC and t-PA production, mRNA levels were stable and correlated with recombinant protein production rate during the

Table 7.3 Reported limiting factors to the rates of recombinant protein production by mammalian cells including APC and t-PA. This table is drawn from Table 1.4 and the APC and t-PA results have been added.

Recombinant Protein	Host Cell	Sample number	cDNA vs. q_P	mRNA vs. q_P	cDNA vs. mRNA	mRNA vs. P_i	P_i vs. q_P	(q_P) Production range (μg/10^{6}cell·day)	Reference
HbsAg	CHO	5	–	+	–	NA	NA	0.1~1	Michel et al., 1985
t-PA	CHO	3	+	+	+	+	+	0.6~10	Kaufman et al., 1985
EPO	CHO	1	NA	+	NA	+	+	NA	Dorner et al., 1989
FVIII	CHO	3	NA	–	NA	+	–	<1.4	Kaufman et al., 1989
vWF	CHO	3	NA	+	NA	+	+	NA	Kaufman et al., 1989
t-PA	Myeloma	14	+	+	+	NA	NA	0.8~8	Hendricks et al., 1989
Protein C	293	15	NA	NA	+	NA	NA	0.02~25	Walls et al., 1989
t-PA	Various	13	–	NA	NA	NA	NA	0.1~11	Jalanko et al., 1990
HbsAg	CHO	3	+	+	+	NA	+, –	0.2~11	Pendse et al., 1992
t-PA	BHK	7	–	+	–	NA	NA	1~20	Hippenmyer and Highkin, 1993
hIGFBP-1	CHO	3	+	NA	NA	NA	NA	0.1~6	Dyring and Mellstrom, 1997
hATIII	CHO	4	NA	NA	NA	NA	+, –	0.4~7	Schroder and Friedl, 1997
TNFrFc	CHO	6	NA	+, –	NA	NA	NA	NA	Morris et al., 1997
APC	BHK	26	– (0.52)	+, – (0.96, -0.8)	– (0.49)	+ (0.97)	+, – (0.96, -0.2)	0.03~2.2	Chapter 4
t-PA	CHO	24	– (0.17)	+ (0.92)	– (0.12)	+ (0.97)	+ (0.98)	1~42	Chapter 6

NA: not available. +: positive correlation greater than 0.85 (where available). –: poor correlation lower than 0.6 (where available). +, –: positive correlation below saturation level then poor correlation at saturation. For the APC and t-PA results, the correlation coefficients are included in parenthesis.

exponential growth. Rapid declines in the APC and the t-PA production rates were observed when the cells entered stationary or decline phases. Although mRNA levels also declined in these phases, they did not correlate as well with protein production rate, especially for CHO cell t-PA production. These results indicate a shift in limiting mechanism that could be further investigated.

Overall, the results in this report could provide some general recommendations for mammalian recombinant protein production. First, our amplification results suggested that bulk amplification provide a less labor-intensive method to obtain high producing clones, at least for non-growth-associated recombinant protein production. Second, stable clones with relatively high production rates should be cloned after adaptation to MTX-free medium without serum. Finally, and most importantly, analysis of intracellular protein content could be used to monitor when intracellular production limitations are reached. This simple analysis indicates at what level further cDNA amplification or vector optimization would be fruitless. If the hypothesis of an apparently 1 pg/cell saturation in the secretory pathway proves correct, Equation 6.2 can be used to estimate the maximum cell specific production rates that could be attained.

CHAPTER 8

FUTURE PERSPECTIVES

In this study, the roles of intracellular factors as the limitations in protein production and the amplification strategy as well as production stability in mammalian cells have been systematically investigated. Although the results clearly demonstrated the distinguished limitation patterns in two different mammalian recombinant protein production systems, this work should be regarded as the preliminary step to understand the limitations in mammalian cell production, and to develop new strategies to increase recombinant protein production rate and to optimize mammalian culture conditions. Advanced investigations need to be carried out to extend our understanding about these issues, and provide us guidelines to apply these concepts in recombinant mammalian production for practical purposes.

8.1 Further Investigation of Production Instability in t-PA Producing CHO Cells

The mechanism which caused the instability of high producing CHO cells in culture is still unclear. Since there was no correlation between cell growth rate and cell specific t-PA production rate, cell apoptosis is the most possible mechanism to dismiss high producing CHO cells in long-term culture. Although the apoptosis analysis in this study did not provide conclusive evidence to verify the relation between instability and cell apoptosis, a higher portion of apoptotic cells was observed in the high producing clone.

Further studies should be conducted using other culture conditions, such as in over-crowded cell culture, different culture pH, different dissolved oxygen concentrations, low cell viability condition, and nutrient-deficient culture to mimic the possible conditions that may occur in the long-term cell culture. These analyses may provide us more information about the effect of apoptosis on long-term protein production rate. Moreover, the results may be useful to develop a new strategy such as co-expression of bcl-2, a apoptosis suppressing protein, with t-PA in the high producing clones to reduce cell apoptosis and preserve these cells in long-term cell culture. This strategy has recently been applied to recombinant mammalian cells to increase cell production rate (Fusseneger et al., 1997), and may have the potential to enhance the stability of t-PA production in high producing CHO cells.

8.2 Production Limitations in Various Cell Culture Methods

The investigation of the intracellular factors reported as discussed in this work was performed with cells in exponential growth and during the whole batch culture. The influence of these intracellular factors on specific protein production rate could also be further investigated in other culture conditions, such as in fed batch culture, semi-continuous culture, or continuous culture. Similar research has been applied to monoclonal antibody production by hybridoma cells (Merten et al., 1994), but no reports for recombinant mammalian cells have been published. These studies could reveal the relation between dilution rate and intracellular limiting factors, and provide information

about the various limitations in different culture stages. These data could be important for selecting culture methods and optimizing culture conditions.

8.3 The Influence of Environmental and Nutritional Factors on the Intracellular Rate Parameters

Environmental factors such as dissolved oxygen level and pH, and nutrients such as glucose, glutamine and amino acids have been shown to affect recombinant protein production rates in culture. However, the influence of these environmental and nutritional factors on intracellular limiting factors has not been fully investigated. Using small-scale, multiple culture wells with various culture conditions and statistical analysis, these extracellular factors can be analyzed for their effects on the rates and limitations of recombinant protein production. These results will be critical for metabolic engineering of recombinant mammalian cells, and provide the critical information to control protein production rate by manipulating culture conditions.

8.4 Maximum Protein Production rate for Different Recombinant Proteins

The mechanism responsible for the difference in maximum protein production rate between APC production by BHK cells and t-PA Production by CHO cells is an interesting topic for further investigation. The difference in host cell types may be part of the reason, but by itself this is hard to fully explain the variation in protein production rate, since both cell types have been widely used with reasonable high recombinant protein

production rates (Table 2.1). Although the different affinity to GRP78 has been reported to be responsible for the distinctive production rates between factor VIII and von Willebrand factor (Kaufman et al., 1989), it is not clear if it is also the case in the production difference between APC and t-PA. Analysis of the association between recombinant proteins and GRP78 or other ER-based processing proteins, and the concentrations of ER-based processing proteins such as PDI, will provide more insight in this issue. Furthermore, coexpression of APC and t-PA in the same host cells may also provide valuable information to help us answer the question why some proteins, such as t-PA and recombinant antibody, have higher maximum production rate than other recombinant proteins, such as APC and factor VIII.

8.5 Limitation Studies of Other Recombinant Protein Production

Two different recombinant protein productions were investigated in this work with distinctive limitation patterns. It is concluded that the limitation on recombinant protein production is highly protein specific. It will be interesting to investigate the intracellular parameters such as cDNA copy number, mRNA level, intracellular protein content, secretion rates, etc., in other recombinant protein productions to confirm the general limitation patterns in mammalian cells, and determine the threshold between different intracellular limitations.

CHAPTER 9

REFERENCES

Al-Rubeai, M., Singh, R. P.,. 1998. Apoptosis in cell culture. Curr. Opin. Biotechnol. **9**: 152-156.

Bae, S. W., Hong, H. J., Lee, G. M. 1995. Stability of transfectomas producing chimeric antibody against the pre-S2 surface antigen of hepatitis B virus during a long-term culture. Biotechnol. Bioeng. **47**: 243-251.

Barsoum, J. 1990. Introduction of stable high-copy-number DNA into Chinese hamster ovary cells by electroporation. DNA and Cell Biol. **9**: 293-300.

Baumal, R., Scharff M. D. 1973. Synthesis, assembly and secretion of mouse immunoglobulin. Transplant. Rev. **14**: 163-183.

Benoist, C., Chambon, P. 1981. in vivo sequence requirements of the SV40 early promoter region. Nature **290**: 304-310.

Bergman, L. W., Kuehl, W. M. 1979. Formation of an intrachain disulfide bond on nascent immunoglobulin chains. J. Biol. Chem. **254**: 8869-8876.

Berkner, K. L., Busby, S. J., Davie, E. W., Hart, C. E., Insley, M., Kisiel, W., Kumar, A. A., Murray, M., O'Hara, P., Woodbury, R. G., Hagen, F. S. 1986. Isolation and expression of cDNAs encoding human factor VII. Cold Spring Harbor Symp. **51**: 531-541.

Bially, H. 1987. Recombinant proteins: virtual authenticity. Bio/technol. **5**: 883-890.

Bibila, T. A., Robinson, D. K. 1995. In pursuit of the optimal fed-batch process for monoclonal antibody production. Biotechnol. Prog. **11**: 1-13.

Bibila, T. A., Flickinger, M. C. 1991. A structured model for monoclonal antibody synthesis in exponentially growing and stationary phase hybridoma cells. Biotechnol. Bioeng. **37**: 210-226.

Bibila, T. A., Flickinger, M. C. 1992. Use of a structured kinetic model of antibody synthesis and secretion for optimization of antibody production systems: 1. Steady-state analysis. Biotechnol. Bioeng. **39**: 251-261.

Bingham, P. M. 1997. Cosuppression comes to the animals. Cell **90**: 385-387.

Boffa, L. C., Gruse, R, J., Allfrey, V. G. 1981. Manifold effects of sodium butyrate on nuclear function. J. Biol. Chem. **256**: 9612-9621.

Boshart, M., Weber, F., Jahn, G., Doirsh-Hasler, Fleckenstein, B., Schaffner, W. 1985. A very strong enhancer is located upstream of an immediate early murine sarcoma virus. Cell **41**: 521-530.

Brown, M. J., Dodd, I., Carey, J. E., Chapman, C. G., Robison, J. H. 1985. Increased yield of human tissue-type plasminogen activator obtained by means of recombinant DNA technology. Thromb. Haemost. **54**: 422-424.

Brown, P. C., Beverley, S. M., Schimke, R. T. 1981. Relationship of amplified dihydrofolate reductase genes to double minute chromosomes in unstable resistant mouse fibroblast cell lines. Mol. Cell. Biol. **1**: 1077-1083.

Capecchi, M. R. 1980. High efficiency transformation by direct microinjection of DNA into cultured mammalian cells. Cell **22**: 479-488.

Carroll, S. M., Gaudray, P., De Rose, M. L., Emery, J. F., Meinkoth, J. L., Nakkim, E., Subler, M., Van Hoff, D. D., Wahl, G. M. 1987. Characterization of an episome produced in hamster cells that amplify a transfected CAD gene at high frequency. Mol. Cell, Biol. **7**: 1740-1745.

Cartwright, T., Crespo, A. 1991. Production of a pharmaceutical enzyme: animal cells or E. coli? In Production of biologicals from animal cells, J. B. G. R. E. Spier, B. Meignier, ed. (Oxford: Butterworth-Heinemann).

Cartwright, T. 1992. Production of tPA from animal cell cultures. In Animal Cell Biotechnology: Academic Press Limited), pp. 217-245.

Cerasi, E. 1975. Insulin secretion: mechanism of the stimulation by glucose. Quarterly Reviews of Biophysics **8**: 1-41.

Chen, C., Okayama, H. 1987. High-efficiency transformation of mammalian cells by plasmid DNA. Mol. Cell. Biol. **7**: 2745-2752.

Choi, Y. S., Knopf, P. M., Lennox, E. S. 1971. Intracellular transport and secretion of an immunoglobulin light chain. Biochemistry **10**: 668-679.

Chomczynski, P., Sacchi, N. 1987. Single-step method of RNA isolation by acid guanidium thiocyanate-phenol-chloroform extraction. Anal. Biochem. **82**: 156-159.

Chuck, A. S., Palsson, B. O. 1992. Population balance between producing and nonproducing hybridoma clones is very sensitive to serum level, state of inoculum, and medium composition. Biotechnol. Bioeng. **39**: 354-360.

Chu, G., Hayakawa, H., Berg, P. 1987. Electroporation for the efficient transfection of mammalian cells with DNA. Nucl. Acids Res. **15**: 1311-1326.

Cockett, M. I., Bebbington, C. R., Yarranton, G. T.,. 1990. High level expression of tissue inhibitor of metalloproteinases in Chinese hamster ovary cells using glutamine synthetase gene amplification. Bio/Technol. **8**: 662-7.

Cogoni, C., Irelan, J. I., Schumacher, M., Schumacher, T. J., Selker, E. U., Macino, G. 1996. Transgene silencing of the *al-1* gene in vegetative cells of *Neurospora* is mediated by a cytoplasmic effector and does not depend on DNA-DNA interactions or DNA methylation. EMBO J. **15**: 3153 - 3163.

Collen, D., Lijnen, H. R. 1986. Tissue-type plasminogen activator: Mechanism of action and thrombolytic properties. Haemostasis **S.3**: 25-32.

Cosmon, D. 1987. Control of messenger RNA stability. Immunol. Today **8**: 16-17.

Cossons, N. H., Hayter, P. M., Tuite, M. F., Jenkins, N. 1991. Stability of amplified DNA in Chinese hamster ovary cells. In Production of biologicals from animal cells in culture, J. B. G. R. E. Spider, and B. Meigner, ed. (Oxford: Butterworth-Heinemann), pp. 309-314.

Cowell, J. K., Miller, O. J. 1983. Occurence and evolution of homogenouslt staining regions may be due to breakage-fusion-bridge cycles following telomere loss. Chromosomes **88**: 216-221.

Cuisset, L., Tichonicky, L., Jaffray, P. and Delpech, M. 1997. The effects of sodium butyrate on transcription are mediated through activation of a protein phophatase. J. Biol. Chem. **272**: 24148-24153.

Cullen, B. R., Lomedico, P. T., Ju, G. 1984. Transcriptional interference in avian retroviruses-Implications for the promoter insertion model of leukaemogenesis. Nature **307**: 241-245.

Curling, E. M., Hayter, P. M., Baines, A. J., Gull, K., Strange, P. G., Jenkins, N. 1990. Recombinant human interferon-gamma. Differences in glycosylation and proteolytic processing lead to heterogeneity in batch culture. Biochem. J. **272**: 333-337.

Dalili, M., Ollis, D. F. 1990. A flow-cytometric analysis of hybridoma growth and monoclonal antibody production. Biotechnol. Bioeng. **36**: 64-73.

Darnell, J., Lodish, H., Baltimore, D. 1990. Chapter 17: Plasma-membrane secretory, and lysosome proteins: Biosynthesis and sorting (New York: Scientific American Books).

Dierks, P., van Ooyen, A., Cochran, M., Dobkin, C., Reiser, J., Weissmann, C. 1983. Three regions upstream from the cap site are required for efficient and accurate transcription of the rabbit β-globin gene in mouse 3T6 cells. Cell **32**: 695-706.

Dolnick, B. J., Berenson, R. J., Bertino, J. R., Kaufman, R. J., Nunberg, J. H., Schimke, R. T. 1979. Correlation of dihydrofolate reductase elevation with gene amplification in a homogeneously staining chromosomal region in L5178Y cells. J. Cell. Biol.

Doms, R. W., Lamb, R. A., Rose, J. K., Helenius, A. 1993. Folding and assembly of viral membrane proteins. Virology **193**: 545-562.

Dorer, D. R., Henikoff, S. 1994. Expansions of transgene repeats cause heterochromatin formation and gene silencing in Drosophila. Cell **77**: 993 - 1002.

Dorner, A. J., Kaufman, R. J. 1990. Analysis of synthesis, processing, and secretion of proteins expressed in mammalian cells. Meth. Enzymol. **185**: 577-596.

Dorner, A. J., Wasley, L. C. and Kaufman, R. J. 1989. Increased synthesis of secreted proteins induces expression of glucose-regulated proteins in butyrate-treated Chinese hamster ovary cells. J. Biol. Chem. **264**: 20602-20607.

Dorner, A. J., Wasley, L. C., Kaufman, R. J. 1992. Overexpression of GRP78 mitigates stress induction of glucose regulated proteins and blocks secretion of selective proteins in Chinese hamster ovary cells. EMBO J. **11**: 1563-1571.

Dorner, A. J., Krane, M. G., Kaufman, R. J. 1988. Reduction of endogenous GRP78 levels improves secretion of a heterologous protein in CHO cells. Mol. Cell Biol. **8**: 4063-4070.

Dorner, A. J., Bole, D. G., Kaufman, R. J. 1987. The relationship of N-linked glycosylation and heavy chain-binding protein association with the secretion of glycoproteins. J. Cell Biol. **105**: 2665-2674.

Downham, M. R., Farrell, W. E., Jenkins, H. A. 1996. Endoplasmic reticulum protein expression in recombinant NS0 myelomas grown in batch culture. Biotechnol. Bioeng. **51**: 691-696.

Dyring, C., Mellstrom, K. 1997. Stable, recombinant expression of human insulin-like growth factor binding protein-1 (hIGFBP-1) in Chinese hamster ovary (CHO) cells. Cytotechnol. **24**: 193-200.

Esmon, C. T. 1987. The regulation of natural anticoagulant pathways. Science **235**: 1348-52.

Esmon, C. T. 1989. The roles of protein C and thrombomodulin in the regulation of blood coagulation. J. Biol. Chem. **25**: 4743-4746.

Farquhar, M. G. 1986. Progress in unraveling pathways of Golgi traffic. Ann. Rev. Cell Biol. **1**: 447-488.

Felgner, P. L., Gadek, T. R., Ringold, G. M., Danielsen, M. 1987. Lipofection: A highly efficient, lipid-mediated DNA-transfection procedure. Proc. Natl. Acad. Sci. USA **84**: 7413-7417.

Finn, G. K., Kurz, B. W., Cheng, R. Z., Shmookler, R. J. 1989. Homologous plasmid recombination is elevated in immortally transformed cells. Mol. Cell. Biol. **9**: 4009-4017.

Flickinger, M. C., Goebel, N. K., Bibila, T., Boyce-Jacino, S. 1992. Evidence for posttranscriptional stimulation of monoclonal antibody secretion by L-glutamine during slow hybridoma growth. J. Biotechnol. **22**: 201-226.

Foster, D. C., Sprecher, C. A., Holly, R. D., Gambee, J. E., Walker, K. M., Kumar, A. A. 1991. Endoproteolytic processing of the dibasic cleavage site in the human protein C precursor in transfected mammalian cells: Effects of sequence alterations on efficiency of cleavage. Biochemistry **29**: 347-354.

Foster, D. C., Rudinski, M. S., Schach, B. G., Berkner, K. L., Kumar, A. A., Hagner, F. S., Sprecher, C. A., Insley, M. Y., Davie, E. W. 1987. Propeptide of human protein C is necessary for γ-carboxylation. Biochemistry **26**: 7003-7011.

Fouser, L. A., Swanberg, S. L., Lin, B.-Y., Benedict, M., Kellerher, K., Cumming, D. A., Riedel, G. E. 1992. High level of expression of a chimeric anti-ganglioside GD2 antibody: genomic kappa sequences improve expression in COS and CHO cells. Bio/Technol. **10**: 1121-1127.

Fusseneger, M. m. M., X., Bailey, J. E. 1997. A novel cytostatic process enhances the productivity of Chinese hamster ovary cells. Biotechnol. Bioeng. **55**: 927-939.

Garoff, H. 1985. Using recombinant DNA techniques to study protein targeting in the eucaryotic cell. Annu. Rev. Cell. Biol. **1**: 403-445.

Gebert, C. A., Gray. P. P. 1994. Expression of FSH in CHO cells: I. Comparison of promoter types and effects of their respective inducers. Cytotechnol. **14**: 39-45.

Gentry, L. E., Webb, N. R., Lim, G. J., Brunner, A. M., Ranchalis, J. E., Twardzik, D. R., Lioubin, M. N., Marquardt, H., Purchio, A. F. 1987. Type I transforming growth factor beta: amplified expression and secretion of mature and precursor polypeptides in Chinese hamster ovary cells. Mol. Cell. Biol. **7**: 3418-3427.

Giguere, V., Hollenberg, S. M., Rosenfeld, M. G., Evans, R. M. 1986. Functional domains of the human glucocorticoid receptor. Cell **46**: 645-652.

Goeddel, D. V., Kohr, W. J., Pennica, D., Vehar, G. A. 1989. Human Tissue Plasminogen Activator. US Patent Application: #4,853,330.

Graham, F. L., van der Eb, A. J. 1973. A new technique for the assay of infectivity of human adenovirus 5 DNA. Virology **52**: 456-467.

Greenall, C., Jenkins, N., Tuite, M., Robinson, D., Cook, D., Freedman, R. 1995. Cell engineering to optimise protein secretion: Analysis of components of the secretory system. In Animal Cell Technology: Developments towards the 21st century, E. C. Beuvery, Griffiths, J. B., Zeijlemaker, W. P., ed. (Dordrecht, NL: Kluwer Academic Publishers), pp. 27-31.

Griffith, M. J., Simons, K. 1986. The trans Golgi network: Sorting at the exit site of the Golgi complex. Science **234**: 438-443.

Grinnell, B. W., Walls, J. D. and Gerlitz, B. 1991. Glycosylation of human protein C affects its secretion, processing, functional activities, and activation by thrombin. J. Biol. Chem. **226**: 9778-9785.

Grinnell, B. W., Walls, J. D., Gerlitz, B., Berg, D. T., McClure, D. B., Ehrlich, H., Bang, N. U., Yan, S. B. 1990. Native and modified recombinant human protein C: Function, secretion, and posttranslational modifications. In Protein C and related anticoagulants, W. N. D. Duane F. Bruley, ed. (Houston: The Woodlands).

Gu, M. B., Todd, P., Kompala, D. S. 1996. Metabolic burden in recombinant CHO cells: Effect of dhfr gene amplification and lacZ expression. Cytotechnol. **18**: 159-166.

Guarna, M. M., Fann, C. H., Busby, S. J., Kilburn, D. G., Piret, J. M. 1995. Effect of cDNA copy number on secretion rate of activated protein C. Biotechnol. Bioeng. **46**: 22-27.

Hames, B. D., Dickwood, D. 1982. Gel Electrophoresis of Proteins: a Practical Approach (New York: Wiley-Liss).

Handeli, S., Klar, A., Meuth, M., Cedar, H. 1989. Mapping replication units in animal cells. Cell **57**: 909-920.

Harlow, E., Lane, D. 1988. Antibodies - A laboratory manual (New York: Cold Spring Harbor Press).

Harris, R. J., Leonard, C. K., Guzzetta, A. W., Spellman, M. W. 1991. O-linked fucose is present in the first epidermal growth factor domain of factor XII but not protein C. Biochemistry **30**: 2311-2314.

Hendricks, M. B., Luchette, C. A., Banker, M. J. 1989. Enhanced expression of an immunoglobulin-based vector in myeloma cells mediated by coamplification with a mutant dihydrofolate reductase gene. Bio/Technol. **7**: 1271-1274.

Hershey, J. W. B. 1989. Protein phosphorylation controls translation rates. J. Biol. Chem. **264**: 20823-20826.

Hershey, J. W. B. 1991. Translational control in mammals. Annu. Rev. Biochem. **60**: 717-755.

Hippenmeyer, P., and Highkin, M. 1993. High level, stable production of recombinant proteins in mammalian cell culture using the herpesvirus VP16 transactivator. Bio/Technol. **11**: 1034-1041.

Hurtley, S. M., Helenius, A. 1989. Protein oligomerization in the endoplasmic reticulum. Annu. Rev. Cell Biol. **5**: 277-307.

Jalanko, A., Pirhonen, J., Pohl, G., Banker, M. L. J. 1990. Production of human tissue-type plasminogen activator in different mammalian cell lines using an Epstein-Barr virus vector. J. Biotechnol. **15**: 155-168.

Jasin, M., Berg, P. 1988. Homologous integration in mammalian cells without target gene selection. Genes and Development **2**: 1353-1363.

Jorgensen, R. A. 1995. Cosuppression, flower color patterns, and metastable gene expression states. Science **268**: 686-691.

Kaufman, R. J., Sharp, P. 1982. Amplification and expression of sequences cotransfected with a modular dihydrofolate reductase complementary DNA gene. J. Mol. Biol. **159**: 601-621.

Kaufman, R. J. 1987. High level production of proteins in mammalian cells. In Genetic Engineering: Principles and Methods, J. Setlow, ed. (New York: Plenum Press), pp. 155-198.

Kaufman, R. J. 1993. Amplification and expression of transfected genes in mammalian cells. In Gene amplification in mammalian cells, R. E. Kellems, ed. (New York: Marcel Dekker, Inc.), pp. 315-343.

Kaufman, R. J., Brown, P., Schimke, R. T. 1979. Amplified dihydrofolate reductase genes in unstably methotrexate-resistant cells are associated with double minute chromosomes. Proc. Natl. Acad. Sci. **76**: 5669-5673.

Kaufman, R. J., Wasley, L. C., Spiliotes, A. J., Gossels, S. D., Latt, S. A., Larsen, G. R., Kay, R. M. 1985. Coamplification and coexpression of human tissue-type plasminogen activator and murine dihydrofolate reductase sequences in Chinese hamster ovary cells. Mol. Cell. Biol. **5**: 1750-1759.

Kaufman, R. J., Wasley, L. C., Davies, M. V., Wise, R. J., Israel, D. I., Dorner, A. J. 1989. Effect of von Willebrand factor coexpression on the synthesis and secretion of factor VIII in Chinese hamster ovary cells. Mol. Cell. Biol. **9**: 1233-1242.

Kaufman, R. J., Sharp, P. A., Latt, S. A. 1983. Evolution of chromosomal regions containing transfected and amplified dihydrofolate reductase sequences. Mol. Cell. Biol. **3**: 699-711.

Kaufman, R. J., Wasley, L. C., Furie, B. C., Shoemaker, C. B. 1986. Expression, purification and characterization of recombinant Y-carboxylated factor IX synthesized in Chinese hamster ovary cells. J. Biol. Chem. **261**: 9622-9628.

Kaufman, R. J. 1987. High level production of proteins in mammalian cells. In Genetic Engineering: Principles and Methods, J. Setlow, ed. (New York: Plenum Press), pp. 155-198.

Kaufman, R. J., Brown, P. C., Schimke, R. T. 1981. Loss and stabilization of amplified dihydrofolate reductase genes in mouse Sarcoma S-180 cell lines. Mol. Cell. Biol. **1**: 1084-1093.

Kaufman, R. J., Davies, M. V., Pathak, V. K., Hershey, J. W. B. 1989. The phosphorylation state of eukarytic initiation factor 2 alters translational efficiency of specific mRNAs. Mol. Cell. Biol. **9**: 946-958.

Kaufman, R. J. 1990. Selection and coamplification of heterologous genes in mammalian cells. Meth. Enzymol. **185**: 537-566.

Kellems, R. E. 1991. Gene amplification in mammalian cells: strategies for protein production. Curr. Opin. Biotechnol. **2**: 723-729.

Kenten, J., Boss, M. 1985. Patent application. **GB 86/00187**: 4/1/85.

Keown, W. A., Campell, C. R., Kucherlapati, R. S. 1990. Methods for introducing DNA into mammalian cells. Meth. Enzymol.

Keyt, B. A., Paoni, N. F., Refino, C. J., Berleau, L., Nguyen, H., Chow, A., Lai, J., Rena, L., Pater, C., Ogez, J., Etcheverry, T., Botstein, D., Bennett, W. F. 1994. A faster-acting

and more potent form of tissue plasminogen activator. Proc. Natl. Acad. Sci. USA **91**: 3670-3674.

Khoury, G., Gruss, P. 1983. Enhancer elements. Cell **33**: 313-314.

Kim, N. S., Kim, S. J., Lee, G. M. 1998b. Clonal variability within dihydrofolate reductase-mediated gene amplified Chinese hamster ovary cells: stability in the absence of selective pressure. Biotechnol. Bioeng. **60**: 679-688.

Kim, S. J., Kim, N. S., Ryu, C. J., Hong, H. J., Lee, G. M. 1998a. Characterization of chimeric antibody producing CHO cells in the course of dihydrofolate reductase-mediated gene amplification and their stability in the absence of selective pressure. Biotechnol. Bioeng. **58**: 73-84.

Kisiel, W., Davie, E. W. 1981. Methods Enzymol. **80**: 320-332.

Kittle, J. D., Pimentel, B. J. 1997. Testing the genetic stability of recombinant DNA cell banks. BioPharm **9**: 48-51.

Koehler, U., Abken, H., Grummt, F., Wienberg, J., Weidle, U. H. 1995. A novel type of unstable homogeneously staining region with a head-to-tail arrangement: spontaneous decay and reintegration of DNA elements into a plethora of new chromosomal sites. Cytogenet. Cell Genet. **68**: 33-38.

Kooistra, T., Schrauwen, Y., Arts, J., Emeis, J. J. 1994. Regulation of endothelial cell t-PA synthesis and release. Int. J. Hematol. **59**: 233-255.

Kornfield, R., Kornfield, S. 1985. Assembly of asparagine-linked oligosaccharides. Ann. Rev. Biochem. **54**: 631-664.

Kromenaker, S. J., Srienc, F. 1994. Stability of producer hybridoma cell lines after cell sorting: a case study. Biotechnol. Prog. **10**: 299-307.

Kruh, J. 1982. Effects of sodium butyrate, a new pharmacological agent, on cells in culture. Mol. Cell. Biochem. **42**: 65-82.

Lanzillo, J. L. 1990. Preparation of digoxigenin-labeled probes by the polymerase chain reaction. BioTechniq. **8**: 621-622.

Lee, A. S., Li, X., Li, L.-J., Little, E. 1993. Molecular approaches toward manipulating the expression of the glucose-regulated proteins in mammalian cells. In Cell Biology and Biotechnology: Novel Approaches to Increased Cellular Productivity, M. S. Oka, Rupp, R. G., ed. (New York: Springer-Verlag), pp. 114-124.

Lee, F., Mulligan, R., Berg, P., Ringold, G. 1981. Glucocorticoids regulate expression of dihydrofolate reductase cDNA in mouse mammary tumor virus chimeric plasmids. Nature **294**: 228-232.

Leibovitch, M. P., Kruh, J. 1979. Effect of sodium butyrate on myoblast growth and differentiation. Biochem. Biophys. Res. Com. **87**: 896-903.

Lengyel, P. 1982. Biochemistry of interferons and their actions. Ann. Rev. Biochem. **51**: 251-282.

Leno, M., Merten, O.-W., Vuillier, F., Hache, J. 1991. IgG production in hybridoma batch culture: kinetics of IgG mRNA, cytoplasmic-, secreted- and membrane-bound antibody levels. J. Biotechnol. **20**: 301-312.

Leno, M., Merten, O.-W., Hache, J. 1992. Kinetic studies of cellular metabolic activity, specific IgG production rate, IgG mRNA stability and accumulation during hybridoma batch culture. Enzyme Microb. Technol. **14**: 135-140.

Lodish, H. F. 1988. Transport of secretory and membrane glycoproteins from the rough endoplasmic reticulum to the Golgi: A rate-limiting step in protein maturation and secretion. J. Biol. Chem. **263**: 2107-2110.

Lodish, H. F., Kong, N., Snider, M., Strous, G. J. A. M. 1983. Hepatoma secretory proteins migrate from the rough endoplasmic reticulum to Golgi at characteristic rates. Nature **304**: 80-83.

Long, G. L. 1986. Structure and evolution of the human genes encoding protein C and coagulation factors VII, IX, and X. Cold Spr. Har. Symp. Quan. Biol. **LI**: 525-529.

Looney, J. E., Hamlin, J. L. 1987. Isolation of the amplified dihydrofolate reductase domain from methotrexate-resistant Chinese hamster ovary cells. Mol. Cell. Biol. **7**: 569-577.

Looney, J. E., Ma, C., Leu, T. H., Flintoff, W. F., Troutman, W. B., Hamlin, J. L. 1988. The dihydrofolate reductase amplicons in different methotrexate-resistant Chinese hamster cell lines share at least a 273-kilobase core sequence, but the amplicons in some cell lines are much larger and are remarkably uniform in structure. Mol. Cell. Biol. **8**: 5268-5279.

Lubiniecki, A., Arathoon, R., Polastri, G., Thomas, J., Wiebe, M., Garnick, R., Jones, A., van Reils, R., Builder, S. 1989. Selected strategies for manufacture and control of recombinant tissue plasminogen activator prepared from cell cultures. In Advances in Animal Cell Biology and Technology for Bioprocesses, J. B. R. E. Spier, Griffiths, J. Stephenno, P. J. Crooy, ed.: Butterworth), pp. 442-457.

Lyles, M. M., Gilbert, H. F. 1991. Catalysis of the oxidative folding of ribocuclease A by protein disulfide isomerase: Dependence of the rate on the composition of the redox buffer. Biochemistry **30**: 619-625.

Ma, C., Martin, S., Trask, B., Hamlin, J. L. 1993. Sister chromatid fusion initiates amplification of the dihydrofolate reductase gene in Chinese hamster cells. Genes Devel. **7**: 605-620.

Maniatis, T., Fritsch, E. F. and Sambrook, J. 1982. Molecular Cloning - A Laboratory Manual. Cold Spring Harbor Press, New York.

Matzke, M. A., Matzke, A. J. M. 1995. How and why do plants inactivate homologous (trans) genes? Plant Physiol. **107**: 679-685.

Maurer, B. J., Lai, E., Hamkalo, B. A., Hood, L., Attardi, G. 1987. Novel submicroscopic extrachromosomal elements containing amplified genes in human cells. Nature **327**: 434-437.

Mayo, K. E., Warren, R., Palmiter, R. D. 1982. The mouse metallothionein-I gene is transcriptionally regulated by cadmium following transfection into human or mouse cells. Cell **29**: 99-108.

McBurney, M. W., Whitemore, G. F. 1975. Mechanism of growth inhibition by methotrexate. Cancer Res. **35**: 586-590.

McClure, D. B., Walls, J. D. and Grinnell, B. W. 1992. Post-translational processing events in the secretion pathway of human protein C, a complex vitamin K-dependent antithrombotic factor. J. Biol. Chem. **267**: 19710-19717.

McIvor, R. S., Goddard, J. M., Simonsen, C. C., Martin Jr., D. W. 1985. Expression of a cDNA sequence encoding human purine nucleotide phophorylase in rodent and human cells. Mol. Cell. Biol. **5**: 1379-1384.

McLauchlan, J., Gaffray, D., Whitton, J. L., Clements, J. B. 1985. The consensus sequence YGTGTTYY located downstream from the AAUAAA signal is required for efficient formation of 3' termini. Nucleic Acid Res. **13**: 1347-1368.

Merten, O. W., Moeurs, D.,Keller, H., Leno, M., Palfi, G. E., Cabanie, L., Couve, E. 1994. Modified monoclonal antibody production kinetics, kappa/gamma mRNA levels, and metabolic activities in a murine hybridoma selected by continuous culture. Biotechnol. Bioeng. **44**: 753-764.

Michel, M.-L., Sobczak, E., Malpiece, Y., Tiollais, P., Rolf, E. 1985. Expression of hepatitis B virus surface antigen genes in Chinese hamster ovary cells. Bio/Technol. **3**: 561-566.

Milbrant, J. D., Heintz, N. H., White, W. C., Rothman, S. M., Hamlin, J. L. 1981. Methotrexate-resistant Chinese hamster ovary cells have amplified a 135 kilobase-pair region that includes the dihydrofolate reductase gene. Proc. Natl. Acad. Sci. USA **78**: 6043-6047.

Moore, A., Donahue, C. J., Hooley, J., Stocks, D. J., Bauer, K. D., Mather, J. P. 1995. Apoptosis in CHO cell batch cultures: examination by flow cytometry. Cytotechnol. **17**: 1-11.

Morris, A. E., Lee, C.-C., Hodges, K., Aldrich, T. L., Krantz, C., Smidt, P. S., Thomas, J. N. 1997. Expression augmenting sequence element (EASE) isolated from Chinese hamster ovary cells. In Animal Cell Technology, M. J. T. Carrondo, ed. (Netherlands: Kluwer Academic Publishers), pp. 529-534.

Morris, T., Marashi, F., Weber, L., Hickey, E., Greenspan, D., Bonner, J., Stein, J., Stein, G. 1986. Involvement of the 5'-leader sequence in coupling the stability of a human H3 histone mRNA with DNA replication. Proc. Natl. Acad. Sci. USA **83**: 981-985.

Morrison, C. J., McMaster, W. R., Piret, J. M. 1997. Differential stability of proteolytically active and inactive recombinant metalloproteinase in Chinese hamster ovary cells. Biotechnol. Bioeng. **53**: 594-600.

Murray, M. J., Kaufman, R. J., LAtt, S. A., Weinberg, R. A. 1983. Construction and use of a dominant, selectable marker: A Harvey sarcoma virus-dihydrofolate reductase chimera. Mol. Cell Biol. **3**: 32-43.

Nover, L. 1987. Expression of heat shock genes in homologous and heterologous systems. Enzyme Microb. Technol. **9**: 130-144.

Nunberg, J. H., Kaufman, R. J., Schimke, R. T., Urlaub, G., Chasin, L. A. 1978. Amplified dihydrofolate reductase genes are localized to a homogeneously staining region of a single chromosome in a methotrexate-resistant Chinese hamster ovary cell line. Proc. Natl. Acsd. Sci., USA **75**: 5553-5556.

Oh, S. K. W., Vig, P., Chua, F., Teo, W. K., Yap, M. G. S. 1993. Substantial overproduction of antibodies by applying osmotic pressure and sodium butyrate. Biotechnol. Bioeng. **42**: 601-610.

Okamoto, M., Nakayama, C., Nakai, M., Yenagi, H. 1990. Amplification and high level expression of a cDNA for human granulocyte-macrophage colony stimulating factor in human lymphoblastoid Namalwa cells. Bio/Technol. **8**: 550-553.

Page, M. J., Sydenham, M. A. 1991. High level expression of the humanized monoclonal antibody Campath-1H in Chinese hamster ovary cells. Bio/Technol. **9**: 64-68.

Pain, V. 1986. Initiation of protein synthesis in mammalian cells. Biochem. J. **235**: 625-637.

Pal-Bhadra, M., Bhadra, U. and Birchler, J. A. 1997. Cosuppression in Drosophila: Gene silencing of alcohol dehydrogenase by *white-adh* transgenes is *Polycomb* dependent. Cell **90**: 479 - 490.

Palermo, D. P., DeGraaf, M. E., Marotti, K. R., Rehberg, E. and Post, L. E. 1991. Production of analytical quantities of recombinant proteins in Chinese hamster ovary cells using sodium butyrate to elevate gene expression. J. Biotechnol. **19**: 35-48.

Pallavicini, M. G., DeTeresa, P. S., Rosette, C., Gray, J. W., Wurm, F. M. 1990. Effects of methotrexate on transfected DNA stability in mammalian cells. Mol. Cell. Biol. **10**: 401-404.

Palmiter, R. D., Behringer, R. R., Quaife, C. J., Maxell, F., Maxwell, I. H., Brinster, R. L. 1987. Cell lineage ablation in transgenic mice by cell-specific expression of a toxin gene. Cell **50**: 435-443.

Parekh, R. B., Dwek, R. A., Thomas, J. R., Opdenakker, G., Rademacher, T. W. 1989. Cell-type-specific and site-specific N-glycosylation of type I and type II human tissue plasminogen activator. Biochemistry **28**: 7644-7662.

Pauletti, G., Lai, E., Attadi, G. 1990. Early appearance and long-term persistence of the submicroscope extrachromosomal elements (amplisomes) containing the amplified DHFR genes in human cell lines. Proc. Natl. Acad. Sci. USA **87**: 2955-2959.

Pendse, G. J., Karkare, S. and Bailey, J. E. 1992. Effect of cloned gene dosage on cell growth and hepatitis B surface antigen synthesis and secretion in recombinant CHO cells. Biotechnol. Bioeng. **40**: 119-129.

Pennica, D., Hlomes, W. E., Kohr, W. J., Harkins, R. N., Vehar, G. A., Ward, C. A., Bennett, W. F., Yelverton, E., Seeburg, P. H., Heyneker, H. L., Goeddel, D. V., Collen, D. 1983. Cloning and expression of human tissue-plasminogen activator cDNA in *E. coli*. Nature **301**: 214-221.

Pinkel, D., Straume, T., Gray, J. W. 1986. Cytogenetic analysis using quantitative, high-sensitivity fluorescence hybridization. Proc. Natl. Acad. Sci. USA **83**: 2934-2938.

Pohl, G., Kallstrom, N., Bergsdorf, N., Wallen, P., Jornvall, H. 1984. Tissue plasminogen activator: Peptide analyses confirm an indirectly derived amino acid sequence, identify the active site serine, establish glycosylation sites and localize variant differences. Biochemistry **23**: 3701-3707.

Potter, H., Weir, L., Leder, P. 1984. Enhancer-dependent expression of human λ-immunoglobulin genes introduced into mouse pre-B lymphocytes by electroporation. Proc. Natl. Acad. Sci. USA **81**: 7161-7165.

Prasad, K. N., and Sinha, P. K. 1976. Effect of sodium butyrate on mammalian cells in culture: A review. In Vitro **12**: 125-132.

Proudfoot, N. J. 1986. Transcriptional interference and termination between duplicated α-globin gene constructs suggests a novel mechanism for gene regulation. Nature **322**: 562-565.

Randy, M., Wallen, P. 1981. A sensitive parabolic rate assay for the tissue plasminogen activator. In Progress in Fibrinolysis, J. F. Dacidson, Nilsson, I. M., Astedt, B., ed. (Edinburgh: Churchill Livingstone), pp. 233-235.

Ratcliffe, J. V., Furie, B., Furie, B. C. 1993. The importance of specific γ-carboxyglutamic acid residues in prothrombin. Evaluation by site-specific mutagenesis. J. Biol. Chem. **268**: 24339-24345.

Reddy, V. B., Garramone, A. J., Sasak, H., Wei, C., Watkins, P., Galli, J., Hsiung, N. 1987. Expression of human uterine tissue-type plasminogen activator in mouse cells using BPV vectors. DNA **6**: 461-472.

Reff, M. E. 1993. High-level production of recombinant immunoglobulins in mammalian cells. Curr. Opin. Biotechnol. **4**: 573-576.

Rehemtulla, A., Roth, D. A., Wasley, L. C., Kuliopulos, A., Walsh, C. T., Furie, B. C., Kaufman, R. J. 1993. *In vitro* and *in vivo* functional characterization of bovine vitamin K-dependent γ-carboxylase expressed in Chinese hamster ovary cells. Proc. Natl. Acad. Sci. USA, **90**: 4611-4615

Riggs, C. D., Bates, G. W. 1989. Stable transformation of tobacco by electroporation: Evidence for plasmid concatenation. Proc. Natl. Acad. Sci. USA **83**: 5602-5606.

Rijken, D. C., Hoylaerts, M., Collen, D. 1982. Fibrinolytic properties of one-chain and two-chain human extrinsic (tissue-type) plasminogen activator. J. Biol. Chem. **257**: 2920-2925.

Rijken, D. C., Collen, D. 1981. Purification and characterization of the plasminogen activator secreted by human melanoma cells in culture. J. Biol. Chem. **256**: 7035-7042.

Robins, D. M., Axel, R., Henderson, A. S. 1981a. Chromosome structure and DNA sequence alterations associated with mutation of transformed genes. J. Mol. Appl. Genet. **1**: 191-203.

Robins, D. M., Ripley, S., Henderson, A., Axel, R. 1981b. Transforming DNA integrates into the host chromosome. Cell **23**: 29-39.

Robinson, A. S., Wittrup, K. D. 1995. Constitutive overexpression of secreted heterologous proteins decreases extractable BiP and protein disulfide isomerase levels in *Saccharomyces cerevisiae*. Biotechnol. Prog. **11**: 171-177.

Robinson, A. S., Hines, V., Wittrup, K. D. 1994. Protein disulfide isomerase overexpression increases secretion of foreign proteins in *Saccharomyces cerevisiae*. Bio/Technol. **12**: 381-384.

Rotondaro, L., Mazzanti, L., Mele, A., Rovera, G. 1997. High-level expression of a cDNA for human granulocyte colony - stimulating factor in Chinese hamster ovary cells. Effect of 3'-noncoding sequences. Mol. Biotechnol. **7**: 231-240.

Rouf, S. A., Moo-Young, M., Chisti, Y. 1996. Tissue-type plasminogen activator: Characteristics, applications and production technology. Biotechnol. Adv. **14**: 239-266.

Ruiz, J. C., Wahl, G. M. 1988. Formation of an inverted duplication can be an initial step in gene amplification. Mol. Cell. Biol. **8**: 4302-4313.

Runstadler, P. W., Gernak, S. R. 1988. Large-scale fluidized-bed, immobilized cultivation of animal cells at high densities. In Animal Cell Technology, R. E. Spier, Griffiths, J. B., ed.: Academic Press, NY), pp. 305-335.

Sanders, P. G. 1990. Protein production by genetically engineered mammalian cell lines. Animal Cell Biotechnol.**4**: 15-69.

Schaffner, W. 1980. Direct transfer of cloned genes from bacteria to mammalian cells. Proc. Natl. Acad. Sci. USA **77**: 2163-2167.

Schroder, M., Friedl, P. 1997. Overexpression of recombinant human antithrombin III in Chinese hamster ovary cells results in malformation and decreased secretion of recombinant protein. Biotechnol. Bioeng. **53**: 547 - 559.

Sgonc, R., Boeck, G., Sietricb, H., Gruber, J., Recbeis, H., Wick, G. 1994. Simultaneous determination of cell surface antigens and apoptosis. Trends in Genetics **10**: 41-42.

Shuster, J. R. 1991. Gene expression in yeast: Protein secretion. Curr. Opin. Biotechnol. **2**: 685-690.

Sinacore, M. S., Brodeur, S., Brennan, S., Cohen, D., Fallon, M., Adamson, S. R. 1995. Population analysis of a recombinant Chinese hamster ovary cell line expressing recombinant human protein cultured in the presence and absence of methotrexate selective pressure. In Animal Cell Technology: Products of Today, Prospects for Tomorrow, R. E. Spier, Griffiths, J. B. and Berthold, W., ed. (Oxford, UK: Butterworth-Heinemann Ltd), pp. 63-68.

Singh, R. P., Al-Rubeai, M., Gregory, C. D., Emery, A. N. 1994. Cell death in bioreactors: A role for apoptosis. Biotechnol. Bioeng. **44**: 720-726.

Sly, W. S., Fischer, H. D. 1982. The phosphomannosyl recognition system for intracellular and intercellular transport of lysosomal enzymes. J. Cell Biochem. **18**: 67-85.

Solymoss, S., Tucker, M. M., Tracy, P. B.,. 1988. Kinetics of inactivation of membrane-bound factor Va by activated protein C. Protein S modulates factor Xa protection. J. Biol. Chem. **263**: 14884-14890.

Southern, E. 1975. Detection of specific sequences among DNA fragments separated by gel electrophoresis. J. Mol. Biol. **98**: 503-517.

Spellman, M. W. 1990. Carbohydrate characterization of recombinant glycoproteins of pharmaceutical interest. Anal. Chem. **62**: 1714-1722.

Stenflo, J., Holme, E., Lindstedt, S., Chandramouli, N., Huang, L., Tam, J., Merrifield, R. 1989. Hydroxylation of aspartic acid in domains homologous to the epidermal growth factor precursor is catalyzed by a 2-oxoglutarate-dependent dioxygenase. Proc. Natl. Acad. Sci. USA **86**: 444-447.

Strauss, W. M. 1987. Preparation of genomic DNA from mammalian tissue. In Current Protocols in Molecular Biology, Ausubel et al., ed. (New York: Green Publishing and Wiley Interscience).

Strous, G. J., and Lodish, H. F. 1980. Intracellular transport of secretory and membrane proteins in hepatoma cells infected by vesicular stomatitis virus. Cell **22**: 709-717.

Sugiura, T. 1992. Effects of glucose on the production of recombinant protein C in mammalian cell culture. Biotechnol. Bioeng. **39**: 953-959.

Sugiura, T., Maruyama, H. B. 1992. Factors influencing expression and post-translational modification of recombinant protein C. J. Biotech. **22**: 353-360.

Suttie, J. W. 1985. Vitamin K-dependent carboxylase. Annu. Rev. Biochem. **54**: 459-477.

Suttie, J. W. 1986. Report of Workshop on expression of vitamin K-dependent proteins in bacterial and mammalian cells, Madison, Wisconsin, USA, April 1986. Thrombosis Research **44**: 129-34.

Suttie, J. W., Hoskins, J. A., Engelke, J., Hopfgartner, A., Ehrlich, H., Bang, N. U., Belagaje, R. M., Schoner, B., Long, G. L. 1987. Vitamin K-dependent carboxylase: Pssible role of the substrate "propeptide" as an intracellular recognition site. Proc. Natl. Acad. Sci., USA **84**: 634-7.

Takeshita, S., Tezuka, K., Takahashi, M., Honkawa, H., Matsuo, A., Matsuishi, T., Hashimoto-Gotoh, T. 1988. Tandem gene amplification *in vitro* for rapid and efficient expression in animal cells. Gene **71**: 9-18.

Tuite, M. F., Freeman, R. B. 1994. Improving secretion of recombinant proteins from yeast and mammalian cells: Rational or empirical design? TIBTECH **12**: 432-434.

Tyler-Smith, C., Bostock, C. J. 1981. Gene amplification in methotrexate-resistant mouse cells III. Interrelationships between chromosome changes and DNA sequence amplification or loss. J. Mol. Biol. **153**: 237-256.

Uetsuki, T., Naito, A., Nagata, S., Kazikro, Y. 1989. Isolation and characterization of the human chromosomal gene for polypeptide chain elongation factor-1α. J. Biol. Chem. **264**: 5791-5796.

Urlaub, G., Chasin, L. A. 1980. Isolation of Chinese hamster ovary cell mutants deficient in dihydrofolate reductase activity. Proc. Natl. Acad. Sci., USA **77**: 4216-4220.

Vehar, G. A. B., W. F., Pennica, D., Ward, C. A., Harkins, R. N., Collen, D. 1984. Charaterization studies of human melanoma cell tissue-type plasminogen activator. Bio/Technol. **12**: 1051-1057.

Verheijen, J. H., Mullaart, E., Chang, G. T. G., Kluft, C., Wijngaards, G. 1982. A simple, sensitive spectrophotometric assay for extrinsic (tissue-type) plasminogen activator applicable to measurements in plasma. Thromb. Haemostas. **48**: 266-269.

Wagner, R. 1997. Metabolic control of animal cell culture processes. In Mammalian Cell Biotechnology in Protein Production, R. W. H. Hauser, ed. (New York: Walter de Gruyter), pp. 193-232.

Walker, F. J. 1981. Regulation of activated protein C by protein S. The role of phospholipid in factor Va inactivation. J. Biol. Chem. **256**: 11128-11131.

Walls, J. D., Berg, D. T., Yan, S. B., Grinnell, B. W. 1989. Amplification of multicistronic plasmids in the human 293 cell line and secretion of correctly processed recombinant human protein C. Gene **81**: 139-149.

Warren, T. G., Hippenmeyer, P. J., Meyer, D. M., Reutz, B. A., Rowold, E., Carron, C. P. 1994. High-level expression of biologically active, soluble forms of ICAM-1 in a novel mammalian-cell expression system. Protein Express Purif. **5**: 498-508.

Wasylyk, B. 1986. Protein coding genes of higher eukaryotes, promoter elements and trans-acting factors. In Maximizing Gene Expression, W. Reznikoff, Gold, L., ed. (Guildford: Butterworth). 112-134

Weidle, U. H., Buckel, P., Wienberg, J. 1988. Amplified expression constructs for human tissue-type plasminogen activator in Chinese hamster ovary cells: instability in the absence of selective pressure. Gene **66**: 193-203.

Wiebe, M. E., Builder, S. E. 1994. Consistency and stability of recombinant fermentations. In Genetic Stability and Recombinant Product Consistency, F. Brown, Lubiniecki, A. S., ed. (Karger: Dev Biol Stand. Basel), pp. 45-54.

Wieland, F. T., Gleason, M. L., Serafini, T. A., Rothman, J. E. 1987. The rate of bulk flow from the endoplasmic reticulum to the cell surface. Cell **50**: 289-300.

Wilson, T., Treisman, R. 1988. Removal of poly(A) and consequent degradation of *c-fos* mRNA facilitated by AU-rich sequences. Nature **336**: 396-399.

Wilson, C., Bellen, H. J., Gehring, W. J. 1990. Position effects on eukaryotic gene expression. Ann. Rev. Cell. Biol. **6**: 679-714.

Windle, B., Draper, B. W., Yin, Y., O'Gorman, S., Wahl, G. M. 1991. A central role for chromosome breakage in gene amplification, deletion formation, and amplicon integration. Genes and Development **5**: 160-174.

Wolffe, A. P., Meric, F. 1996. Coupling transcription to translation: A novel site for the regulation of eukaryotic gene expression. Int. J. Biochem. Cell Biol. **28**: 247-257.

Wood, W. I., Capon, D. J., Simonsen, C. C., Berman, P. W., Eaton, D. L., Gitschier, J., Keyt, B., Seeburg, P. H., Smith, D. H., Hollingshead, P., Wion, K. L., Delwart, E., Tuddenham, E. G. D., Vehar, G. A., Lawn, R. M. 1984. Expression of active human factor VIII from recombinant DNA clones. Nature **312**: 330-337.

Wurm, F. M. 1997. Aspect of gene transfer and gene amplification in recombinant mammalian cells. In Mammalian Cell Biotechnology in Protein Production, R. W. H. Hauser, ed. (New York: de Gruyter), pp. 90-91.

Wurm, F. M., Pallavicini, M. G. 1993. Effects of methotrexate on recombinant sequences in mammalian cells. In Gene Amplification in Mammalian Cells, R. E. Kellems, ed. (New York: marcel Dekker), pp. 85-94.

Wurm, F. M., Petropoulos, J. 1994. Plasmid integration, amplification and cytogenetics in CHO cells: Questions and comments. Biologicals **22**: 95-102.

Wurm, F. M., Gwinn, K. A., Kingston, R. E. 1986. Inducible overproduction of the mouse c-myc protein in mammalian cells. Proc. Natl. Acad. Sci. USA **83**: 5414-5418.

Wurm, F. M., Pallavicini, M. G., Arathoon, R. 1992. Integration and stability of CHO amplicons containing plasmid sequences. Dev. Biol. Stand. **76**: 69-82.

Wurm, F. M. 1997. Aspect of gene transfer and gene amplification in recombinant mammalian cells. In Mammalian Cell Biotechnology in Protein Production, R. W. H. Hauser, ed. (New York: de Gruyter), pp. 90-91.

Yan, S. B., Grinnell, B. W. 1989. Post-translational modifications of proteins: Some problems left to solve. TIBS **14**: 264-268.

Yan S. C., R., P., Chao, Y. B., Walls, J. D., Berg, D. T., McClure, D. B., Grinnell, B. W. 1990. Characterization and novel purification of recombinant human protein C from three mammalian cell lines. Bio/Technol. **8**: 655-661.

Yeo, K. T., Parent, J. B., Yeo, T. K., and Olden, K. 1985. Variability in transport rates of secretory glycoproteins through the endoplasmic reticulum and Golgi in human hepatoma cells. J. Biol. Chem. **260**: 7896-7902.

Zettlmeissl, G., Ragg, H., Karges, H. E. 1987. Expression of biologically active human antithrombin III in Chinese hamster ovary cells. Bio/Technol. **5**: 720-725.

Zhang, L., Jhingan, A., Castellino, F. J. 1992. Role of individual γ-carboxyglutamic acid residues of activated human protein C in defining its *in vitro* anticoagulant activity. Blood **80**: 942-952.

Zheng, H., Wilson, J. H. 1990. Gene targeting in normal and amplified cell lines. Nature **344**: 170-173.